Preparation of Phosphinate-based Ionic Liquids for Rare Earth Recovery

A thesis

submitted in partial fulfillment

of the requirements for the degree

of

Master of Science (Research) in Chemistry

at

The University of Waikato

by

Sinead Sanders

THE UNIVERSITY OF
WAIKATO
Te Whare Wānanga o Waikato

2023

Abstract

The rare earth elements are vital components in many modern technologies, including green energy technology such as wind turbines and electric vehicles, however the extraction and separation of these elements remains a problem. Due to the similar chemical properties of these elements, achieving pure single elemental concentrations of the REEs is difficult, often requiring multiple steps in the separation process, as well as the use of large volumes of harmful organic solvents. With the demand of these elements projected to grow in the coming decades, greener and more efficient extraction and separation methods need to be developed.

In this work, a series of hydrophobic ionic liquids were prepared through simple neutralisation and protonation reactions. The successful synthesis and characterisation of camphyl phenyl phosphinic acid is also described and used as an anion precursor in IL preparation. Five phosphinate-based ionic liquids were successfully prepared and tested for the separation of the rare earth elements, as well as for cobalt/nickel separations. Both liquid-liquid extraction methods using a neat IL, and column chromatography methods using supported ionic liquids were tested. Results showed selectivity towards the heavy rare earth elements, achieving a La/Yb separation factor as high as 55.3. For the liquid-liquid extraction experiments, La extraction efficiencies of 99% were achieved for a majority of the tested ILs. For the Yb column extractions, high extraction efficiencies were also achieved, ranging from 85.5 - 99.9%. Repeated extractions of cobalt and nickel showed the stability of the column, with minimal decrease in extraction efficiencies over 10 repeated runs, and an average separation factor of 2.79 across these runs.

Acknowledgements

There are a great number of people who I wish to thank, each of whom has supported me and helped me get to the finish line in some shape or form. I am incredibly grateful for each of you, I wouldn't be here without you all.

I would firstly like to thank my primary supervisor, Bill Henderson, for his guidance and support throughout this degree, as well as his passion and enthusiasm in teaching during my undergraduate degree. You have contributed a great deal to my growing interest in, and knowledge of, chemistry, and for that I will be forever grateful.

To my secondary supervisor, Megan Grainger, thank you for your help and guidance throughout this journey. Thank you for being there to answer all my questions about ICP-MS and for being a great support and a second pair of eyes overlooking my results and calculations. Thank you for being a friendly and approachable face, and for your speedy replies and willingness to help me when I needed it.

I would also like to thank Jenny Stockdill for all her help around the lab, Danielle Blackwell for her help with running ICP-MS samples, and Helen Turner for her help with preparing samples for and using the SEM.

I thank AusIMM and Waikato Graduate Women for their financial support throughout my masters degree.

Thanks also goes to those who I had the pleasure of sharing the D-block lab space with. Particular thanks goes to Matthew, thank you for helping me get settled into the lab when I was feeling very much out of my depth, and thank you for all the support you've shown me since then, from answering all my silly questions and giving advice, to the chats which were sometimes a well-needed distraction. I would also like to thank Ryland and Graham for their help with cleaning up my XRD crystal structures.

A special thanks also goes to my friends and family who have been a great support during this time. Thank you to Mum, for always being there, I appreciate everything you do for me, thank you for being my biggest supporter – you're the best. To my friends, thank you for your friendship and support, I feel truly grateful to have such a great bunch around me. Particular thanks goes to Niamh, Chloe and Elikah, for our gaming sessions, our chats, and our little outings, which gave me a much-needed break from studying and writing.

Finally, I wish to thank Grannie Cáit. You taught me the value of a curious mind and inspired me to never stop learning. For that, I will be forever grateful.

Table of Contents

List of Figures

List of Tables

List of Abbreviations

REE	Rare Earth Element
HREE	Heavy Rare Earth Element
LREE	Light Rare Earth Element
IL	Ionic Liquid
SIL	Supported ionic liquid
SILP	Supported ionic liquid phase
PIM	Polymer Inclusion Membrane
$[(EH)_2NH_2]^+$	Bis(2-ethylhexyl) ammonium
$[(EH)_3NH]^+$	Tris)2-ethylhexyl) ammonium
$[hex_2POO]^-$	Di-n-hexyl phosphinate
$[oct_2POO]^-$	Di-n-octyl phosphinate
$[CamHPOO]^-$	Camphyl phosphinate
$[CamPhPOO]^-$	Camphyl phenyl phosphinate
D2EPHA	Di(2-ethylhexyl)phosphoric acid
P507	2-ethylhexyl phosphinic acid mono(2-ethylhexyl) ester
TBP	Tributyl phosphate
TRPO	Trialkylphosphine oxide
EDTA	Ethylenediaminetetraacetic acid
$CDCl_3$	Deuterated chloroform
HCl	Hydrochloric acid
NMR	Nuclear Magnetic Resonance Spectroscopy
ESI-MS	Electrospray Ionisation mass spectrometry
FTIR	Fourier Transform Infrared Spectroscopy
XRD	X-Ray Diffraction
ICP-MS	Inductively Coupled Plasma Mass Spectrometry
SEM	Scanning electron microscope
cm^{-1}	wavenumber
ν	frequency (IR, in cm^{-1})
s	singlet (NMR)
d	doublet (NMR)

q	quartet (NMR)
δ	Chemical shift (NMR)
ppm	parts per million
ppb	parts per billion
m/z	mass-to-charge ratio (ESI-MS)
Å	Angstrom
MHz	Megahertz

Chapter 1
Introduction

1.1 Rare Earth Elements

1.1.1 Introduction

The rare earth elements (REEs) describe the group of 17 elements within the lanthanide group, as well as scandium and ytterbium. [1] Across the lanthanide group, the gradual filling of the 4f orbitals are observed. These elements are often further split into the light rare earth elements (LREEs) and the heavy REEs (HREEs). These groups are typically defined by the electron configuration of the elements, with the LREEs including the elements with unpaired electrons, from lanthanum to gadolinium, and the HREEs describing those with paired electrons, elements terbium to lutetium. [1] Many of the REEs are essential in the manufacturing of much of our modern technology, and are present in smart phones, television screens, monitors and more. They are also important components in green energy technology such as solar panel cells, rechargeable batteries, and wind turbines. Some of the most common applications for the individual elements are given in Table 1.1.

A report from the US Department of Energy in 2011 reported the rare earths as critical elements for clean energy technology in the future, accounting for both their high supply risk, and their high importance in clean energy technology. [2] The European Commission has released similar reports, with their most recent published in 2020. Their report included the heavy rare earths and light rare earths in their list of critical raw materials. [3] It also predicted an increase in the demand for many REEs in the coming decades. For example, the demand for praseodymium, dysprosium, and neodymium was predicted to increase up to 3-, 4- and 12-fold respectively by 2050. [4] In 2015, the British Geological Society placed the rare earth elements at the top of their element risk list, considering factors such as production concentration, recycling rate, governance (production rates as well as amount in reserves). [5]

Table 1.1: Some of the common applications of individual rare earth elements[6]

Element	**Use**
Scandium (Sc)	High strength Al-Sc alloys, electron beam tubes
Yttrium (Y)	Capacitors, phosphors, lasers, superconductors
Lanthanum (La)	Glasses, ceramics, catalysts, phosphors, pigments
Cerium (Ce)	Polishing agent, additive to glass, phosphors, catalysts, UV filters
Praseodymium (Pr)	Pigment, ceramics, component in scintillator of medical CAT scans, used in electric vehicle motors and wind turbine generators
Neodymium (Nd)	Neodymium-iron-boron permanent magnets, CRT displays, pigment, Nd-based YAG lasers used in medical applications, lasers, IR filters
Promethium (Pm)	Beta radiation source, fluid cracking catalysts
Samarium (Sm)	Sm-Co permanent magnets, microwave filters
Europium (Eu)	Phosphors
Gadolinium (Gd)	Mixed with ETDA as contrast agent in patients for MRI scans, ceramics, glasses, crystal scintillators
Terbium (Tb)	Phosphors, fluorescent lamps
Dysprosium (Dy)	Component in NdFeB magnets used in EVs, phosphors, ceramics
Holmium (Ho)	Ceramics, lasers, nuclear industry
Erbium (Er)	Ceramics, dyes for glass, optical fibers, lasers, nuclear industry
Thulium (Tm)	Electron beam tubes, visualisation of images in medicine
Ytterbium (Yb)	Metallurgy, chemical industry
Lutetium (Lu)	Single crystal scintillators

China has long been the main producer of REEs, but both environmental and geopolitical factors have increased the need for greener and more sustainable methods of REE mining and recycling. The processes involved in the mining and extracting or REEs are notorious for their impact on the surrounding environment. For example, in Baotou, where a large amount of China's REEs are produced, extraction and separation processes have created large amounts of acidic and radioactive waste, containing hydrofluoric acid, sulfuric acid and sulfur oxides, as well as radioactive elements such as thorium.[7] Much of the difficulty faced in the recovery of rare earth elements is due to their natural abundances and chemical properties. While the rare earth elements are abundant within the earth's crust, they often occur together with other rare earths, and in low concentrations. Therefore, a lot of work is required to mine significant amounts of these elements, and even more work is required to separate individual elements due to the chemical and physical similarities of these elements. Furthermore, the abundance varies between elements, generally decreasing with increasing atomic number. The lanthanides also follow the Oddo-Harkins rule, which states that elements with even atomic numbers will be more abundant than those with odd atomic numbers. [8] Many REE applications require a single pure rare earth element, so the separation process is of high importance.

1.1.2 Chemistry of the REEs

Across the lanthanide series, the metallic and ionic radii of the elements generally decrease in size, with Eu and Yb being exceptions having larger metallic radii than the other lanthanide elements[9]. This is thought to be due to both electrostatic effects and relativistic effects. This phenomenon is known as the 'lanthanide contraction.' This similarity in size contributes to the challenge faced when separating individual REEs. [9]

For most of the lanthanide elements, the +3 oxidation state is the most stable, owing to the fourth ionisation energy which is higher than the sum of the first 3 ionisation energies[10]. However, for some elements the +2 and +4 oxidation states do exist, but these tend to be more common in their solid state. For example, Eu^{2+} and Yb^{2+} adopt their +2 oxidation state more easily due to the stability of a half-full or full set of f-orbitals. [9] Across the series of lanthanide elements, the ionic radii generally decrease with increasing atomic number, however neighbouring elements are sufficiently similar to make the separation of individual elements difficult.

The processes used in the separation of individual REEs exploit the small differences in properties between neighbouring elements. Initial separation methods often used fractional crystallisation which separated the REEs based on the differences in solubilities of salts. More recently, solvent extraction methods have been applied. These methods involve the use of a complexing agent which acts as the extractant in the organic phase, and which is loaded using a REE-containing aqueous phase. Separation using solvent extraction methods occur based on changes in stability across the lanthanides. With small changes to pH, different lanthanide (Ln^{3+}) ions are extracted. While this process does successfully produce high purity REEs, multiple extractions (up to 1500) are required to reach this purity. [9]

1.1.3 Rare Earth Recycling

With only a finite supply of REEs available on earth, and both the increasing demand for rare earths and environmental impact of their mining, many researchers and organisations are realising the need to develop effective and efficient methods for rare earth recycling from secondary materials. "Urban mining" of REEs describes the extraction of these elements from pre-consumer waste, and post-consumer waste from end-of-life products. [11] The recycling of these elements is often a challenge as they are used in small concentrations, and separation often requires multiple steps. [11] Having said that, there are methods being developed and used for the recycling of REEs, including the use of both hydrometallurgical and pyrometallurgical methods to reuse the REEs found in NdFeB magnets, phosphors, and Ni-MH batteries. [12]

Some industrial and commercial companies have taken steps to recycle REEs used in their products. In 2012, Honda decided to work with Japan Metals & Chemicals (JMC) to extract and recycle rare earths found in their nickel metal hydride batteries used in hybrid and electric vehicles. [13] Rhodia (now owned by Solvay) joined Umicore to help recycle the REEs in Ni-MH batteries. [14] With efforts to recycle their iPhones, Apple is also working to recycle and reuse the REEs found in their phones. In a 2020 report, they reported that their iPhone 12 was made using 98% recycled REEs. [15]

1.1.4 Organophosphorus acid extractants

Organophosphorus compounds have been used as extractants since the 1950s, with one of the common applications being a solvent extraction method using di(2-ethylhexyl) phosphoric acid (D2EHPA) (Figure 1.1) and tri-n-octylphosphine oxide (TOPO) for the separation of uranium from sulphuric acid. [16] Diluted in kerosene, DEHPA has also been applied to lanthanide separation solvent extraction methods capable of high extraction efficiencies and able to tune the selectivity towards certain REEs by altering the pH. [9]

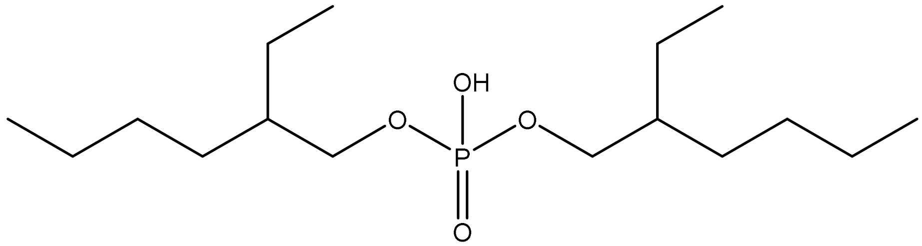

Figure 1.1: Structure of di(2-ethylhexyl) phosphoric acid (DEHPA)

In the time since, many similar extractants have been created and considered for the separations of many compounds and elements. The types of acid extractants include a range of phosphoric acids, phosphonic acids and phosphinic acids (Figure 1.2), as well as a few thiophosphinic acids. For the separations of interest in this work, phosphinic acids appear to be superior for extractions. For example, for the separation of cobalt and nickel, to which extractants similar to those used for REE separation are applied, there is a general trend showing that phosphinic acids achieve better separations than phosphonic and phosphoric acids. [17]

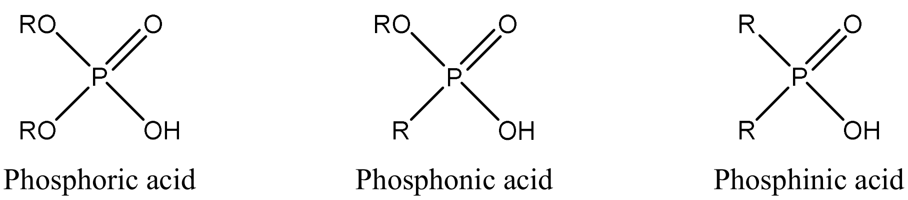

Figure 1.2: Common organophosphorus acid extractants

Cytec (acquired by Solvay in 2015) produces a range of organophosphorus acid extractants, including alkyl phosphinic acid, bis(2,4,4-trimethylpentyl)phosphinic acid (Cyanex 272), and its thio analogues, Cyanex 301 and 302 (Figure 1.3). Cyanex 272 was designed for cobalt/nickel separation from weakly acidic sulfate liquors and Solvent extraction methods using this extractant became widely used for cobalt/nickel extractions.

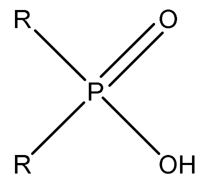

Cyanex272

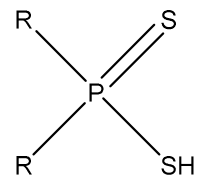

Cyanex301

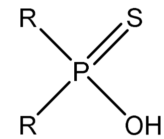

Cyanex302

R = 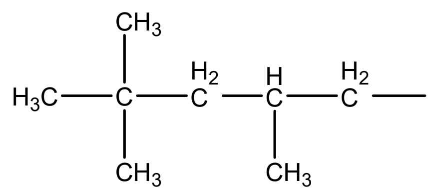

Figure 1.3: Structure of Cyanex272, 301, and 302

For the separation of the REEs, acid extractants, including some of those mentioned above, have been used. For example, in the Mountain Pass mine in California, DEHPA was used as an extractant in kerosene, with selectivity altered through changes to pH. [18] For the same purpose, organophosphorus acids have been used as rare earth extractants by Thorium Ltd, Megon Company and Denison Mines. Other common organophosphorus extractants include 2-ethylhexyl phosphinic acid mono(2-ethylhexyl) ester (P507) and tributyl phosphate (TBP) whose structures are given in Figure 1.4 and Figure 1.5 respectively. [19] These extractants have successfully been applied for the separation of most of the rare earth elements.

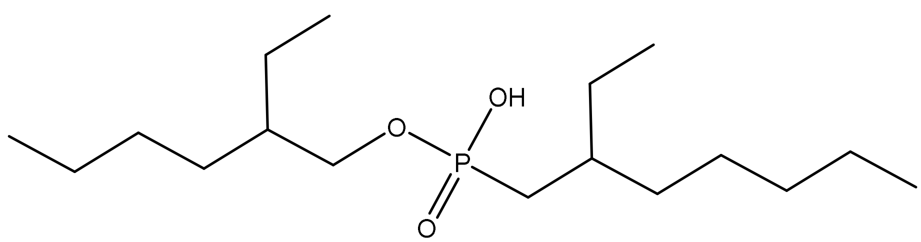

Figure 1.4: Structure of P507

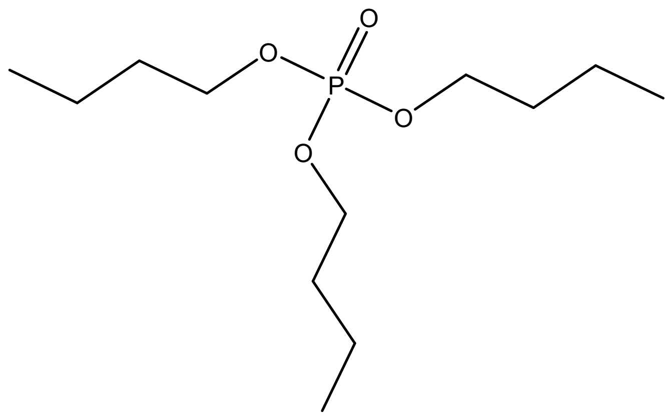

Figure 1.5: Structure of TBP

P507 has become a widely utilised extractant across China, achieving up to 99.99% purity of individual rare earth elements. [20] While the method using P507 still proves difficult when stripping heavy REEs, it is currently considered to be one of the best methods for rare earth separations.

1.2 Ionic liquids (ILs)

Ionic liquids are defined as salts which are liquids and refer to salts with low melting points (below 100 °C). [21] Due to their unique properties, they have been considered as green alternatives to commonly used volatile organic solvents. Some of these properties include their low volatility, low flammability, negligible vapour pressure, and their ease of recyclability. It should be noted that properties are not universal across all ionic liquids, varying based on the properties of the cation and anion used, and the way these interact with each other. [22] These alterable properties have also led to ILs being described as ‘designer solvents’ as properties such as solubility, melting point, and viscosity, can be altered through changes to, and functionalisation of, the anion and cation. [21] The addition of various functional groups to the ions allows ILs to be designed and optimised for specific tasks and applications, including their use as solvents in separations, [23, 24] catalysts, [25] electrolytes in batteries, [26] and corrosion inhibitors[27-29].

Walden was the first to describe room temperature ionic liquids in 1914, with his discovery of ethylammonium nitrate (Figure 1.6), found to have a melting point of 13-14 °C. [30] Further research on ILs was slow in the following decades. In 1948, a patent for ionic liquids made from aluminium chloride and ethylpyridinium halides was processed, and later reported for their use as electrolytes. [31]

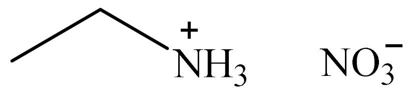

Figure 1.6: Ethylammonium nitrate

One of the main drawbacks of these early ILs was their low stability in water and air. However, following the work of Wilkes and Zaworotko in 1992, who reported their discovery of a series of ionic liquids which were both air and water stable, interest in ILs was piqued. Wilkes and Zaworotko created ILs using 1-ethyl-3-methylimidazolium cations with a variety of anions (**Figure 1.7**).[30]

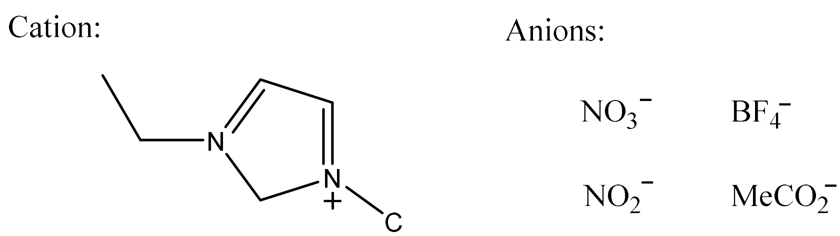

Figure 1.7: 1-ethyl-3-methylimidazolium cation and range of anions used by Wilkes and Zaworotko.

Since the discovery of water- and air- stable ionic liquids, the amount of research and literature involving ILs has increased tremendously, with many books and reviews written about these interesting liquids.[21, 32, 33] Reviews include general overviews on ionic liquids, their properties and structure,[34] as well as reviews on their applications as catalysts,[35] and separation media.[36] Reviews also cover the biological activity of ILs[37], and their use in energy technologies[38], and the pharmaceutical industry.[39]

1.2.1 Preparation of Ionic Liquids

ILs can be prepared using a variety of methods and ions. Some of the most commonly used ions for creating ILs are shown in Figure 1.8. The main methods used to prepare ILs include anion exchange and quaternisation reaction methods. Quaternisation reactions typically involve the conversion of a tertiary amine or phosphine to a quaternary ammonium or phosphonium salt.[33] This can occur by protonation whereby a proton is gained by the tertiary amine or phosphine as shown in *Equation 1.1*.

$$NR_3 + R'_2PO_2H \longrightarrow [NR_3H][R'_2PO_2]$$

R, R' = alkyl groups

Equation 1.1: Protonation of tertiary amine and phosphinic acid to form IL

The conversion can also occur through alkylation where an alkyl group is added to the tertiary compound. This route typically involves the reaction of the tertiary phosphine or amine with an alkyl halide. An example of this route is shown in *Equation 1.2*.

$$PR_3 + R'X \longrightarrow [NR_3R'][X]$$

X = F, Cl, Br, I

R, R' = alkyl group

Equation 1.2: Alkylation of tertiary phosphine and alkyl halide to form IL

While routes involving halide salts offer some advantages, there is also a desire for halide-free routes as halides can often contaminate the final IL and affect the application of the IL. Some halide-free routes used to create ILs include anion exchange methods, such as anion metathesis and neutralisation reactions. These methods essentially involve the exchange of anions from two starting materials to create a new ionic liquid. Neutralisation reactions of this kind occur between an acid and a base. An example of this reaction using a phosphinic acid and an ammonium hydroxide is shown in *Equation 1.3*. These reactions tend to result in the formation of water as a by-product which can be removed by vacuum.

$$R_2PO_2H + \ R'_4NOH \longrightarrow [R'_4N][R_2PO_2] + H_2O$$

R, R' = alkyl

Equation 1.3: Neutralisation reaction of phosphinic acid and quaternary ammonium hydroxide to form IL.

Finally, anion metathesis reactions occur through the exchange of ions between a quaternary salt and an alkali metal salt. An example of an anion metathesis route to create IL is shown in *Equation 1.4*.

$$[PR_4][X] + MZ \longrightarrow [PR_4][Z] + MX$$

Where R = alkyl

M = alkali metal

Z = anion

Equation 1.4: Anion metathesis route used to form IL

The properties of the anion and cation have significant effects on the properties of the final ionic liquid and when selecting ions to include in novel ionic liquids, a range of considerations can be made. For example, ions with molecular asymmetry, delocalised charge, or large side chains may be selected to achieve a liquid salt with a low melting point. [40] The combination of different sized ions can also aid in producing a liquid. [40]

Hydrophilicity of an IL is often determined by the anion used, relying largely on the number and length of alkyl side chains present, as well as the hydrogen bonding ability of the anion[41]. The viscosities and melting points of ILs can be altered by changing the molecular weights of the ions, with an increase in molecular weight often resulting in an increase in viscosity and a decrease in melting point temperature. [42] This increase is viscosity is often attributed to an increased strength of intermolecular forces present in longer chains. [43] In many cases, low viscosities are desired, so ions are selected to ensure the melting point remains low as well. A low melting point IL can be achieved by using ions with low symmetry as well those with poor packing efficiency. [43] Unsymmetrical ions can limit the crystallinity of the IL, thus also lowering the melting point. [42] However, there are also other factors which influence the melting point, for example, delocalised charges in ions can help reduce electrostatic interactions, thus lowering the melting point. This is observed with common imidazolium and pyridinium cations. In the early ILs, the use of a large organic cation was a large factor in the low melting point of ILs through reduced ion association between ions. [30]

Cations

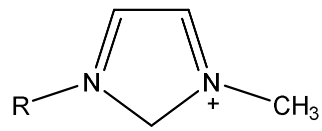

1-alkyl-3-methylimidazolium

(C_n-mim$^+$)

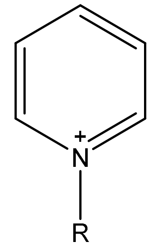

1-alkylpyridinium

(C_n-Py$^+$)

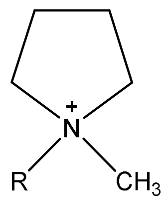

1-alkyl-1-methylpyrrolidinium

(C_nC_1Pyrr$^+$)

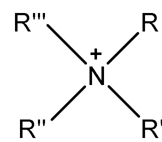

Tetraalkylammonium

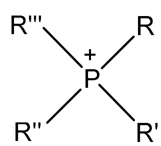

Tetraalkylphosphonium

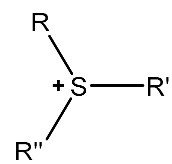

Trialkylsulfonium

Anions

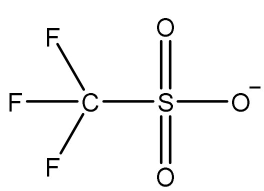

Trifluoromethylsulfonate

(TfO$^-$)

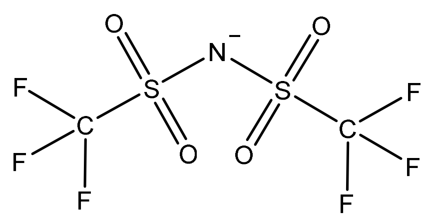

Bis(trifluoromethylsulfonyl)imide

(NTf_2^-)

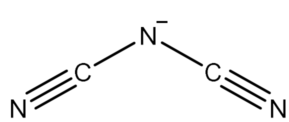

Dicyanamide

(DCA$^-$)

Cl^-, Br^-, I^-, BF_4^-, PF_6^-, PO_4^{3-},

$CH_3CO_2^-$

Figure 1.8: Structures of some of the most common anions and cations found in ILs

1.2.2 Phosphorus-containing Ionic Liquids

Early research on ILs largely focused on nitrogen based ILs, namely those consisting of imidazolium and pyrrolidinium cations. Research on phosphonium-based ionic liquids was initially slow, likely owing to the high cost and air-sensitivity of the common trialkylphosphine starting materials. [44] Phosphonium ILs are typically made using a tertiary alkyl phosphine with a halo-alkane, or active esters to produce a quaternary phosphonium salt. [45]

Compared to ammonium based ILs, phosphonium ionic liquids can offer some advantages depending on the desired purpose or application. For example, phosphonium ionic liquids tend to be more thermally stable than ammonium and imidazolium based alternatives, although they also commonly have higher viscosities compared to ammonium ILs. [46] The larger thermal stability can be advantageous when recycling phosphonium ionic liquids, as the presence of decomposition products is less likely to be observed. Furthermore, the higher thermal stability can make phosphonium ILs more suitable for processes which occur at higher temperatures. Phosphonium ILs also lack the acidic proton present in many imidazolium based ILs. The presence of this acidic proton can be a disadvantage to imidazolium-based ILs in basic conditions, as the cation becomes deprotonated, forming a carbene which is stabilised by the two neighbouring nitrogen atoms. [47] Because of this, phosphonium-based ILs tend to perform better in basic conditions. [48]

With increasing interest in phosphonium IL came the increase in commercial availability of a selection of these types of ILs. For example, Cytec Industries, who have long manufactured a range of phosphines and their derivatives, supply a wide variety of quaternary phosphonium-based ionic liquids. [46] Many of these ILs have been applied to separations of a variety of compounds and elements, including the heavy metals and rare earth elements. For example, Cyphos IL 101 has been able to separate cobalt from nickel, [49] as well as cobalt and lithium from spent Li-batteries, [50] while Cyphos IL 104 has been used for rare earth separation. [51-53]

1.2.3 Ionic liquid Applications for Separations and Extractions

One of the major applications which ionic liquids have been considered for is in separation methods. Solvent extraction is a common method used for the separation of metals from solution. This method typically makes use of organic solvents for separations, but there are numerous reports showing the success of ionic liquids used for the separation a variety of metal separations. In some solvent extraction methods, the IL acts as both the extractant and the solvent, whereas in others an extractant is added to the IL phase to improve separations. In cases where the IL is the extractant, an organic solvent is often required to dilute a viscous IL to improve the mixing of the liquid phases.

Thanks to their designability, ILs have shown their potential in separation methods for a vast range of elements and compounds. For example, phosphonium ionic liquids have been used for the separation of many elements and compounds, including cobalt and nickel[54], the lanthanide elements[51], and sulfur from fuels[55]. Separation methods using ILs have also been considered for the platinum group metals[56], organic compounds such as acetylsalicylic acid[57] and insecticides[58], and gas separations, such as carbon dioxide from nitrogen or methane. [59]

1.2.4 Supported Ionic Liquids (SILs)

While liquid-liquid extraction is one of the most commonly used methods for metal separations with ILs, it comes with some disadvantages such as the need for a high volume of IL, the leaching of ILs into the aqueous phase, the often high viscosity of ILs which limits mixing of phases, and the limited extraction efficiency of trace metals. [60] The immobilisation of ionic liquids through the addition of solid supports can be beneficial to overcoming some of these drawbacks, particularly in catalysis and separation methods. The immobilisation of ILs onto a support has been found to stabilise the IL, making it less prone to leaching, while maintaining the advantageous properties of the neat IL. In some cases, metal separation is improved using SILs as they can accelerate the transport rate, and shorten the diffusion distance. [61] Examples of supported ionic liquids for metal separations has been discussed in many review articles. [61-63]

IL immobilisation occurs by depositing a thin film of the ionic liquid on the chosen support, commonly achieved by either chemisorption or physisorption. Chemisorption is used to covalently bond the IL to the support, whereas physisorption uses physical methods such as stirring, impregnation, or the sol-gel method. [64] Chemisorption methods are typically carried out by reacting a functionalised support with an IL which has a functional group such as trimethylsilyl-, thiol-, or ether-.[65] The reaction will result in the formation of covalent bonds between the support and the ionic liquid which offers some advantages over physisorption methods, such being less prone to leaching. [66] In their review on covalently supported ionic liquids, Xin and Hao describe some of the methods employed for making these SILs, as well as their applications. [65] For physisorption, where the IL often simply coats the chosen support, stirring methods are often used, whereby the IL is simply mixed with the support and a low boiling point solvent. The solvent is removed, leaving behind the SIL. [67]

A range of supports have been successfully utilised, including polymer supports, silica supports, membranes and metal organic frameworks. For example, for the separation of indium from iron-rich goethite residues, van Roosendael et al. [68] created a SIL through impregnation of Amberlite XAD-16N polymer support with IL Aliquat 336 iodide, [A336][I]. The SIL was easily prepared by shaking the support and the IL dissolved in acetone for 24 hours and high selectivity towards indium was achieved.

Polymer inclusion membranes (PIMs) are popular supports for making SILs. Separations utilising these are typically set up with a feed phase and a receiving phase, with a membrane between the two phases. For example, Regel-Rosocka et al. [69] tested a PIM with Cyphos IL 101 and Cyphos IL 104 as ion carriers for the separation of zinc(II) and iron. The cellulose triacetate polymer membrane was set up with a continuous flow of the feed and receiving phase through the PIM and achieved zinc(II) extraction efficiencies as high as 99.9 % using 0.8 M Cyphos IL 101.

Chromatographic methods have also been applied under the scope of supported ionic liquids. In these methods, the ionic liquid coats an inert, porous support such as silica, alumina, or porous polymers. These methods offer similar advantages to other SILs discussed. However, they also come with some disadvantages. For example, column chromatographic extraction methods are commonly associated with lower metal ion retention which causes difficulties with large sample volumes. [70] This can be fixed with the use of larger columns, however this results in longer extraction times, larger volumes of extractant and higher costs. Another drawback of many chromatographic extractions is the stability of the column and the reusability of the column. As the SILs in the column are typically made through physisorption methods, the SIL is at risk of deteriorating over the course of multiple extractions as the extractant is not bonded chemically to the chosen support. [70] Despite these disadvantages, there are still promising methods being reported and published for the separation of a range of elements and compounds.

In an example of a chromatographic column separation, Avdibegovic and Binnemans used a supported ionic liquid phase, betainium sulfonyl(tri-fluoromethanesulfonylimide) poly(styrene-co-divinylbenzene) for the separation of REEs from spent NdFeB and SmCo magnets. [71] With this SILP, they reached recoveries of 82% and 90% for neodymium and samarium respectively. They also reported high selectivity towards the trivalent REEs over the divalent iron and cobalt also present in the magnet leachate, however there was no report on the stability and reusability of the column in this method. In another example, by the same authors using the same supported ionic liquid phase, a column chromatography separation method was tested to separate the REEs from bauxite residue. Results showed the SILP preferentially removed the REEs over other elements present in the residue, with fast adsorption and good reusability of the column. [72]

1.2.5 Ionic Liquids for Rare Earth Recovery

The separation of REEs using ILs has been described and tested using a range of ionic liquids, and new ionic liquids and separation methods are often reported. For example, in 2021, Dashti et al. described the separation of light, medium and heavy REEs from a chloride medium using a phosphonium IL made from Cyanex 572 and TBP. [73] They were able to separate the heavy REE, erbium, from the lighter praseodymium and neodymium elements with separation factors of 30.08 and 29.95 respectively.

In another method, Zhang et al. discussed their findings with their novel carboxylic acid functionalised phosphonium based ionic liquid (Figure 1.9).[74] The undiluted hydrophobic acidic extractant showed good extraction and selectivity towards scandium(III) in a mixture of six different REEs, as well as good selectivity towards the rare earth elements over the first row transition metals. Their method showed changing selectivity when the pH was altered, with selectivity for scandium(III) increasing with acidity.

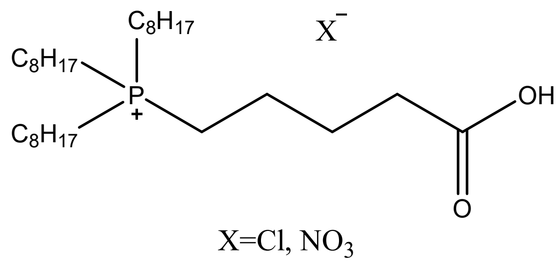

Figure 1.9: Structure of carboxylic acid functionalised ILs used by Zhang et al. for REE separations

Due to the successes of P507 in rare earth separation, many studies have considered it as an ion precursor in ILs to explore possible improvements to separations which ILs may offer. For example, Shen et al., used the IL [A336][P507] (Figure 1.10) with a sulfuric acid medium for the separation of the mid-heavy REEs from solution. This method demonstrated the stability of the ionic liquid, with little change to the extraction efficiencies of Eu(III) over five cycles. With changes to the pH, extractant concentration, and salting out agent, extraction efficiencies over 90% were achieved for HREEs, Tm(III) and Lu(III). [75]

Using the same IL, Chen et al. prepared a polymer inclusion membrane (PIM) with the ionic liquid as the extractant for the extraction of the heavy REE, lutetium. [76] This method also showed promising results, with good stability and reusability of the column over 10 cycles.

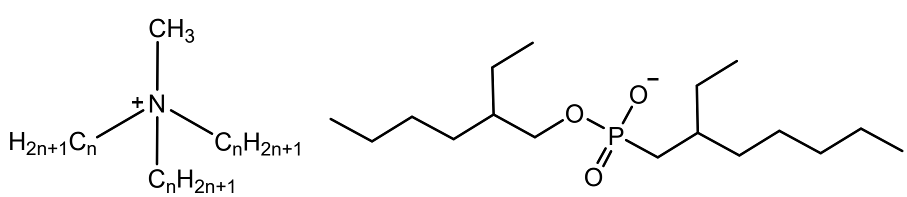

Figure 1.10: Structure of IL [A336][P507]

Xu et al. also utilised the extractant P507 to explore the abilities of a similar ionic liquid, [N1888][P507] for the separation of the heavy rare earths (Figure 1.11). This IL was reported to have good extractabilities of the HREEs, however the addition of trialkylphosphine oxide (TRPO) extractant was shown to improve extractions. [77] Using this mixture of IL and TRPO, extraction efficiencies for Yb and Lu reached 99% with the system showing selectivity towards the heavy REEs.

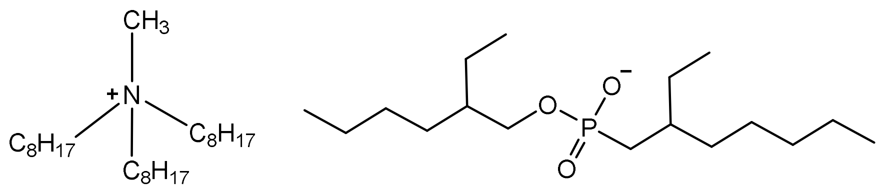

Figure 1.11: Structure of IL [N1888][P507]

Other phosphonium ionic liquids have also been tested for rare earth recovery. For example, with the addition of a silica support, Mohamed et al. [78] explored the ability of commercially available Cyphos-104 for the separation of neodymium(III) and gadolinium(III) from aqueous solution. The IL impregnated silica was shown to have increased sorption ability compared to silica alone. In fact, the sorption of Nd and Gd increased from 18% and 20% without impregnation to 67% and 89.45% with impregnation respectively. The ions were also successfully stripped using nitric acid, and the impregnated silica was regenerated and reused for further separations.

In another method, Dupont et al. explored the use of nitrogen-based IL [Hbet][TF_2N] (bentainium bis(trifluoromethylsulfonyl)imide) for the recycling of of $Y_2O_3:Eu^{3+}$ (YOX) from recycled phosphor waste. [79] The chosen IL (Figure 1.12) was shown to have high selectivity towards the YOX phosphor under mild conditions, and able to separate it from other phosphors present.

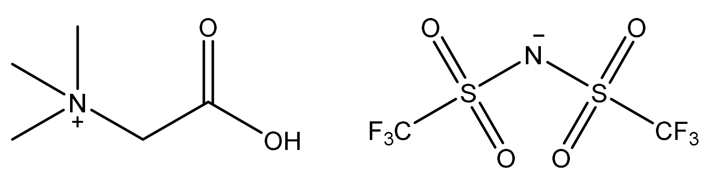

Figure 1.12: Structure of IL [Hbet][TF_2N]

For the recycling of important metal oxides from NdFeB permanent magnets, the ionic liquid liquid trihexyl(tetradecyl)phosphonium nitrate was applied for the separation of cobalt from an aqueous nitrate solution. Subsequent separations of REEs Nd and Dy were carried out with complexing agent ethylenediaminetetraacetic acid (EDTA) was used for liquid-liquid extractions. High purities of Nd, Dy and Co oxides were successfully obtained. [80]

1.3 Aims of Research

The application of ILs for REE separation has become a topic of interest for many researchers in the field, with many publications documenting various experiments and testing a wide range of ILs for this purpose. However, due to the difficulties faced in REE separations, there is still an ongoing desire to find improvements to separation methods, including improvements to extraction efficiencies and selectivity.

Considering the ongoing effort to find better methods for rare earth separation, the aim of this work was to prepare a series of ionic liquids and consider their application as green rare earth extractants. These ILs were created using phosphinic acids as starting materials, similar to those organosphosphorus acid extractants used in industrial REE separations. Synthesis of phosphinic acid starting materials is also attempted, including synthesis of those which are derived from camphene, a monoterpene which can be obtained from a renewable feedstock. The ionic liquids were also used to create supported ionic liquids, through the use of inexpensive, inert and robust glass beads. The SILs were used to create a column separation method for the REEs.

1.4 References

[1] Voncken, J. H. L., The rare earth elements: A special group of metals. In *The Rare Earth Elements: An Introduction*, Voncken, J. H. L., Ed. Springer: 2016.

[2] *Critical materials strategy*; U.S. Department of Energy: 2011.

[3] Commission, E. *Study on the EU's list of critical raw materials - final report*; European Commission: 2020.

[4] *Critical materials for strategic technologies and sectors in the EU - a foresight study,*; European Commission: 2020.

[5] *Risk list 2015*; British Geological Society: 2015.

[6] Gupta, C. K.; Krishnamurthy, N., *Extractive metallurgy of rare earths*. Second edition. ed.; Taylor & Francis, CRC Press: Boca Raton, FL, 2016.

[7] Huang, X. W.; Long, Z. Q.; Wang, L. S.; Feng, Z. Y., Technology development for rare earth cleaner hydrometallurgy in China. *Rare Metals* **2015,** *34* (4), 215-222.

[8] Migaszewski, Z. M.; Gałuszka, A., The characteristics, occurrence, and geochemical behavior of rare earth elements in the environment: A review. *Critical Reviews in Environmental Science and Technology* **2015,** *45* (5), 429-471.

[9] Aspinall, H. C., *Chemistry of the f-block elements*. Gordon and Breach Science Publishers: 2001.

[10] Kaltsoyannis, N.; Scott, P., *The f elements*. Oxford Science Publications: 1999.

[11] Dutta, T.; Kim, K. H.; Uchimiya, M.; Kwon, E. E.; Jeon, B. H.; Deep, A.; Yun, S. T., Global demand for rare earth resources and strategies for green mining. *Environmental Research* **2016,** *150*, 182-190.

[12] Omodara, L.; Pitkäaho, S.; Turpeinen, E. M.; Saavalainen, P.; Oravisjärvi, K.; Keiski, R. L., Recycling and substitution of light rare earth elements, cerium, lanthanum, neodymium, and praseodymium from end-of-life applications: A review. *Journal of Cleaner Production* **2019,** *236*, 117573.

[13] Honda motors, Japan metals & chemicals establish rare earth metals recycling project. https://www.recyclingtoday.com/article/honda-japan-metals-hybrid-metals-recycling-rare-earth/ (accessed 12/11/2021).

[14] Umicore. Battery recycling. https://csm.umicore.com/en/battery-recycling/our-recycling-process/ (accessed 21/01/2021).

[15] *Product environment report: iPhone 12*; Apple Inc.: 2020.

[16] Beltrami, D.; Cote, G.; Mokhtari, H.; Courtaud, B.; Moyer, B. A.; Chagnes, A., Recovery of uranium from wet phosphoric acid by solvent extraction processes. *Chemical Reviews* **2014,** *114* (24), 12002-12023.

[17] Flett, D. S., Solvent extraction in hydrometallurgy: The role of organophosphorus extractants. *Journal of Organometallic Chemistry* **2005,** *690* (10), 2426-2438.

[18] Nicol, M.; Fleming, C. A.; Preston, J. S., Application to extractive metallurgy. *Comprehensive Coordination Chemistry* **1987,** *6*, 779-842.

[19] Mwewa, B.; Tadie, M.; Ndlovu, S.; Simate, G. S.; Matinde, E., Recovery of rare earth elements from acid mine drainage: A review of the extraction methods. *Journal of Environmental Chemical Engineering* **2022**, 107704.

[20] Li, D., Development course of separating rare earths with acid phosphorus extractants: A critical review. *Journal of Rare Earths* **2019,** *37* (5), 468-486.

[21] Freemantle, M., *An introduction to ionic liquids*. The Royal Society of Chemistry: UK, 2010.

[22] Lei, Z.; Chen, B.; Koo, Y.-M.; MacFarlane, D. R., Introduction: Ionic liquids. ACS Publications: 2017; Vol. 117, pp 6633-6635.

[23] Huang, Y.; Zhang, Y.; Xing, H., Separation of light hydrocarbons with ionic liquids: A review. *Chinese Journal of Chemical Engineering* **2019,** *27* (6), 1374-1382.

[24] Lee, S. G., Functionalized imidazolium salts for task-specific ionic liquids and their applications. *Chemical Communications* **2006,** (10), 1049-1063.
[25] Zhang, Q.; Zhang, S.; Deng, Y., Recent advances in ionic liquid catalysis. *Green Chemistry* **2011,** *13* (10), 2619-2637.
[26] Lewandowski, A.; Świderska-Mocek, A., Ionic liquids as electrolytes for Li-ion batteries: An overview of electrochemical studies. *Journal of Power Sources* **2009,** *194* (2), 601-609.
[27] Cao, S.; Liu, D.; Ding, H.; Wang, J.; Lu, H.; Gui, J., Task-specific ionic liquids as corrosion inhibitors on carbon steel in 0.5 M HCl solution: An experimental and theoretical study. *Corrosion Science* **2019,** *153*, 301-313.
[28] Cao, S.; Liu, D.; Zhang, P.; Yang, L.; Yang, P.; Lu, H.; Gui, J., Green brönsted acid ionic liquids as novel corrosion inhibitors for carbon steel in acidic medium. *Scientific Reports* **2017,** *7* (1), 8773-8773.
[29] Ortega Vega, M. R.; Mattedi, S.; Schroeder, R. M.; Fraga Malfatti, C., 2 ‐ hydroxyethylammonium oleate protic ionic liquid as corrosion inhibitor for aluminum in neutral medium. *Materials and Corrosion* **2021,** *72* (3), 543-556.
[30] MacFarlane, D. R.; Kar, M.; Pringle, J. M.; MacFarlane, D. R., *Fundamentals of ionic liquids : From chemistry to applications*. John Wiley & Sons, Incorporated: Newark, Germany, 2017.
[31] Freemantle, M., Chapter 2:. In *An introduction to ionic liquids*, The Royal Society of Chemistry: UK, 2010.
[32] Plechkova, N. V.; Seddon, K. R., *Ionic liquids completely uncoiled : Critical expert overviews*. John Wiley & Sons, Incorporated: Hoboken, New Jersey, 2015.
[33] MacFarlane, D.; Kar, M.; Pringle, J. M., *Fundamentals of ionic liquids : From chemistry to applications*. Wiley-VCH: Weinheim, Germany, 2017.
[34] Kianfar, E.; Mafi, S., Ionic liquids: Properties, application, and synthesis. *Fine Chemical Engineering* **2021**, 22-31.
[35] Welton, T., Ionic liquids in catalysis. *Coordination chemistry reviews* **2004,** *248* (21-24), 2459-2477.
[36] Han, X.; Armstrong, D. W., Ionic liquids in separations. *Accounts of Chemical Research* **2007,** *40* (11), 1079-1086.
[37] Egorova, K. S.; Gordeev, E. G.; Ananikov, V. P., Biological activity of ionic liquids and their application in pharmaceutics and medicine. *Chemical Reviews* **2017,** *117* (10), 7132-7189.
[38] Macfarlane, D. R.; Tachikawa, N.; Forsyth, M.; Pringle, J. M.; Howlett, P. C.; Elliott, G. D.; Davis, J. H.; Watanabe, M.; Simon, P.; Angell, C. A., Energy applications of ionic liquids. *Energy and Environmental Science* **2014,** *7* (1), 232-250.
[39] Kemp, T. J., Ionic liquids: Pharmaceutical potential. *Science Progress* **2012,** *95* (2), 224-230.
[40] Castner Jr, E. W.; Wishart, J. F., Spotlight on ionic liquids. *The Journal of Chemical Physics* **2010,** *132* (12), 120901.
[41] Zhou, T.; Chen, L.; Ye, Y.; Chen, L.; Qi, Z.; Freund, H. r.; Sundmacher, K., An overview of mutual solubility of ionic liquids and water predicted by COSMO-RS. *Industrial & Engineering Chemistry Research* **2012,** *51* (17), 6256-6264.
[42] Curnow, O. J., Ionic liquids: Some of their remarkable properties and some of their applications. *Chemistry in New Zealand* **2012,** *76*, 118-122.
[43] Zhao, H., Current studies on some physical properties of ionic liquids. *Physics and Chemistry of Liquids* **2003,** *41* (6), 545-557.
[44] Blundell, R. K.; Licence, P., Quaternary ammonium and phosphonium based ionic liquids: A comparison of common anions. *Physical Chemistry Chemical Physics* **2014,** *16* (29), 15278-15288.

[45] Chang, T., Robertson, A., Kamenetzky, E., Rivera, C., Du, L., Harris, D., Piquette, M., Nucciarone, D., Crutchfield, C., Characterization of phosphonium ionic liquids with emphasis on mass spectrometry and chromatography. In *Ionic liquids IV: Not just solvents anymore*, Brennecke, J.; Rogers, R. D.; Seddon, K. R., Eds. American Chemical Society: 2007; Vol. IV.
[46] Bradaric, C. J.; Downard, A.; Kennedy, C.; Robertson, A. J.; Zhou, Y., Industrial preparation of phosphonium ionic liquids. *Green Chemistry* **2003,** *5* (2), 143-152.
[47] Chowdhury, S.; Mohan, R. S.; Scott, J. L., Reactivity of ionic liquids. *Tetrahedron* **2007,** *63* (11), 2363-2389.
[48] Fraser, K. J.; MacFarlane, D. R., Phosphonium-based ionic liquids: An overview. *Australian Journal of Chemistry* **2009,** *62* (4), 309-321.
[49] Wellens, S.; Goovaerts, R.; Möller, C.; Luyten, J.; Thijs, B.; Binnemans, K., A continuous ionic liquid extraction process for the separation of cobalt from nickel. *Green Chemistry* **2013,** *15* (11), 3160-3164.
[50] Xu, L.; Chen, C.; Fu, M. L., Separation of cobalt and lithium from spent lithium-ion battery leach liquors by ionic liquid extraction using Cyphos IL-101. *Hydrometallurgy* **2020,** *197*, 105439.
[51] Kumari, A.; Sinha, M. K.; Sahu, S. K.; Pandey, B. D., Solvent extraction and separation of trivalent lanthanides using Cyphos IL 104, a novel phosphonium ionic liquid as extractant. *Solvent Extraction and Ion Exchange* **2016,** *34* (5), 469-484.
[52] Ma, L.; Zhao, Z.; Dong, Y.; Sun, X., A synergistic extraction strategy by [N1888][SOPAA] and Cyphos IL 104 for heavy rare earth elements separation. *Separation and Purification Technology* **2017,** *174*, 474-481.
[53] Wang, Y.; Chen, L.; Yan, Y.; Chen, J.; Dai, J.; Dai, X., Separation of adjacent heavy rare earth lutetium(III) and ytterbium(III) by task-specific ionic liquid Cyphos IL 104 embedded polymer inclusion membrane. *Journal of Membrane Science* **2020,** *610*, 118263.
[54] Jing, X.; Wu, Z.; Zhao, D.; Li, S.; Kong, F.; Chu, Y., Environmentally friendly extraction and recovery of cobalt from simulated solution of spent ternary lithium batteries using the novel ionic liquids of [$C_8H_{17}NH_2$][Cyanex272]. *ACS Sustainable Chemistry & Engineering* **2021,** *9* (6), 2475-2485.
[55] Moghadam, F. R.; Azizian, S.; Bayat, M.; Yarie, M.; Kianpour, E.; Zolfigol, M. A., Extractive desulfurization of liquid fuel by using a green, neutral and task specific phosphonium ionic liquid with glyceryl moiety: A joint experimental and computational study. *Fuel* **2017,** *208*, 214-222.
[56] Lanaridi, O.; Sahoo, A. R.; Limbeck, A.; Naghdi, S.; Eder, D.; Eitenberger, E.; Csendes, Z.; Schnürch, M.; Bica-Schröder, K., Toward the recovery of platinum group metals from a spent automotive catalyst with supported ionic liquid phases. *ACS Sustainable Chemistry & Engineering* **2020,** *9* (1), 375-386.
[57] Bernardo, S. C.; Araújo, B. R.; Sousa, A. C.; Barros, R. A.; Cristovão, A. C.; Neves, M. C.; Freire, M. G., Supported ionic liquids for the efficient removal of acetylsalicylic acid from aqueous solutions. *European Journal of Inorganic Chemistry* **2020,** *2020* (24), 2380-2389.
[58] Francisco, R.; Almeida, C.; Sousa, A. C.; Neves, M. C.; Freire, M. G., High performance of ionic-liquid-based materials to remove insecticides. *International Journal of Molecular Sciences* **2022,** *23* (6), 2989.
[59] Scovazzo, P.; Kieft, J.; Finan, D. A.; Koval, C.; DuBois, D.; Noble, R., Gas separations using non-hexafluorophosphate $[PF_6]^-$ anion supported ionic liquid membranes. *Journal of Membrane Science* **2004,** *238* (1), 57-63.
[60] Lupa, L.; Negrea, P.; Popa, A., Use of ionic liquids in solid-liquid separation processes. In *Progress and developments in ionic liquids*, IntechOpen: 2017.

[61] Zhu, L.; Guo, L.; Zhang, Z.; Chen, J.; Zhang, S., The preparation of supported ionic liquids (SILs) and their application in rare metals separation. *Science China Chemistry* **2012,** *55* (8), 1479-1487.

[62] Imdad, S.; Dohare, R. K., A critical review on heavy metals removal using ionic liquid membranes from the industrial wastewater. *Chemical Engineering and Processing-Process Intensification* **2022**, 108812.

[63] Zante, G.; Boltoeva, M.; Masmoudi, A.; Barillon, R.; Trébouet, D., Supported ionic liquid and polymer inclusion membranes for metal separation. *Separation & Purification Reviews* **2021**, 1-17.

[64] Meijiboom, R., Haumann, M., Muller, T. E., Szesni, N., Synthetic methodologies for supported ionic liquid materials. In *Supported Ionic Liquids : Fundamentals and Applications*, Fehrmann, R.; Riisager, A.; Haumann, M., Eds. John Wiley & Sons, Incorporated: Weinheim, Germany, 2014.

[65] Xin, B.; Hao, J., Imidazolium-based ionic liquids grafted on solid surfaces. *Chemical Society Reviews* **2014,** *43* (20), 7171-7187.

[66] Fehrmann, R.; Riisager, A.; Haumann, M., *Supported ionic liquids: Fundamentals and applications*. John Wiley & Sons: 2014.

[67] Fehrmann, R.; Riisager, A.; Haumann, M., Introduction. In *Supported Ionic Liquids : Fundamentals and Applications*, Fehrmann, R.; Riisager, A.; Haumann, M., Eds. John Wiley & Sons, Incorporated: Weinheim, GERMANY, 2014.

[68] Van Roosendael, S.; Regadío, M.; Roosen, J.; Binnemans, K., Selective recovery of indium from iron-rich solutions using an aliquat 336 iodide supported ionic liquid phase (SILP). *Separation and Purification Technology* **2019,** *212*, 843-853.

[69] Regel-Rosocka, M.; Nowak, Ł.; Wiśniewski, M., Removal of zinc(II) and iron ions from chloride solutions with phosphonium ionic liquids. *Separation and Purification Technology* **2012,** *97*, 158-163.

[70] Hawkins, C.; Momen, M. A.; Dietz, M., Application of ionic liquids in the preparation of extraction chromatographic materials for metal ion separations: Progress and prospects. *Separation Science and Technology* **2018,** *53* (12), 1820-1833.

[71] Avdibegović, D.; Binnemans, K., Chromatographic separation of rare earths from aqueous and ethanolic leachates of NdFeB and SmCo magnets by a supported ionic liquid phase. *RSC Advances* **2021,** *11* (14), 8207-8217.

[72] Avdibegović, D.; Regadío, M.; Binnemans, K., Efficient separation of rare earths recovered by a supported ionic liquid from bauxite residue leachate. *RSC Advances* **2018,** *8* (22), 11886-11893.

[73] Dashti, S.; Sadri, F.; Shakibania, S.; Rashchi, F.; Ghahreman, A., Separation and solvent extraction of rare earth elements (Pr, Nd, Sm, Eu, Tb, and Er) using TBP and Cyanex 572 from a chloride medium. *Minerals Engineering* **2021,** *161*, 106694.

[74] Zhang, Y.; Guo, W.; Liu, D.; Xu, J., Rational design of novel carboxylic acid functionalized phosphonium based ionic liquids as high-performance extractants for rare earths. *Journal of Rare Earths* **2021,** *39* (11), 1435-1441.

[75] Shen, L.; Chen, J.; Chen, L.; Liu, C.; Zhang, D.; Zhang, Y.; Su, W.; Deng, Y., Extraction of mid-heavy rare earth metal ions from sulphuric acid media by ionic liquid [A336][P507]. *Hydrometallurgy* **2016,** *161*, 152-159.

[76] Chen, L.; Chen, J., Asymmetric membrane containing ionic liquid [A336][P507] for the preconcentration and separation of heavy rare earth lutetium. *ACS Sustainable Chemistry & Engineering* **2016,** *4* (5), 2644-2650.

[77] Xu, H.; Zhang, L.; Pang, Z.; Wang, Z.; Li, W.; Deng, J., The study on extraction behavior of [N1888][P507] and TRPO for heavy rare earths. *Minerals Engineering* **2022,** *176*, 107339.

[78] Mohamed, W.; Metwally, S.; Ibrahim, H.; El-Sherief, E.; Mekhamer, H.; Moustafa, I. M.; Mabrouk, E., Impregnation of task-specific ionic liquid into a solid support for removal of neodymium and gadolinium ions from aqueous solution. *Journal of Molecular Liquids* **2017,** *236*, 9-17.
[79] Dupont, D.; Binnemans, K., Rare-earth recycling using a functionalized ionic liquid for the selective dissolution and revalorization of $Y_2O_3:Eu^{3+}$ from lamp phosphor waste. *Green Chemistry* **2015,** *17* (2), 856-868.
[80] Riaño, S.; Binnemans, K., Extraction and separation of neodymium and dysprosium from used NdFeB magnets: An application of ionic liquids in solvent extraction towards the recycling of magnets. *Green Chemistry* **2015,** *17* (5), 2931-2942.

Chapter 2
Synthesis of Phosphinic Acids and Phosphonium Cations

2.1 Introduction

Hydrophosphination reactions involve the formation of a P-C bond, with one of the common ways to achieve this being though a radical-catalysed addition reaction of hypophosphorus acid (H_3PO_2) with an alkene. Williams and Hamilton were among the first to report this method, with reaction occurring through the use of peroxide as radical initiator to produce a dialkylphosphinic acid (Figure 2.1).[1]

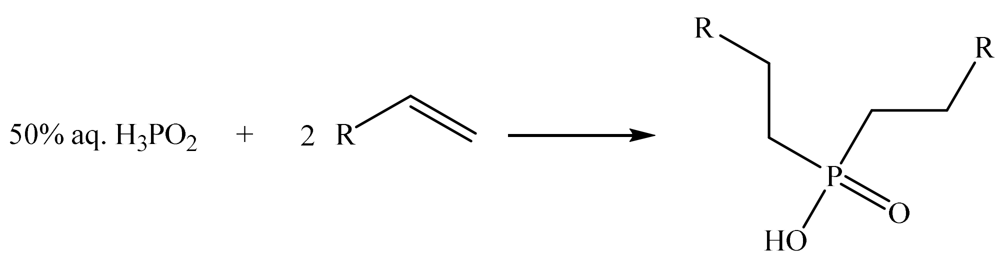

Figure 2.1:Radical reaction of hypophosphorus acid reported by Williams and Hamilton

Further work was done by Nifant'ev et al. to develop this reaction, improving yields of the original method by carrying out the reaction in acidic conditions.[2] While this produces high yields in some cases, the acidic nature makes the reaction conditions quite harsh and therefore unsuitable for some functional groups. Further work by Deprèle and Montchamp resulted in a new method involving a reaction of sodium hypophosphite with an alkene and triethylborane initiator at room temperature for two hours.[3] These mild conditions allow for a wider range of functional groups to be used, and therefore a larger range of possibilities for reactions of this kind.

Other work on hydrophosphination reactions have involved the testing of a range of methods and conditions, with initiators such as peroxides, azobisisobutyronitrile (AIBN),[4] manganese(III) acetate,[5] and silver(I) fluoride[6]. There have also been promising results from reactions tested at room temperature under neutral conditions, solvent-free reactions,[7] and microwave reactions.[8]

The proposed mechanism for the radical addition reaction of hypophosphorus acid with an alkene is shown in Figure 2.2. On the alkene, there are two carbon sites on which the P-C bond may form. Generally, a minor and major product will form, with the favoured product forming where the P bonds to the carbon which is less sterically hindered. [9]

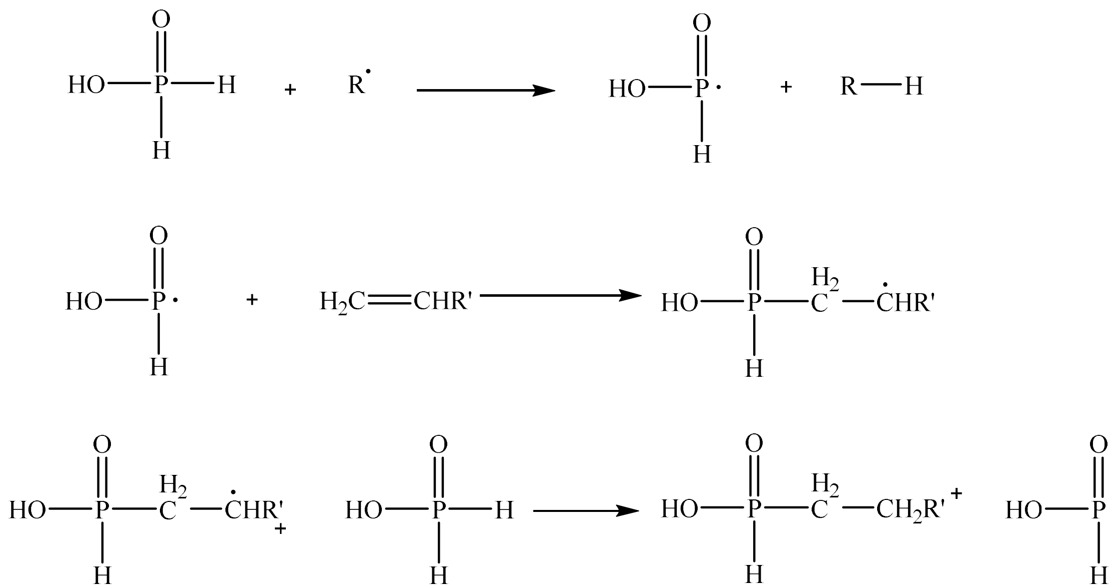

Figure 2.2: Reaction mechanism for the radical-catalysed addition of hypophosphorus acid to alkenes

2.1.1 Phosphorus Mannich Reaction

Mannich reactions are well documented condensation reactions named after Carl Mannich who was one of the first to describe this type of reaction in 1912. [10] A Mannich reaction typically occurs between formaldehyde, a compound with an active hydrogen, and a primary or secondary amine. This general reaction is shown in Scheme 2.1. In this type of reaction, new C-N and C-C bonds are formed with the formaldehyde providing a CH_2 group which bonds with the nitrogen from the amine, as well as with the R' group in the compound with the active hydrogen.

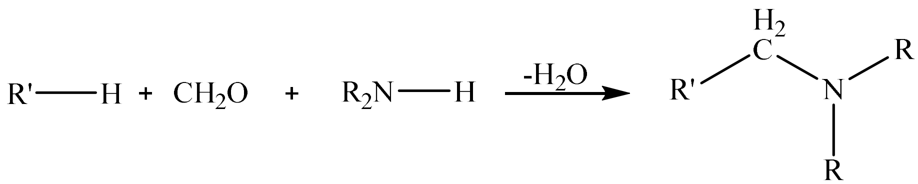

Scheme 2.1: Reaction scheme of general Mannich condensation reaction between formaldehyde, an amine, and a compound with an active hydrogen.

In the time since Mannich reported this reaction, many developments have been made to improve the reaction and widen the scope and applications of this reaction. For example, Mannich reactions are used in the synthesis of the pain relief drug, Tramadol and anaesthetic Falicain, as well as natural product synthesis. [11]

Phosphorus Mannich-type reactions have also been reported in the synthesis of aminophosphinic acids and aminophosphonates. Phosphinic acids contain an acidic hydrogen bonded to the phosphorus which can be used as the active hydrogen for a Mannich condensation reaction with an amine and formaldehyde to form an aminophosphinic acid. Reactions of this kind have been reported achieving reasonable yields. For example, Keglevich et al. achieved yields ranging between 49-98 % for their microwave assisted synthesis of cyclic aminomethylphosphonates and aminomethyl-aryl phosphinic acids. [12]. In another example, Varga reported yields between 30-90% for the synthesis of N,N,N',N'-tetrasubstituted bis(aminomethyl) phosphinic acids.[13]

2.1.2 Camphene

Terpenes are a type of natural product, defining the largest class of secondary metabolites.[14] They are built from isoprene units, 2-methylbuta-1,3-diene, containing five carbons. Terpenoids also fall into the class of terpenes but tend to contain other functional groups or oxidised methyl groups which have been lost or relocated.[15] These compounds are commonly used in perfumery, cosmetics, and medical treatments.[14]

Camphene (Figure 2.3) is a bicyclic monoterpene which is also produced as a byproduct of the paper and pulp industry, forming as an important secondary intermediate in the conversion of α-pinene to camphor.[14] It is also found naturally in the leaf oils of a range of plants, most commonly eucalypt, *Eucalyptus kirktomiana*, as well as ginger and rosemary.

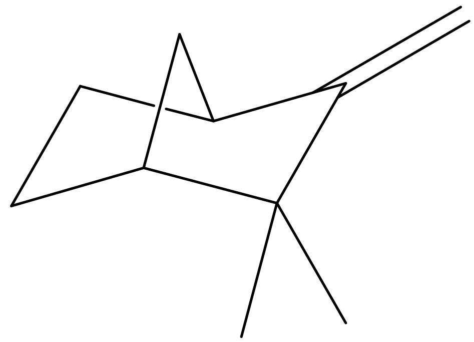

Figure 2.3: Structure of camphene

In this work, camphene is used as a starting material for the synthesis of camphyl phenyl phosphinic acid. Its origins make it a reasonably green, renewable and inexpensive material. Furthermore, being a lipophilic and branched compound, it may be useful in the preparation of IL, helping increase the lipophilicity and the selectivity of created ILs.

2.1.3 Hydroxymethyl phosphonium salts

Discussion surrounding hydroxymethyl phosphonium salts typically concerns tetrakis(hydroxymethyl)phosphonium chloride (THPC), whose structure is given in Figure 2.4. This salt, and other hydroxymethyl phosphonium salts, can be useful as precursors to hydroxymethyl phosphines, such as triskis(hydroxymethyl) phosphine (THP) through the elimination of formaldehyde (CH_2O).[16]

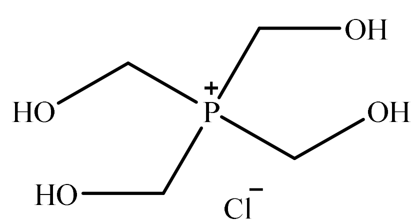

Figure 2.4: Structure of tetrakis(hydroxymethyl) phosphonium chloride (THPC)

One common reaction often reported when using THPC is a phosphorus Mannich reaction, similar to that discussed previously in this chapter. However, in this work, an alkylation reaction using THPC as a starting material was considered, similar to that described in a patent by Woodward et al. [17] to form tri-n-butylphosphine. When reacted with base, THPC forms tris(hydroxymethyl)phosphine (THP), as shown in Figure 2.5. This can undergo alkylation with a haloalkane to form a phosphonium salt, as shown in Figure 2.6.[16]

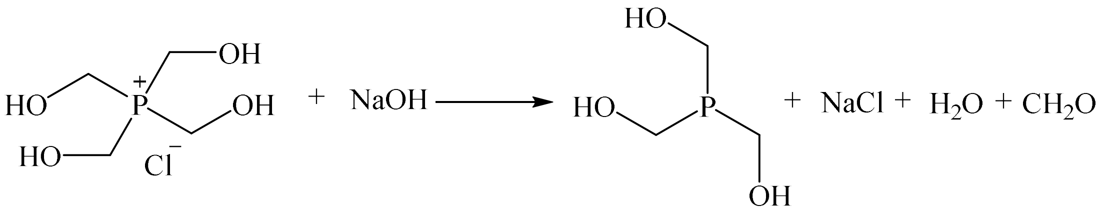

Figure 2.5: Reaction of THPC with base to form THP

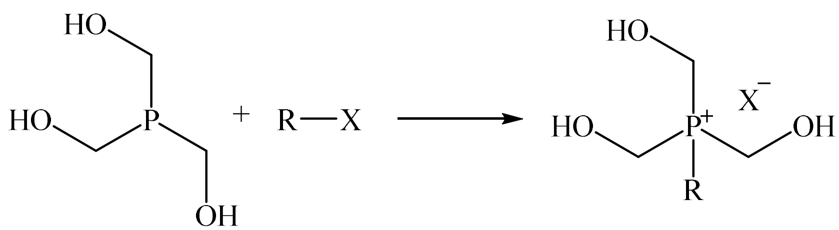

Figure 2.6: Reaction of THP with haloalkane to form tris(hydroxymethyl) alkyl phosphonium cation. R = alkyl group, X = Cl, Br, I

Upon further reaction with base and a haloalkane, the hydroxymethyl groups can be substituted to form the $[RP(CH_2OH)_3]^+$, $[R_2P(CH_2OH)_2]^+$, $[R_3P(CH_2OH)]^+$ and $[R_4P]^+$ phosphonium cations, with formaldehyde and water forming as a by-product.

2.1.4 Aims of this chapter

In this work, three different reactions are attempted with the goal of producing phosphinic acid anion precursors and phosphonium cations to be used in the preparation of a series of novel ionic liquids.

A hydrophosphination reaction will be tested involving the addition of camphene to phenylphosphinic acid, taking place using a similar previously reported method. [9] This method will be a method adapted from a previous method for the synthesis of camphyl phosphinic acid.[9, 18]. The second reaction attempted is a phosphorus Mannich-type reaction between camphyl phosphinic acid, diisobutylamine and formaldehyde to form aminophosphinic acid, camphyl [diisobutyl-aminomethyl] phosphinic acid. The use of camphene and camphene derived products are used as camphene is a green, renewable, and inexpensive starting material.

Finally, the alkylation of THPC using 1-bromooctane and 1-bromobutane will be attempted. It was expected that the reaction would produce a product containing a mixture of phosphonium ions with varying degrees of alkylation with different combinations of butyl and octyl alkyl groups. A mixture of cations would be less likely to crystallise, and would therefore be more likely to form as a liquid when preparing ionic liquid. Cyanex 923 is a similar extractant which contains a mixture of trialkylphosphine oxides. This phosphine oxide mixture includes varying amounts of compounds with the general formulae R_3PO, $R_2R'PO$, RR'_2PO and R'_3PO where R and R' represent n-octyl and n-hexyl groups respectively.

2.2 Experimental

2.2.1 Materials

Phenyl phosphinic acid, 75% benzoyl peroxide, diisobutyl amine, deuterated chloroform and toluene were all sourced from Sigma Aldrich. Sodium hydroxide pellets, camphene, 1-bromooctane, and cobalt(II) acetate tetrahydrate were sourced from BDH chemicals. Concentrated hydrochloric acid, formaldehyde, 1-bromobutane, and petroleum spirits were sourced from Ajax Fine Chemicals. Glacial acetic acid and heptane were sourced from Merck. Tetrakis(hydroxymethyl) phosphonium chloride (THPC) was sourced from Albright and Wilson Ltd. UK. Methanol, ethanol, isopropanol, diethyl ether and dichloromethane were all drum grade.

2.2.2 General Procedures and Instrumentation

Elemental microanalysis:
Elemental microanalysis was carried out externally at Macquarie University in Sydney, Australia.

Nuclear Magnetic Resonance Spectroscopy (NMR):
^{1}H, ^{13}C and ^{31}P NMR spectra of products were obtained using a JEOL ECZR 600 MHz NMR spectrometer. Samples were prepared by dissolving product in $CDCl_3$. Spectra were processed using the Delta 6.1.0 program.

Electrospray Ionisation Mass Spectrometry (ESI-MS):

The mass spectra of samples were prepared by dissolving the sample in methanol in Eppendorf tubes. Samples were centrifuged prior to testing to separate undissolved material from the dissolved sample. Spectra were recorded using a Bruker Daltonics MicroTOF electrospray ionisation mass spectrometer, with a capillary exit voltage of 150 V and a skimmer 1 voltage of 50 V unless otherwise stated.

Fourier Transform Infrared Spectroscopy (FTIR):

Samples were prepared as KBr disks. Infrared spectra were recorded using a Perkin Elmer Spectrum 100 FTIR spectrometer with an observed range of 4000-450 cm^{-1}.

Melting Point:

The melting point of solid samples was measured using a Reichert Thermopan melting point machine. Samples were prepared on microscope slide and covered with a cover slip. A melting point range was recorded at sign of first melting to the full melting of sample.

X-Ray Diffraction (XRD):

XRD data was produced externally by the School of Chemical Sciences at Auckland University. Crystal structural data collected on a Rigaku XtaLAB Synergy-S single crystal X-ray diffractometer. The crystal was kept at 100.0(3) K during data collection. The structure was solved on Olex2[19] using the olex2.solve[20] structure solution program using Charge Flipping and refined with olex2.refine[20] refinement package using Gauss-Newton minimisation.

2.2.3 Synthesis of CamPhPOOH (1)

The method of synthesis for camphyl phenyl phosphinic acid was adapted from a previous method. [9] Phenyl phosphinic acid (25 g) and melted camphene (40 mL) was added to 95% ethanol (160 mL) and brought to reflux. The mixture was refluxed for a total of 15 hours with benzoyl peroxide added at regular intervals (roughly 1 hour) until a total of 2 g had been added. Once the reaction mixture had finished refluxing, water (20 mL) was added, and volatiles were removed by rotary evaporation.

The crude product was extracted into a sodium hydroxide solution (15 g, in 100 mL water), and the aqueous phase was washed with diethyl ether. The aqueous phase was acidified with concentrated HCl. The solid produced was filtered by vacuum filtration and washed with petroleum spirits.

To further purify the product, it was dissolved in glacial acetic acid and the solution was filtered by gravity filtration before adding water to force the product out of solution. The white crystals were filtered by vacuum filtration.

Single crystals suitable for XRD data collection were grown by dissolving the product in a hot 2:1 heptane:toluene mixture, with crystals forming with the slow cooling of the mixture. The crystals were removed from solution by vacuum filtration. m.p 181-182 °C ESI-MS $[M-H]^-$ m/z 277.33, calculated m/z 277.14. Elemental C 69.00%, H 7.19% (Theoretical: C 69.05%, H 8.33%).

NMR: $^{31}P\{^{1}H\}$: δ 48.5 [s]

^{1}H: δ 10.5 [1H, s, br, OH], 7.73-7.69 [2H, dd, J 7.57 Hz, H_{12}], 7.47-7.44 [1H, t, ^{3}J 7.57 Hz, H_{14}], 7.39-7.36 [2H, td, ^{3}J 7.57 Hz, ^{4}J 3.44 Hz, H_{13}], 2.14 [1H, s, br, H_4] 1.825-1.68 [3H, m], 1.67 [1H, s, br, H_1], 1.49-1.43 [2H, m], 1.19-1.12 [3H, m], 1.05 [1H, d, ^{2}J 9.64 Hz, $H_{7'}$], 0.83 [3H, s, Me'], 0.70 [3H, s, Me"]

$^{13}C\{^{1}H\}$: δ 133.8 [d, $^{1}J_{P\text{-}C}$ 128.6 Hz, C11], 131.8 [s, C14], 131.1 [d, $^{3}J_{P\text{-}C\text{-}C\text{-}C}$ 10.1 Hz, C12/16], 128.4 [d, $^{2}J_{P\text{-}C\text{-}C}$ 13.0 Hz, C13/15], 48.5 [s, C1], 43.8 [d, $^{2}J_{P\text{-}C\text{-}C}$ 4.33 Hz, C3], 42.3 [d, $^{3}J_{P\text{-}C\text{-}C\text{-}C}$ 4.33 Hz, C4], 37.6 [d, $^{3}J_{P\text{-}C\text{-}C\text{-}C}$ 11.7 Hz, C2], 37.0 [s, C7], 31.8 [s, C10], 28.4 [d, $^{1}J_{P\text{-}C}$ 99.7 Hz, C8], 42.6 [s, C6], 22.1 [s, C9], 20.2 [s, C5].

FTIR: υ(P=O) region 1185.5, 1141.9, 1131.2, strong, υ(P-OH), υ(P-Ph) region 1082.7, 1068.6, 984.7, 959.3.

2.2.4 Synthesis of CamPhPOOH cobalt complex 1a

1 (0.25 g) was dissolved in a solution of NaOH (0.04 g NaOH, 20 mL EtOH). This was added to a solution of cobalt(II) acetate tetrahydrate (0.14 g) dissolved in ethanol (10 mL). This was gently stirred before being left to evaporate. The pink solution formed blue crystals as the ethanol evaporated. The final yield of the product was not recorded.
For the collection of XRD data, single crystals of the cobalt complex were grown from the crude product by slow evaporation in methanol.

2.2.5 Synthesis of CamP(O)(OH)($CH_2N^iBu_2$) 2

Camphyl phosphinic acid (2.00 g) was dissolved in isopropanol (40 mL). Diisobutylamine (2.4 mL) and HCl (conc, 5 mL) was added to the solution. The mixture was heated to reflux before adding excess formaldehyde (10 mL) dropwise and left to reflux for 2.5 hours. Once removed from reflux, water (50 mL) was added, and the volatiles were removed by rotary evaporation. The product was dissolved in dichloromethane (30 mL) and washed with water. The DCM layer was separated from the aqueous layer and volatiles removed by rotary evaporation. The remaining product was left to dry under vacuum. The resulting product was a viscous, clear, yellow liquid. (Yield of crude product: 36%) ESI-MS $[M-H]^-$ m/z 342.3.

2.2.6 Attempted synthesis of hydroxymethyl alkyl phosphonium ions

Tetrakis(hydromethyl) phosphonium chloride (1.99 g), 1-bromooctane (3.23 g) and 1-bromobutane (2.34 g) were each dissolved in 25 mL methanol and added to a round bottom flask and refluxed. Sodium hydroxide pellets (1.99 g) were dissolved in a mixture of water (50 mL) and methanol (10 mL). Once the refluxing mixture started boiling, the sodium hydroxide solution was added dropwise over 3.5 hours. Once the reaction had finished, the reaction mixture was analysed by ESI-MS.

2.3 Results and Discussion

2.3.1 Camphyl phenyl phosphinic acid synthesis

Using a method based on a previous thesis method,[9] the reaction to produce **1** was done initially by adding benzoyl peroxide to a refluxing reaction mixture containing camphene and phenyl phosphinic acid in two 1 g quantities, with work-up steps involving a base extraction. However, this method produced a low yield (7.7%) and so the method was altered in an attempt to improve this.

To determine whether the low yield was due to insufficient reaction time or incomplete reaction, a change of solvent from ethanol to propanol was tested. It was expected that the use of propanol would allow the reaction mixture to be brought up to a higher refluxing temperature, and therefore decrease reaction time. However, the change of solvent produced a significantly lower yield than the initial method. In this reaction, benzoyl peroxide acts as a radical initiator, producing radicals which act as catalysts and allow the reaction to occur. It is suggested that with the higher temperature in the propanol reaction mixture, the radicals are being produced faster than the reaction occurs. As a result, the radicals decompose faster than the desired reaction occurs, therefore a low yield was achieved.

Following this attempt, the reaction solvent was changed back to ethanol, but the peroxide was added in smaller amounts over shorter periods of time. This would provide a more regular and steadier production of radicals at a lower temperature. Using this final method, an improved yield of 34 % was achieved.

2.3.2 Characterisation of 1

The results from the proton, carbon and phosphorus NMR indicated the presence and purity of the desired product. The ^{1}H NMR spectrum for **1** is given in Figure 2.8. The integration values of the ^{1}H spectrum showed the expected 23 hydrogens were present within the compound and the proton shifts aligned with what was expected in good agreement with previous work.[9] The structure and numbering scheme used for NMR peak assignments is given in Figure 2.7.

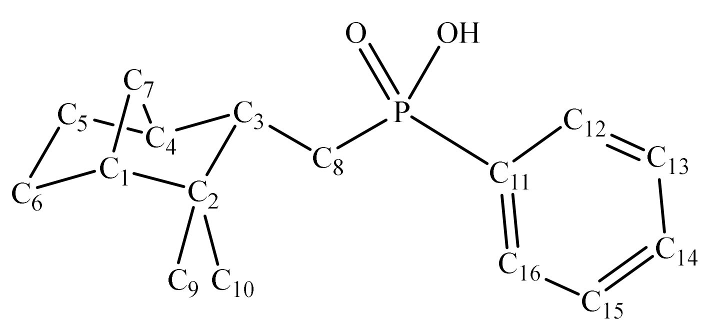

Figure 2.7: Structure and numbering scheme of product **1**

The five protons with shifts between 7.73 and 7.69 ppm were assigned as the phenyl group protons. The triplet of triplets present at 7.39 ppm represented 2 protons with ortho- and meta- coupling constants of 7.57 Hz and 3.44 Hz respectively. This was assigned as the H_{13} protons. The triplet at 7.47 ppm was assigned to the H_{14} protons as integration showed it represented only one carbon. This peak was weakly showing as a triplet of triplets, with ^{3}J and ^{4}J couplings of 7.57 Hz and 1.38 Hz. The final peak presented as a doublet of doublets at 7.73 ppm. The two coupling constants for these peaks were calculated to be 7.57 Hz and 11.71 Hz. The 7.57 Hz coupling constant was assigned as the ^{3}J coupling constant as this was equal to the other ^{3}J couplings within the phenyl ring. The assignment of the camphyl group protons was a challenge, and many peaks could not be assigned confidently due to significant overlap of peaks.

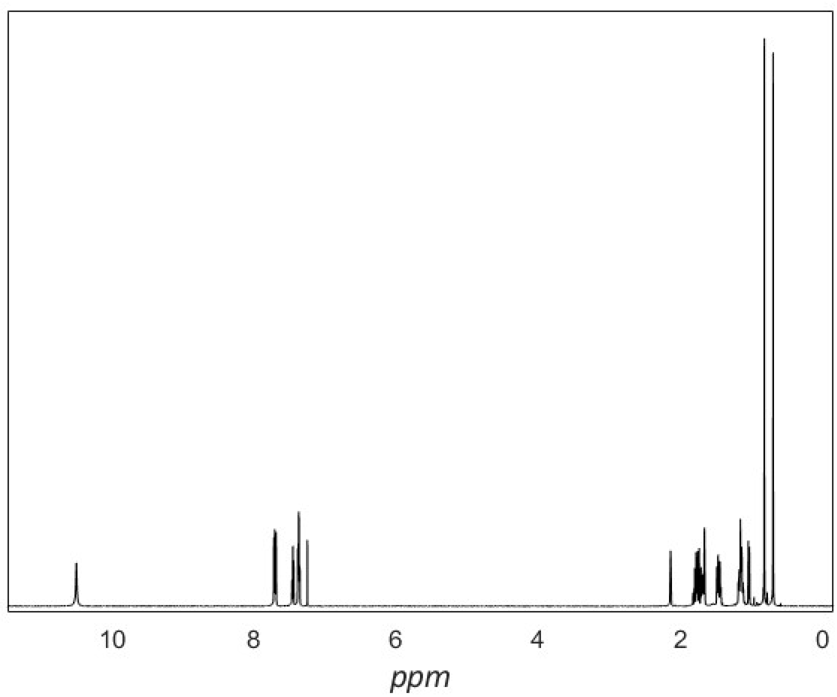

Figure 2.8: ^{1}H NMR spectrum of **1** in $CDCl_3$

The $^{13}C\{^1H\}$ spectra, shown in Figure 2.9 also aligned with the expected product, showing 14 different carbon environments present within the sample. This was to be expected with 16 carbons present in the product, two of which shared the same environment. Among the peaks, there were six doublets present due to J-coupling between phosphorus and the nearby carbon atoms. As is expected, the ^{1}J coupling constants were large, measured to be 99.7 Hz and 128.6 Hz for the coupling occurring between phosphorus and C8 and C11 respectively. ^{2}J and ^{3}J couplings were also observed in the spectrum.

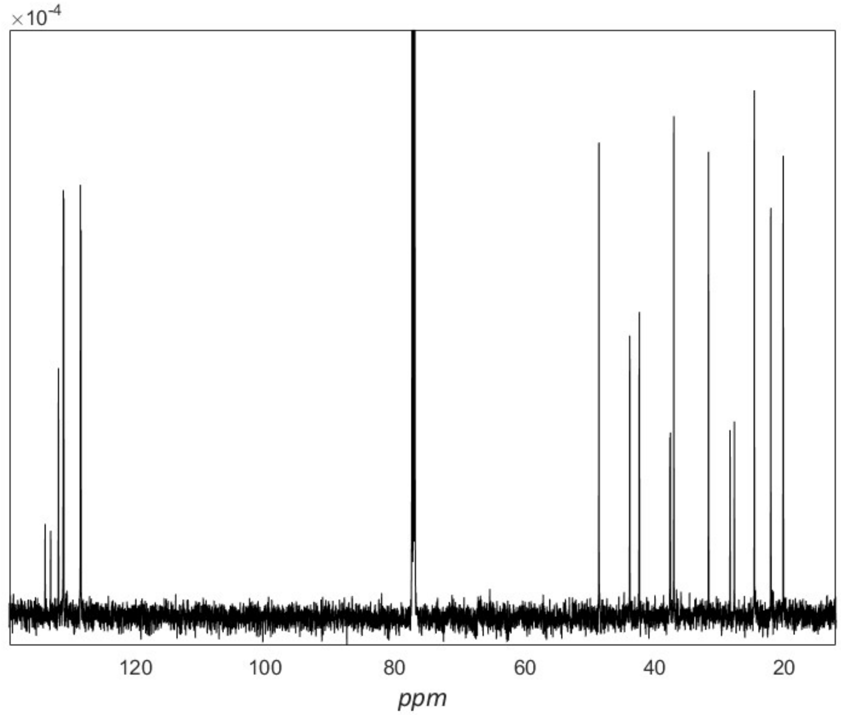

Figure 2.9: $^{13}C\{^{1}H\}$ NMR spectrum of **1** in $CDCl_3$

The $^{31}P\{^{1}H\}$ decoupled spectrum showed a single peak at 48.5 ppm representing the single phosphorus in the compound. The lack of other peaks was also used as an indication of the purity of the product, with the single peak providing no evidence of by-products or leftover phenyl phosphinic acid in the sample.

The negative ion mode ESI mass spectrum of the final purified product, **1**, also confirmed the presence of the desired product and showed the purity of the sample. Two main ion peaks were observed at m/z values of 277.2 and 555.4, which were assigned as the $[M-H]^-$ and $[2M-H]^-$ ions. This is shown in the ESI-MS in Figure 2.11.

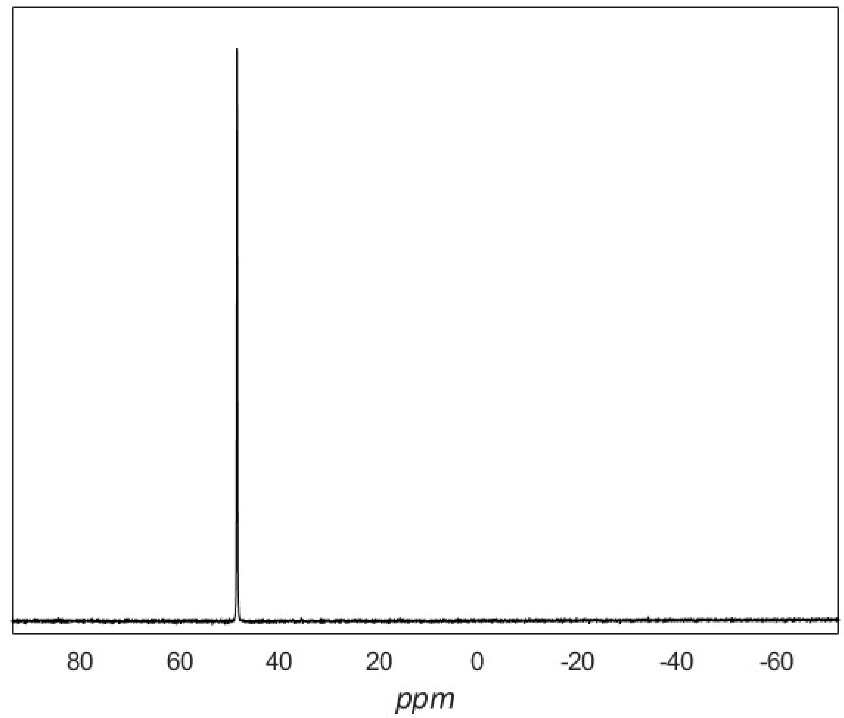

Figure 2.10: $^{31}P\{^{1}H\}$ spectrum of **1** in $CDCl_3$

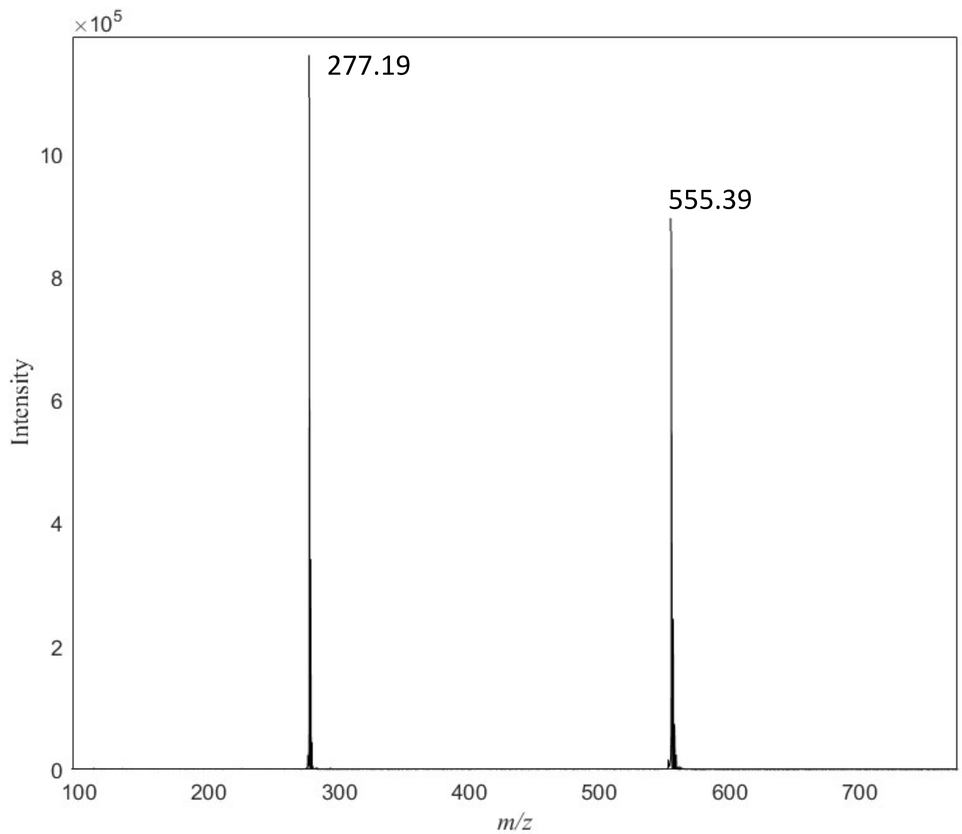

Figure 2.11: ESI-MS of product **1** in negative ion mode

The elemental analysis results further confirmed the purity and presence of the desired product. For the duplicate results received, the %C were very close to the theoretical value. The hydrogen values were slightly lower than expected, however this is consistent with results found by Kuveke et al. in their study of elemental analysis results from laboratories around the world. [21] In this study, they found Macquarie University to provide reliable results for carbon in elemental analysis, but the hydrogen results were on average lower than the expected values.

2.3.3 XRD of 1

Single crystals suitable for XRD data collection were grown by dissolving the product in a hot 2:1 heptane:toluene mixture, with crystals forming with the slow cooling of the mixture. The resulting crystal structure is shown in Figure 2.12. The XRD data showed the crystals grew in the orthorhombic space group, Pbca. This is a centrosymmetric space group, with both enantiomers of **1** present within the structure, related through a centre of inversion. Crystallographic data for **1** are shown in Table 2.1, with selected bond lengths and angles reported in Table 2.2.

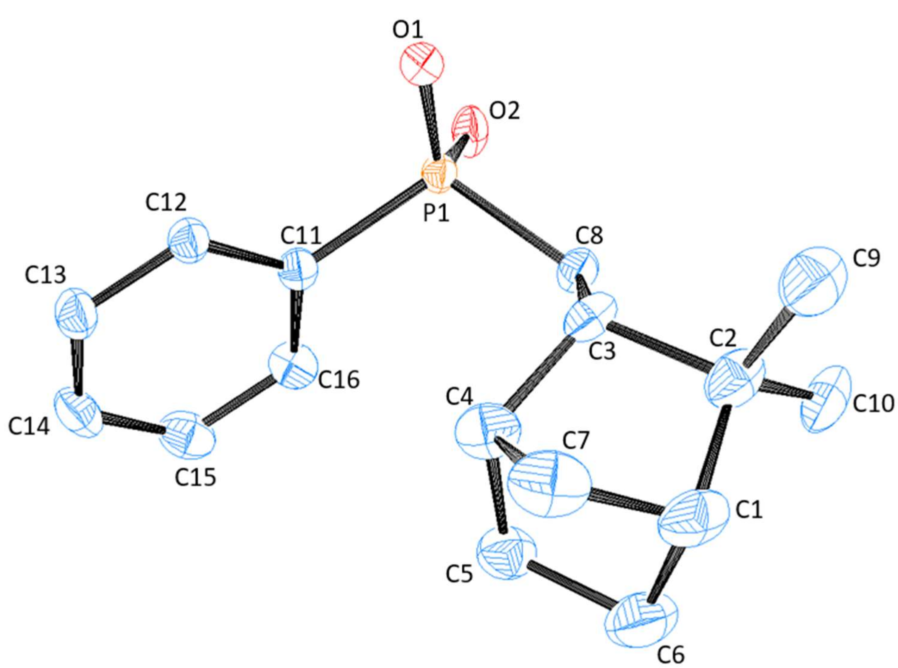

Figure 2.12: XRD structure of **1**, hydrogens removed for clarity. Ellipsoids at 50% probability.

Table 2.1: Crystallographic Data collected for **1**

CamPhPOOH	
Formula	$C_{16}H_{22}O_2P$
Formula weight	277.326
Crystal system	orthorhombic
Space group	Pbca
a/Å	6.3240(1)
b/Å	14.9795(2)
c/Å	31.6113(5)
Volume/ Å^3	2994.55(8)
Z	8
ρcalc g/cm^3	1.230
μ/mm^{-1}	1.587
Crystal size/mm^3	0.1 x 0.1 x 0.1
Radiation/ Å	Cu Kα (λ = 1.54184)
2Θ range for data collection/°	11.2 to 148.4
Reflections collected	19463
Independent reflections	3018 [R_{int} = 0.0356, R_{sigma} = 0.0252]
Data/restraints/parameters	3018/0/176
Goodness of fit on F^2	1.047
Final R indexes	R_1 = 0.0476, wR_2 = 0.1192
Final R indexes [all data]	R_1 = 0.0528, wR_2 = 0.1226
Largest diff. peak/hole/ e Å^{-3}	0.59/-0.34

Table 2.2: Selected bond lengths for CamPhPOOH **1**

CamPhPOOH	**Length (Å)/Angle (°)**
P1-O1	1.4973(14)
P1-O2	1.5516(14)
P1-C11	1.7982(19)
P1-C8	1.7983(19)
O2-P1-O1	115.88(8)
C11-P1-O1	110.03(9)
C11-P1-O2	107.51(8))
C8-P1-O1	109.90(9)
C8-P1-C11	110.75(9)
C8-P1-O2	102.53(8)

Hydrogen bonding is present between molecules, occurring between the hydrogen of the hydroxyl group and the double bonded oxygen. This hydrogen bonding pattern is consistent with the hydrogen bonding observed in other phosphinic acids, with links between the hydrogen bonds creating a "zigzag" pattern between molecules with each phosphorus-bonded oxygen appearing to form intermolecular hydrogen bonds with the hydroxy group of a neighbouring molecule, shown in Figure 2.13. Similar patterns are observed for compounds such as bis(3-nitrophenyl)phosphinic acid (CSD Code: BECPOQ), diphenylphosphinic acid[22] and [2,4,6-tris(trifluoromethyl)phenyl]-phosphinic acid[23]. The strength of the hydrogen bond also appears to be similar to these examples. In the latter example, Cornet et al. found the hydrogen bond O···O distance to be 2.509(4) Å. [23] In the former, the this distance was measured to be 2.429 Å. These are all comparable to the same distance measured in the crystal structure of **1**, with a O-O distance of 2.500(2) Å.

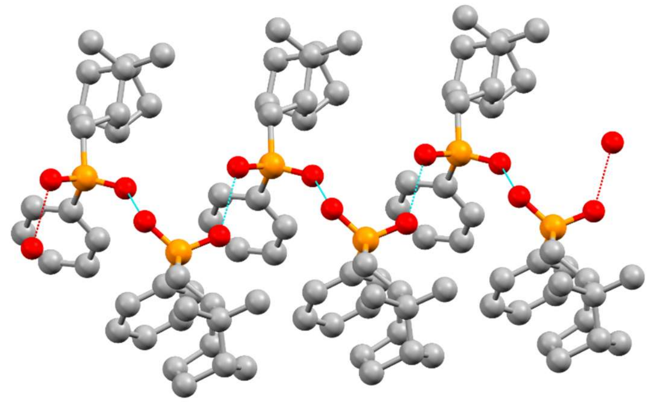

Figure 2.13: Hydrogen bond interactions of **1** forming "zig zag" pattern. The atoms are colour coded with grey, red, and orange representing carbon, oxygen and phosphorus respectively.

2.3.4 Cobalt Complex 1a

The synthesis of a cobalt complex using the product **1** was attempted due to the similarity of extractants used in rare earth separations and cobalt separation methods, as well as the colour change which is easily observed as cobalt changes from octahedral (pink) to tetrahedral (blue). Therefore, successful formation of a cobalt complex may give a good indication of the applicability of this phosphinic acid for the separation of the REEs. To form the cobalt complex, one mole equivalent of cobalt(II) acetate was dissolved in a ethanol solution containing 2 molar equivalents of sodium hydroxide with two mole equivalents of **1** and stirred. This attempted synthesis of a cobalt complex appeared successful, as the pink-to-blue colour change was observed as the solid crystal complex **1a** formed by slow evaporation. The coordination of the ligand to cobalt was confirmed through XRD data which showed the complex crystallised in a monoclinic crystal system, in the $P2_1/c$ space group. The table of crystallographic data is shown in Table 2.3.The structure showed that the cobalt complex formed a polymer, with three ligands bridging two cobalt atoms through the P-bonded oxygen atoms, and an additional ligand linking one asymmetric unit to the next. The asymmetric unit of the structure is shown in Figure 2.14.

Table 2.3: Crystallographic Data collected for **1a**

Formula	$Co_2C_{64}H_{88}O_8P_4$
Formula weight	1166.93
Crystal system	monoclinic
Space group	$P2_1/c$
a/Å	14.4822(3)
b/Å	23.7584(5)
c/Å	18.8858(4)
β/°	100.283(2)
Volume/ Å^3	6393.7(2)
Z	4
ρcalc g/cm^3	1.084
μ/mm^{-1}	5.407
Crystal size/mm^3	0.14 x 0.05 x 0.01
Radiation/ Å	Cu Kα (λ = 1.54184)
2Θ range for data collection/°	6.038 to 148.484
Reflections collected	130518
Independent reflections	12813 [R_{int} = 0.2223, R_{sigma} = 0.0936]
Data/restraints/parameters	12813/282/357
Goodness of fit on F^2	1.146
Final R indexes	R_1 = 0.1631, wR_2 = 0.3924
Final R indexes [all data]	R_1 = 0.2050, wR_2 = 0.4362
Largest diff. peak/hole/ e Å^{-3}	2.26/-1.11

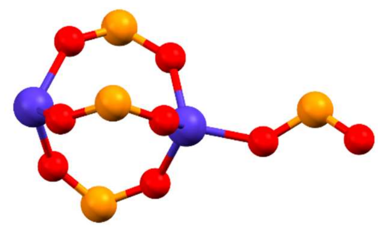

Figure 2.14: Asymmetric unit of **1a** with carbons and hydrogens removed. Orange, red, and blue coloured atoms represent phosphorus, oxygen, and cobalt respectively.

Although the XRD data for this complex was ample to provide a good idea of the overall structure of the complex, the data collected were not high quality. This may be due to a few different factors, including the quality of the crystals themselves as well as the nature of the structure. Difficulty was faced with growing crystals suitable for XRD data collection, with multiple attempts at growing crystals by slow evaporation, only three to four produced were of high enough quality for XRD. The deterioration of the crystals also meant that once good crystals had successfully grown, they would deteriorate before good quality XRD data could be collected, or during data collection.

Furthermore, the bulky structure of the complex may have also contributed to the quality of the crystal structure. The large groups within the ligand are likely susceptible to disorder, and the camphyl phenyl phosphinic ligand used has two enantiomers present which may be superpositioned and is likely to contribute to poor quality data. [24]

The crystal structure showed some interesting features. For example, the linkage between ligands and cobalt form a polymeric chain, the core structure of which is shown in Figure 2.15. This shows the alternating triply and singly phosphinate bridges connecting tetrahedral cobalt atoms along the chain.

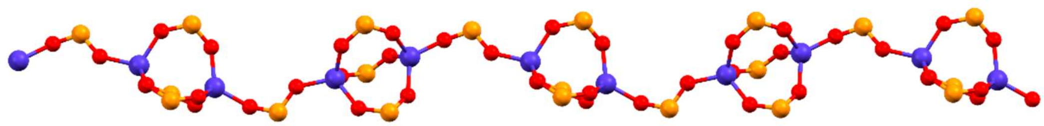

Figure 2.15: Linkage of polymer formed in **1a** with carbons removed.

While the alternating singly and triply bridged metals found in **1a** type of structure is present in literature it appears as though many polymeric structures form in a way as is shown in Figure 2.16. This structure contains continuous chains of ligands bridging metals doubly. [25] It is suggested that the differences in the bridging motifs is due to the ability of the metals to achieve their ideal tetrahedral geometry.

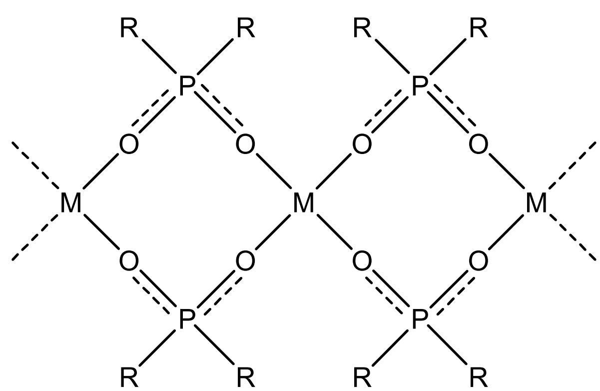

Figure 2.16: Common arrangement of dinucleating phosphinate ligands in polymer chain

Although the bridging pattern observed in **1a** does not appear to be the most common, there are many examples of complexes forming with a similar structure. For example, catena(μ_2-di-n-butylphosphinato)-di-beryllium (CSD Code: HICZAU) also contains three double-bridged phosphinate ligands between Be centres, and an additional ligand bridging these units to create a polymeric chain. [26] Cobalt(II) and zinc(II) complexes formed with di-n-butylphosphinate and diphenylphosphinate have also been found to form with this bridging pattern creating a chain polymer similar to **1a**. [27]

In their study of 552 alkyl and aryl phosphinate metal salts in the Cambridge Structural Database, Carson et al. found the μ_2-bridging dinucleating motif (Figure 2.17) like the one formed in this work, to be the most common, with variations to the number of bridging ligands and the ways in which the ligands bridge to various metal atoms, forming both polymeric and oligomeric structures. [25]

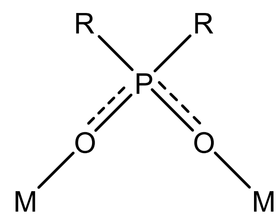

Figure 2.17: Most common coordination mode found for phosphinate ligands in metal salts[25]

Figure 2.18 shows the view of the polymer chain of **1a**, showing a spiral helix structure with the inner inorganic core, and the carbons forming an outer layer to the structure. This columnar structure is similar to the polymeric calcium phosphinate described by Henderson et al, who formed a calcium salt with camphyl phosphinic acid ligands was described as having a buckled ladder-like structure. [24]

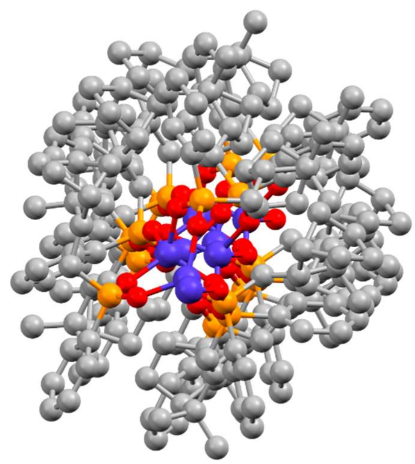

Figure 2.18: View of **1a** down polymer chain. Hydrogens omitted. Colours coded as follows: carbon – grey, phosphorus – orange, oxygen – red, cobalt – blue.

2.3.5 Synthesis of camphyl [diisobutyl-aminomethyl] phosphinic acid **2**

To form **2** a mixture of diisobutylamine with formaldehyde and camphyl phosphinic acid was refluxed under acidic condition. The reaction was carried out with the intention of forming another phosphinic acid to use as an anion precursor for the preparation of hydrophobic ionic liquids. It was expected that the two isobutyl groups would be sufficiently large and bulky to achieve hydrophobic properties in an IL. Unfortunately, a pure product of **2** was difficult to achieve.

The ESI-MS in negative ion mode appeared to show a reasonably pure product, with the main $[M-H]^-$ peak assigned at m/z 342 (Figure 2.19). The proton decoupled ^{31}P NMR spectrum of the initial product showed two phosphorus peaks, indicating the presence of two phosphorus atoms in different environments (Figure 2.10). This was likely due to unreacted starting material within the sample, or possibly a result of an intermediate product or side reaction. The ^{31}P coupled spectrum was also run of this sample, and showed splitting of the peak at 31.0 ppm into a doublet of quartets, and the peak at 42.7 ppm as a single quartet. The doublet of quartets was identified to be due to the presence of starting material, camphyl phosphinic acid, which would include coupling to CH_2 protons, the OH proton, as well as the directly bonded P-H proton. This was confirmed by running the coupled spectrum of the starting material. Therefore, the quartet at 42.7 ppm was assigned as the desired product, **2**.

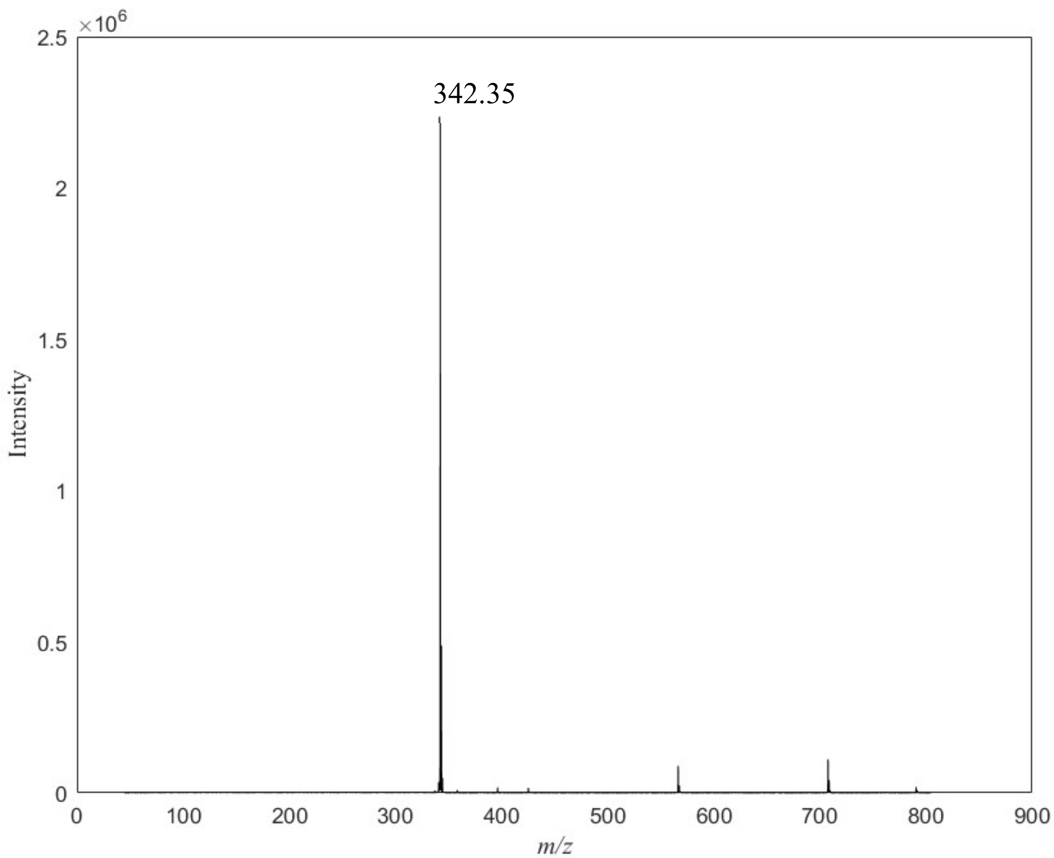

Figure 2.19: ESI-MS of product **2** in negative ion mode

Steps to extract and purify the sample were mostly unsuccessful. Base extraction of the product using sodium hydroxide resulted in a significant loss of product and NMR results still showed the second phosphorus peak in the $^{31}P\{^{1}H\}$ decoupled spectrum.

With attempts to purify the product proving to be a challenge, and purified products being obtained in low yields, further work on this compound were abandoned due to time constraints. Therefore, full characterisation of the compound is not provided in this work and **2** was not considered for further use in the synthesis of ionic liquids. Further work could be done in the future to improve the reaction method to produce higher yields, and to produce a purer product.

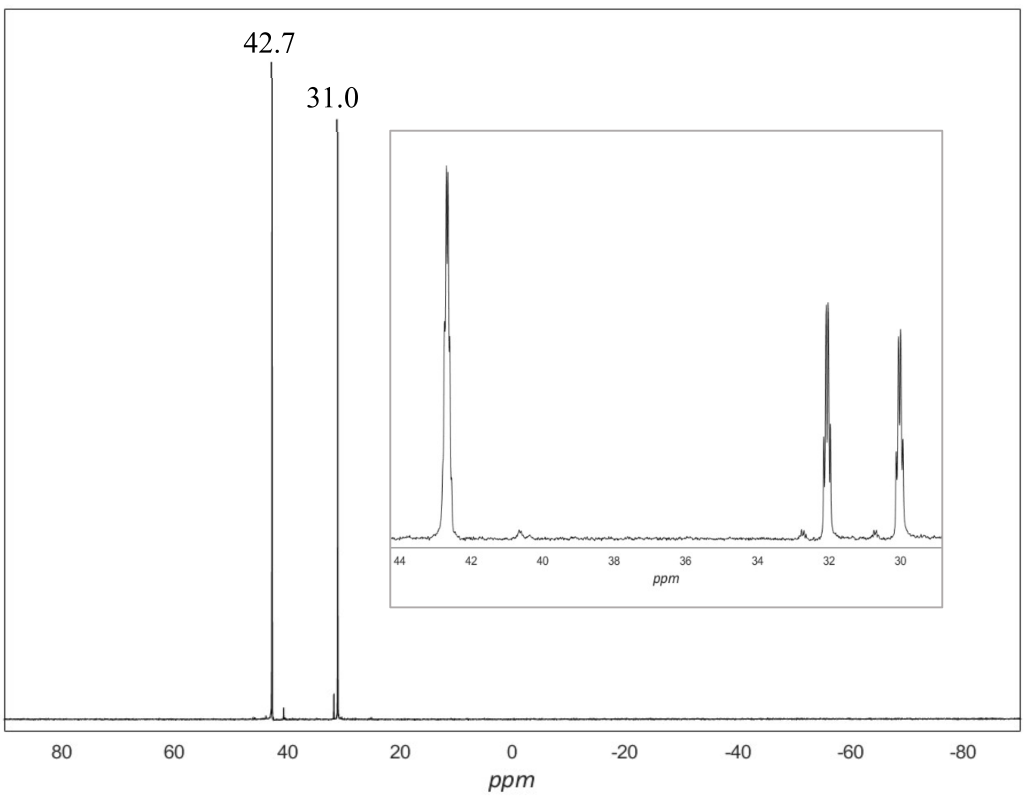

Figure 2.20: $^{31}P\{^{1}H\}$ NMR spectrum of **2** in $CDCl_3$ with inner box showing the coupled ^{31}P spectrum with splitting pattern for the observed peaks.

2.3.6 Attempted synthesis of phosphonium cations using $P(CH_2OH)_4Cl$ (THPC)

In the initial experiment reacting THPC with an alkylating agent, a reaction using two different alkylating groups, 1-bromo-octane and 1-bromo-butane, was attempted to form a mixture of phosphonium cations. It was expected that this reaction would not create a pure single product, but rather a mixture of cations with varying degrees of alkylation and different combinations of alkyl groups. This impure mixture of phosphonium cations could have been advantageous as an extractant for the REEs as the mixture would have been more likely to be a liquid, being less likely to crystallise than a single pure product. This mixture could have been used much like Cyanex 923, an extractant which contains a mixture of trialkylphosphine oxides containing hexyl and octyl alkyl groups.

Characterisation of the reaction mixture following the initial reaction showed evidence that some alkylation had occurred, with peaks for the $[octyl_4P]^+$ and $[octyl_3butP]^+$ cations present within the mass spectrum at m/z 483.6 and 427.5 respectively (Figure 2.21). There was a range of other peaks present within the spectrum, many of which could not be confidently assigned. For example, peaks present at m/z 331.3 and 387.4 were tentatively assigned to represent $[oct_2BuPO + H]^+$ and $[oct_3PO + H]^+$ respectively. However, these were not confidently assigned as for each of these peaks, there were peaks present 22 m/z below at m/z 309.3 and 365.4. With this being the difference between a $[M+H]^+$ and an $[M+Na]^+$ ion, it would be possible that the peaks at m/z 331.3 and 387.4 are $[M+Na]^+$ peaks. Furthermore, when this experiment was repeated using only 1-bromobutane as the alkylating agent, a peak at m/z 331 was present again, this time as one of the most intense peaks in the spectrum. Therefore, the assignment of $[oct_2BuPO + H]^+$ is unlikely, with no 1-bromooctane being present within the reaction mixture.

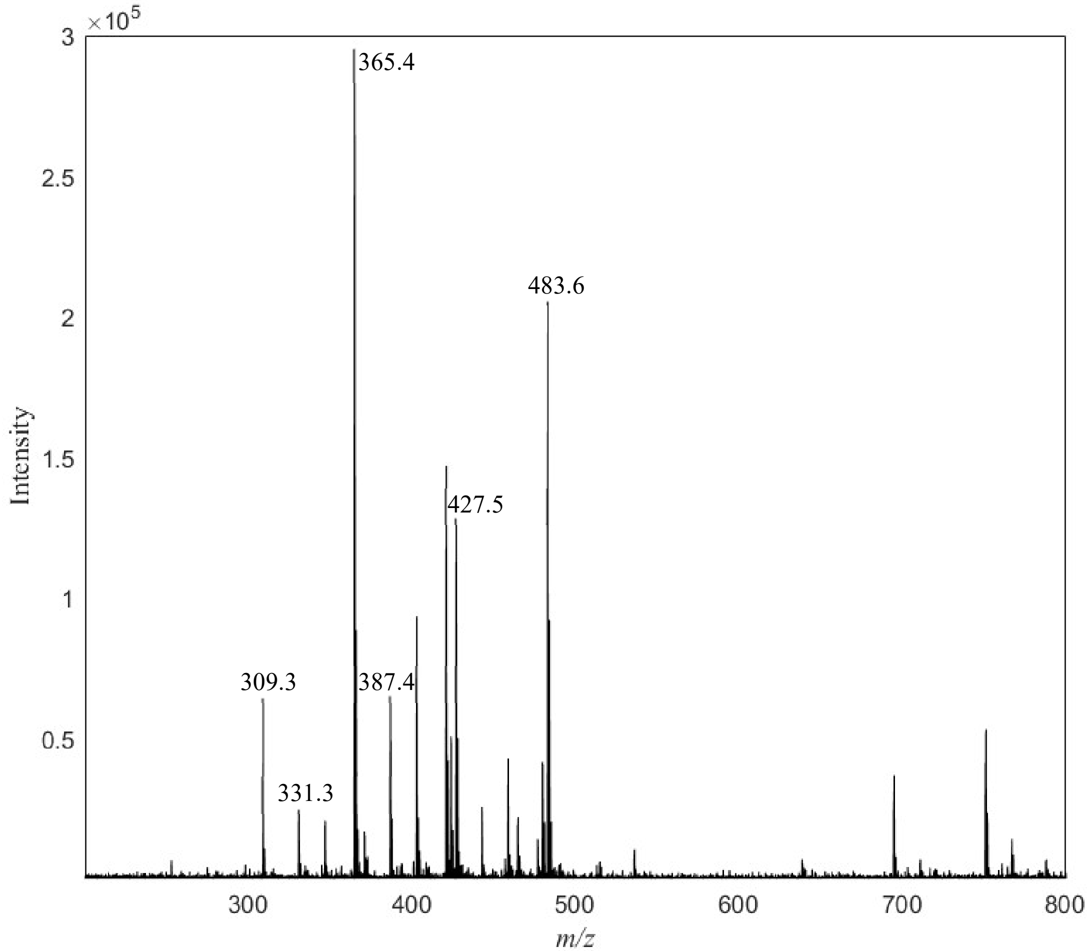

Figure 2.21: ESI-MS of reaction mixture resulting from reaction of THPC with 1-bromooctane and 1-bromobutane in positive ion mode

This second reaction attempt did appear to produce a tetrabutylphosphonium cation, shown by the peak at m/z 259 in the mass spectrum. The other two main peaks present in the spectra were found at 331 and m/z 639 which were unable to be assigned, but likely represent $[M+Na]^+$ and $[2M+Na]^+$ of the unidentified compound. A repeat of this reaction under nitrogen was carried out to reduce the potential oxidisation of phosphines within the reaction mixture. Tertiary phosphines are known to be sensitive to oxygen and decompose/oxidise quickly. Although THP is known to be moderately air stable compared to other tertiary phosphines, oxidation to the corresponding phosphine oxide may still occur. [28, 29] Therefore, the reaction was tested under nitrogen to reduce the chance of oxidation, and give an indication as to whether peaks found in previous product mixture were oxidised product peaks. However, the experiment under nitrogen found similar results, also producing a peak at m/z 309.

While results from the mass spectra of various attempted THPC reactions showed evidence that the tetraoctyl phosphonium and tetrabutyl phosphonium cations had been formed, due to time constraints and the appearance of other unidentified peaks in the spectra, further work on the synthesis and purification of a phosphonium cation mixture was deemed unfeasible for this project.

2.4 Conclusion

This chapter described the methods used and discussed the characterisation results for the successful synthesis of camphyl phenyl phosphinic acid. Characterisation using ^{1}H, ^{13}C and ^{31}P NMR, XRD, elemental analysis, and ESI-MS showed the presence of the pure product. With the success of this synthesis, camphyl phenyl phosphinic acid was used in further work as an ion precursor in the synthesis of ionic liquids described in the following chapter.

Other syntheses were attempted, including the synthesis of $CamP(O)(OH)(CH_2N^iBu_2)$. This synthesis showed some success, with ESI-MS providing some evidence of the desired starting material. Unfortunately, further work on this was not pursued due to difficulties faced with low yields and purification of the product. The reaction of THPC with bromoalkanes was also carried out with the aim of producing a mixture of phosphonium cations. Despite showing some evidence of phosphonium cations in the ESI-MS results, further work on this reaction was also abandoned due to time constraints and a complicated mass spectrum with a series of unidentified peaks.

2.5 References

[1] Williams, R. H.; Hamilton, L. A., Disubstituted phosphine oxides and disubstituted phosphinic acids. II. The di-n-alkyl series 1. *Journal of the American Chemical Society* **1955,** *77* (12), 3411-3412.

[2] Montchamp, J. L., Recent advances in phosphorus–carbon bond formation: Synthesis of H-phosphinic acid derivatives from hypophosphorous compounds. *Journal of Organometallic Chemistry* **2005,** *690* (10), 2388-2406.

[3] Deprele, S.; Montchamp, J.-L., Triethylborane-initiated room temperature radical addition of hypophosphites to olefins: Synthesis of monosubstituted phosphinic acids and esters. *The Journal of Organic Chemistry* **2001,** *66* (20), 6745-6755.

[4] Antczak, M. I.; Montchamp, J.-L., AIBN-initiated radical reactions of ethyl phosphinate. *Synthesis* **2006,** *2006* (18), 3080-3084.

[5] Li, D. P.; Pan, X. Q.; An, L. T.; Zou, J. P.; Zhang, W., Manganese(III)-mediated selective diphenylphosphinoyl radical reaction of 1, 4-diaryl-1-butynes for the synthesis of 2-phosphinoylated 3, 4-dihydronaphathalenes. *The Journal of Organic Chemistry* **2014,** *79* (4), 1850-1855.

[6] Li, Z.; Fan, F.; Zhang, Z.; Xiao, Y.; Liu, D.; Liu, Z. Q., A silver-initiated free-radical intermolecular hydrophosphinylation of unactivated alkenes. *RSC Advances* **2015,** *5* (35), 27853-27856.

[7] Huang, Z.; Chen, Y.; Kanan, M. W., Hypophosphite addition to alkenes under solvent-free and non-acidic aqueous conditions. *Chemical Communications* **2022,** *58* (13), 2180-2183.

[8] Mimeau, D.; Delacroix, O.; Gaumont, A. C., Regioselective uncatalysed hydrophosphination of alkenes: A facile route to P-alkylated phosphine derivatives. *Chemical Communications* **2003,** (23), 2928-2929.

[9] Leach, M. T. O. Organophosphorus chemistry of camphene. PhD Thesis, University of Waikato, 1999.

[10] Tramontini, M.; Angiolini, L., *Mannich bases-chemistry and uses*. CRC Press: 1994; Vol. 5.

[11] Arend, M.; Westermann, B.; Risch, N., Modern variants of the Mannich reaction. *Angewandte Chemie International Edition* **1998,** *37* (8), 1044-1070.

[12] Keglevich, G.; Szekrenyi, A.; Sipos, M.; Ludanyi, K.; Greiner, I., Synthesis of cyclic aminomethylphosphonates and aminomethyl ‐ arylphosphinic acids by an efficient microwave ‐ mediated phospha ‐ mannich approach. *Heteroatom Chemistry: An International Journal of Main Group Elements* **2008,** *19* (2), 207-210.

[13] Varga, T. R., Synthesis of bis (aminomethyl)-phosphinic acids via a Mannich reaction. *Synthetic Communications* **1997,** *27* (17), 2899-2903.

[14] Sell, C. S., Chapter 5: Bicyclic monoterpenoids. In *Fragrant introduction to terpenoid chemistry*, Royal Society of Chemistry: Cambridge, United Kingdom, 2003; pp 99-101.

[15] Perveen, S.; Al-Taweel, A., *Terpenes and terpenoids: Recent advances*. BoD–Books on Demand: 2018.

[16] Frank, A. W.; Daigle, D. J.; Vail, S. L., Chemistry of hydroxymethyl phosphorus compounds: Part III. Phosphines, phosphine oxides, and phosphonium hydroxides. *Textile Research Journal* **1982,** *52* (12), 738-750.

[17] Woodward, G.; Padda, R. S.; Regius, C. T. Organophosphines. 2002.

[18] Henderson, W.; Hoye, P. A. T. Camphyl phosphonic acid. 1994.

[19] Dolomanov, O. V.; Bourhis, L. J.; Gildea, R. J.; Howard, J. A.; Puschmann, H., Olex2: A complete structure solution, refinement and analysis program. *Journal of Applied Crystallography* **2009,** *42* (2), 339-341.

[20] Bourhis, L. J.; Dolomanov, O. V.; Gildea, R. J.; Howard, J. A.; Puschmann, H., The anatomy of a comprehensive constrained, restrained refinement program for the modern computing environment–olex2 dissected. *Acta Crystallographica Section A: Foundations and Advances* **2015,** *71* (1), 59-75.
[21] Kuveke, R. E.; Barwise, L.; van Ingen, Y.; Vashisth, K.; Roberts, N.; Chitnis, S. S.; Dutton, J. L.; Martin, C. D.; Melen, R. L., An international study evaluating elemental analysis. *ACS Central Science* **2022,** *8*, 855-863.
[22] Gholivand, K.; Fallah, N.; Valmoozi, A. A. E.; Gholami, A.; Dusek, M.; Eigner, V.; Pooyan, M.; Mohammadpanah, F., Synthesis and structural characterization of phosphinate coordination polymers with tin(IV) and copper(II). *Journal of Molecular Structure* **2020,** *1202*, 127369.
[23] Cornet, S. M.; Dillon, K. B.; Howard, J. A.; Monks, P. K.; Thompson, A. L., Hydrogen bonding and short contacts in [2, 4, 6-tris(trifluoromethyl)phenyl] phosphinic acid. *Acta Crystallographica Section C: Crystal Structure Communications* **2009,** *65* (5), o195-o197.
[24] Henderson, W.; Leach, M. T.; Nicholson, B. K.; Sabat, M., Self-assembly of a columnar polymeric calcium phosphinate derived from camphene. *Journal of the Chemical Society, Dalton Transactions* **1995,** (12), 2109-2110.
[25] Carson, I.; Healy, M. R.; Doidge, E. D.; Love, J. B.; Morrison, C. A.; Tasker, P. A., Metal-binding motifs of alkyl and aryl phosphinates; versatile mono and polynucleating ligands. *Coordination Chemistry Reviews* **2017,** *335*, 150-171.
[26] Giancotti, V.; Giordano, F.; Ripamonti, A., The structure of beryllium di‐n‐butyphosphinate poymer. *Die Makromolekulare Chemie: Macromolecular Chemistry and Physics* **1968,** *120* (1), 96-102.
[27] Giancotti, V.; Ripamonti, A., Isomorphism and polymorphism in zinc(II) and cobalt(II) phosphinate polymers. *Journal of the Chemical Society A: Inorganic, Physical, Theoretical* **1969**, 706-713.
[28] Saravana Bharathi, D.; Sridhar, M. A.; Shashidhara Prasad, J.; Samuelson, A. G., The first copper(I) complex of tris(hydroxymethyl)phosphine. *Inorganic Chemistry Communications* **2001,** *4* (9), 490-492.
[29] Moiseev, D. V.; James, B. R., Air-stability of aqueous solutions of $(HOCH_2)_3P$ and $(HOCH_2CH_2CH_2)_3P$. *Inorganica Chimica Acta* **2011,** *379* (1), 23-27.

Chapter 3
Preparation of Ionic Liquids

3.1.1 Ionic Liquid Synthesis

Some of the different methods used to make ionic liquids have been discussed previously in Chapter 1. There were two methods of interest for this work which were used to form a series of ILs. The first method used was a neutralisation reaction between a phosphinic acid and tetrabutylphosphonium hydroxide. The second method was a protonation method between bis- and tris- (2-ethylhexyl) amines and a range of phosphinic acids. As these ILs were to be applied to methods for REE separations with ion precursors selected in the hopes of ensuring the formed salts would (1) form as a liquid (2) be hydrophobic and (3) be suitable for REE separation. Some of these considerations have been briefly discussed in Chapter 1. In order to make the IL more hydrophobic, ion precursors with large alkyl side chains were selected. The presence of these were also to help lower the melting point of the IL. Finally, phosphinic acid anion precursors were selected as these were likely to be suitable to REE extractions due to the success of organophosphorus extractants, particularly phosphinic acids, for REE separations.

3.2 Experimental

3.2.1 Materials

Tetrabutylphosphonium hydroxide (40 % w/w), bis(2-ethylhexyl) amine, and tris(2-ethylhexyl) amine were sourced from Sigma Aldrich. 65 % nitric acid was sourced from Merck. Cyanex272 was sourced from Cyanamid. Ethanol was drum grade. Di-n-hexyl phosphinic acid and di-n-octyl phosphinic acid were supplied using previously reported method. [1] Camphyl phosphinic acid was also prepared using a previously described method. [2] Camphyl phenyl phosphinic acid was prepared using the method described in Chapter 2. Phenolphthalein indicator used was a 2% solution in ethanol.

3.2.2 General Methods and Instrumenatation

ESI-MS:

The mass spectra of ionic liquids were prepared by dissolving the sample in methanol in Eppendorf tubes. Samples were centrifuged prior to testing to separate undissolved material from the dissolved sample. Spectra were recorded using a Bruker Daltonics MicroTOF electrospray ionisation mass spectrometer, with a capillary exit voltage of 150 V and a skimmer 1 voltage of 50 V unless otherwise stated. ESI-MS results for ionic liquids report the cation, $[C]^+$, and the anion $[A]^-$.

ICP-MS:

Samples were prepared for ICP-MS analysis by diluting to suitable concentration (roughly 500 ppb for REEs). 9.8 mL diluted sample was added to a 15 mL falcon tube with 0.2 mL concentrated nitric acid. ICP-MS analysis was carried out internally when available, or externally by Analytica Laboratories, Hamilton. All samples were made up with type 1 water as required for ICP-MS analysis.

3.2.3 Synthesis of [P(butyl)$_4$][(hexyl)$_2$POO]

Di-hexylphosphinic acid (2.97 g) was dissolved in ethanol (20 mL) and a drop of phenolphthalein indicator solution was added. Tetrabutylphosphonium hydroxide was added until the mixture turned a pale pink to indicate the completion of the reaction (roughly 15 mL). The solvent and some of the water by-product was removed by rotary evaporation. The product was dried further under vacuum until it reached a constant mass, resulting in a clear, colourless and slightly viscous liquid. ESI-MS $[C]^+$ m/z 259.3 $[A]^-$ m/z 233.2.

3.2.4 Synthesis of [P(butyl)$_4$][Cyanex272] 4

Ionic liquid **3** was prepared by a similar method to **2.** Cyanex 272 (5.43 g) was added as the anion precursor, and tetrabutylphosphonium hydroxide used as the cation precursor. The product was a clear, colourless liquid. ESI-MS $[C]^+$ m/z 242.3 $[A]^-$ m/z 289.2.

3.2.5 Synthesis of $[(EH)_3NH][(octyl)_2POO]$ 5

Di-n-octylphosphinic acid (2.71 g) was added tris(2-ethylhexyl)amine (3.30 g). The mixture was placed in a water bath (60-70 °C) and left to stir until a clear liquid formed. The sample formed as a white solid as it cooled to room temperature. Melting Point: 30-78 °C. ESI-MS $[C]^+$ m/z 354.4 $[A]^-$ m/z 289.2.

3.2.6 Synthesis of $[(EH)_2NH_2][(octyl)_2POO]$ 6

Di-n-octylphosphinic acid (2.29 g) was added to bis(2-ethylhexyl)amine (1.93 g), following the same method described to make **4**. The product was a clear, colourless liquid. ESI-MS $[C]^+$ m/z 242.3 $[A]^-$ m/z 289.2.

3.2.7 Synthesis of $[(EH)_3NH][(cam)HPOO]$ 7

Using the same method described for **5**, camphyl phosphinic acid (2.00 g) was added to tris(2-ethylhexyl)amine (3.75 g). This produced a clear colourless liquid which partially crystallised upon cooling. ESI-MS $[C]^+$ m/z 354.4 $[A]^-$ m/z 201.1.

3.2.8 Synthesis of $[(EH)_2NH_2][(cam)HPOO]$ 8

Using the same method described for **4**, camphyl phosphinic acid (1.98 g) was added to bis(2-ethylhexyl) amine (2.53 g), forming a clear yellow viscous liquid. ESI-MS $[C]^+$ m/z 242.3 $[A]^-$ m/z 201.1.

3.2.9 Synthesis of $[(EH)_3NH][(cam)(Ph)POO]$ 9

Camphyl phenyl phosphinic acid (0.97 g) and tris(2-ethylhexyl) amine (1.23 g) was dissolved in ethanol (20 mL). The mixture was stirred at room temperature for 1 hour. The solvent was removed by rotary evaporation to give a white waxy solid. ESI-MS $[C]^+$ m/z 354.4 $[A]^-$ m/z 277.2.

3.2.10 Synthesis of $[(EH)_2NH_2][(cam)(Ph)POO]$ 10

Using the same method described for **8**, camphyl phenyl phosphinic acid (1.21 g) was added to bis(2-ethylhexyl)amine (1.06 g). The product was a slightly viscous clear pale-yellow liquid. ESI-MS $[C]^+$ m/z 242.3 $[A]^-$ m/z 277.1.

3.2.11 Synthesis of $[(EH)_3NH][Cyanex272]$ 11

Cyanex 272 (4.99 g) was mixed with tris(2-ethylhexyl) amine (6.06 g) for 1 hour until a single homogenous layer formed. The product was a clear colourless liquid. ESI-MS $[C]^+$ 354.4 m/z $[A]^-$ 289.2 m/z.

3.2.12 Synthesis of $[(EH)_2NH_2][Cyanex272]$ 12

Cyanex 272 (7.96 g) was mixed with bis(2-ethylhexyl) amine (6.66 g) for 1 hour until a single homogenous layer formed. The product was a clear, pale-yellow liquid. ESI-MS $[C]^+$ 242.3 m/z $[A]^-$ 289.3 m/z.

3.2.13 Solubility tests of ionic liquids

Visual solubility tests were carried out by mixing a few drops of each ionic liquid in an excess of water. Those which did not appear to dissolve in water were further tested using the following solubility test.

The ionic liquid (1 g) was added to 20 mL water and stirred using a magnetic stir bar for 24 hours to create a saturated solution. The aqueous layer was centrifuged for 2 minutes at 2500 rpm to separate any remaining IL droplets from the water. The samples were prepared for ICP-MS analysis and tested for phosphorus content.

3.3 Results and Discussion

3.3.1 Ionic Liquid Preparation

Two methods were used to prepare a series of ILs. The initial neutralisation method was used to successfully make two ionic liquids (Figure 3.1). However, the samples required long drying times to remove the water, which was produced as a by-product, and present in the tetrabutylphosphonium hydroxide used.

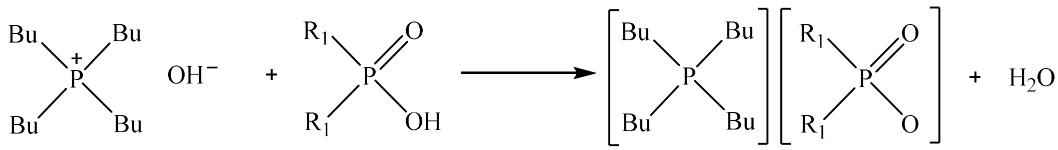

2 R_1= hexyl
3 R_1= 2,4,4-trimethylpentyl

Figure 3.1: Neutralisation reaction used to create ILs

The protonation method was successfully used to make ILs **5-12** (Figure 3.2). The structures of the cations and anions used in the protonation method are shown in Figure 3.3. For those made using Cyanex272, no solvent or heat was required, and with no by-product produced, no further steps were required once the ionic liquid had formed. It should be noted that $[Cyanex272]^-$ reported in square brackets does not strictly describe the phosphinic acid, Cyanex272, but rather the corresponding phosphinate.

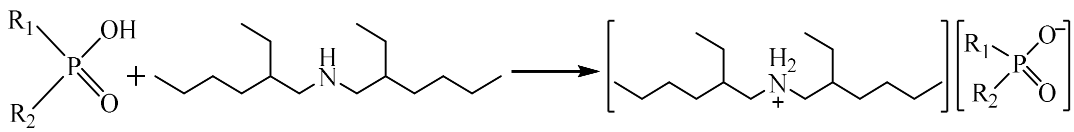

Figure 3.2: Protonation reaction of phosphinic acid and amine to produce ionic liquids **5-12**

Unlike Cyanex272. the other anion precursors are all solid at room temperature, which resulted in difficulty when stirring the anion and cation precursors. Without the presence of heat or a solvent, the reaction failed to produce the desired single homogenous liquid layer. For the ionic liquids produced using anion precursors di-n-octyl phosphinic acid and camphyl phosphinic acid, heating the reaction mixture helped the desired IL reaction to occur. For these reactions, $[(EH)_2NH_2][(oct)_2POO]$ and $[(EH)_2NH_2][camHPOO]$ formed as liquids, however, $[(EH)_3NH][(oct)_2POO]$ and $[(EH)_3NH][camHPOO]$ did not result in a liquid, but rather produced white mushy solids. The melting point test for $[(EH)_3NH][(oct)_2POO]$ showed a wide melting point range (30-78 °C). This suggests an impure product, which may be due to impurities within the starting materials, or may be due to the presence of starting materials within the sample as the amine used is liquid at room temperature, whereas di-n-octyl phosphinic acid is reported to have a higher melting point of 82 °C. [1]

Cations

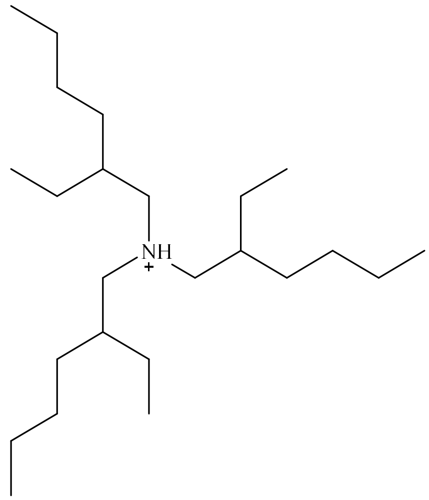

Tris(2-ethylhexyl) ammonium

$[(EH)_3NH]^+$

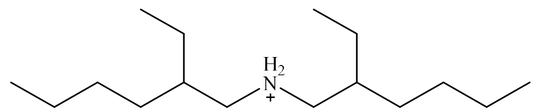

Bis(2-ethylhexyl) ammonium

$[(EH)_2NH_2]^+$

Anions

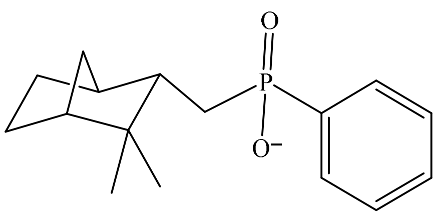

Camphyl phenyl phosphinate

$[CamPhPOO]^-$

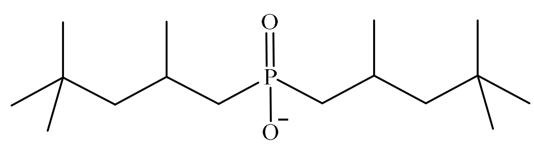

Cyanex272

$[Cyanex272]^-$

Camphyl phosphinate

$[CamHPOO]^-$

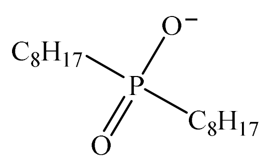

Di-n-octyl phosphinate

$[oct_2POO]^-$

Figure 3.3: Structure of cations and anions used to make hydrophobic ionic liquids.

A solvent was used to produce the ionic liquids using the anion precursor camphyl phenyl phosphinic acid. The heating of this reaction mixture did not work for this reaction, likely due to the higher melting point of camphyl phenyl phosphinic acid. The use of a solvent allowed the reaction to be carried out without heat but required an additional step to remove the solvent. The ionic liquids produced using this method also resulted in a white mushy solid when paired with the $[(EH)_3NH]^+$ cation, but a clear homogeneous liquid when paired with $[(EH)_2NH_2]^+$. This difference in melting point is likely due to the difference in size between the two cations, with the extra ethyl-hexyl group on the $[(EH)_3NH]^+$ cation resulting in more intermolecular forces between molecules, therefore raising the melting point.

3.3.2 Characterisation of ILs by ESI-MS

Each of the ILs prepared for this work were characterised by ESI-MS. When the capillary exit voltage was set at 150 V, the main ion peak observed in both the positive and negative ion modes were the expected peaks of the cation and anion respectively. At a lower capillary exit voltage of 90 V, more aggregates of ions appeared, as would be expected and as is observed in the literature. [3]

It is the positive ion mode mass spectra which are often of more interest as these often show a wider range of ion aggregates and more interesting grouping of ions which tend to involve both the cation (C) and anion (A). This is the case for $[(EH)_2NH_2]$[CamHPOO] whose mass spectrum is shown in Figure 3.4. In this example, the $[C]^+$ ion was observed at m/z 242.3, with other peaks assigned to represent the $[CA+H]^+$, $[C_2A]^+$ and $[2CA+H]^+$ ion aggregates at m/z 444.4, 685.7 and 887.8 respectively. For most reports of IL characterisation by MS, the most common aggregates which appear in the positive ion mode are of the type $[C_nA_{n-1}]^+$. [3-6] However, in the mass spectra obtained in this work, only the $[C_2A]^+$ cluster is observed, and this appears in a minority of spectra for the ILs.

ILs tested in negative ion mode at 90 V commonly produced peaks representing the $[A]^-$ ion. However, for some ILs, peaks representing aggregates of the molecular ion expected for the starting material are also observed. This can be seen in the example given for IL $[(EH)_2NH_2]$[CamHPOO] shown in Figure 3.5, where the $[A]^-$ is observed at m/z 201.1, and the $[2M-H]^-$ and $[3M-H]^-$ aggregates for the starting material are observed at m/z 403.2 and 605.3.

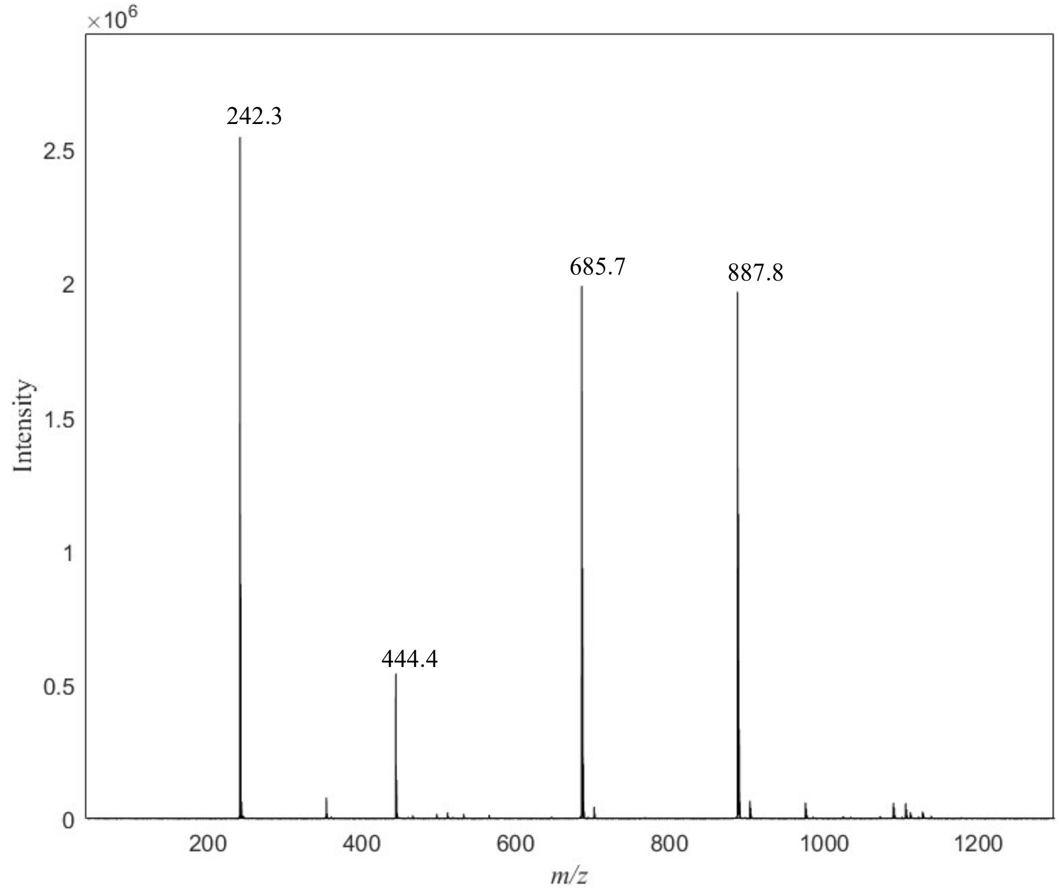

Figure 3.4: ESI-MS of $[(EH)_2NH_2][CamHPOO]$ in positive ion mode with a capillary exit voltage of 90V.

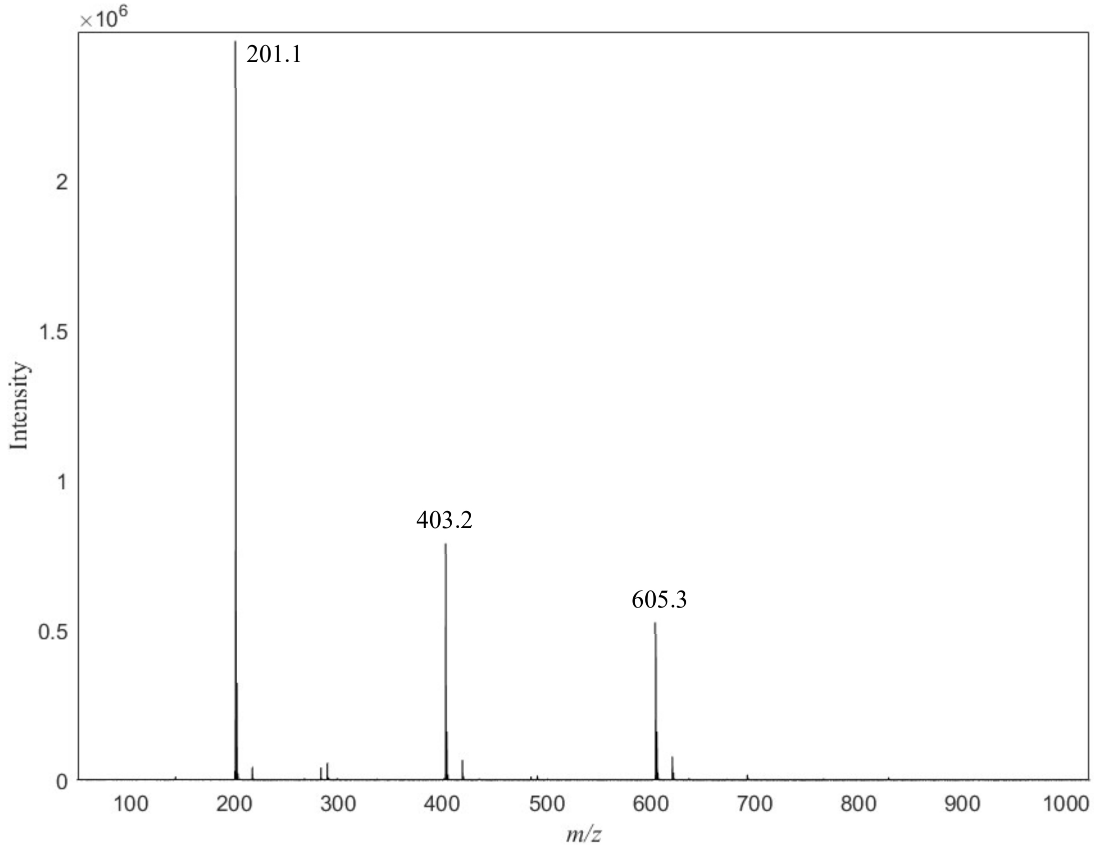

Figure 3.5: ESI-MS of $[(EH)_2NH_2][CamHPOO]$ in negative ion mode with a capillary exit voltage of 90V.

3.3.3 Solubility tests

Solubility tests were initially carried out visually, adding a drop of each IL to 10 mL water. Despite being previously reported as immiscible in water, [1] these visual solubility tests showed that the ionic liquids **2** and **3** were soluble in excess water. Therefore, these ionic liquids were not considered for neither the quantitative solubility tests, nor any further separation tests. The remaining ILs did not appear to dissolve in excess water, and their solubility was further tested using a quantitative test.

In the quantitative solubility tests, none of the ionic liquids were observed to have dissolved in water after 24 hours of stirring. It was therefore assumed that a saturated solution had formed as there was still plenty of undissolved material left.

From the ICP-MS results, the total IL in the saturated solution was determined from the phosphorus concentration. An example of this calculation is given in Appendix A with the results from these tests shown in Table 3.1.

Table 3.1: Results of solubility tests for ILs in water

Ionic Liquid	**Solubility (g/L)**	**Solubility (mol/L)**
$[(EH)_2NH_2][Cyanex272]$	0.293	0.000550
$[(EH)_3NH][Cyanex272]$	0.183	0.000552
$[(EH)_2NH_2][(octyl)_2POO]$	0.216	0.000406
$[(EH)_3NH][(octyl)_2POO]$	0.389	0.000604
$[(EH)_2NH_2][camHPOO]$	2.814	0.00634
$[(EH)_3NH][camHPOO]$	6.444	0.0116
$[(EH)_2NH_2][camPhPOO]$	1.318	0.00253
$[(EH)_3NH][camPhPOO]$	0.263	0.000416

These results show that the ionic liquids containing the $[camHPOO]^-$ anion have the highest solubility in water, while those containing the $[(octyl)_2POO]^-$ anion have some of the lowest solubilities in water. Computational studies as well as experimental studies have shown that the anion tends to have the predominant effect on the solubility of ILs in water with the cation alkyl chain length and cation family have a secondary influence on solubility. [7, 8] In their computational study, Zhou et al. [7] found that it was the hydrogen bonding between the anion and the water which had the largest effect on solubility.

The effect of the anion appeared to be inconsistent throughout the results, with ILs containing the $[(EH)_3NH]^+$ cation being more soluble than those containing the $[(EH)_2NH_2]^+$ where the anion is $[(octyl)_2POO]^-$ and $[camHPOO]^-$ while the opposite is true for the remaining ILs. Due to the additional ethyl-hexyl group present in the $[(EH)_3NH]^+$ cation, it would be expected that ILs containing this cation have lower solubilities as this group would decrease the polarity as well as the charge density on the cation. Additionally, $[(EH)_2NH_2]^+$ cation has two hydrogens which could be expected to increase solubility of the ionic liquids containing this ion as stabilisation through hydrogen bonding occurs in aqueous solution. However, the results suggest that there may be other factors contributing to the solubility, for example the interaction between the anion and cation may also affect solubility.

While the results from these solubility tests show the ionic liquids dissolving in water to some extent, it was decided that they were all sufficiently immiscible in water to be classed as hydrophobic. The calculated results showed that for most of the ILs, less than one gram of the IL would dissolve in one litre of water. However, compared to other hydrophobic ILs, the solubilities of those prepared in this work are quite high. [8, 9]

3.3.4 Suitability for Separation Experiments

Following the IL preparation experiments, five ionic liquids were deemed to be suitable for the separation experiments as they were found to be both liquid at room temperature and deemed sufficiently hydrophobic for the separation experiments. Some ionic liquids were disregarded as they were discovered to be soluble in water, while others had melting points above room temperature. The ILs chosen for the separation experiments were $[(EH)_2NH_2]$[Cyanex272], $[(EH)_3NH]$[Cyanex272], $[(EH)_2NH_2][(octyl)_2POO]$, $[(EH)_2NH_2]$[camHPOO], and $[(EH)_2NH_2]$[camPhPOO].

3.4 Conclusion

In this chapter, the successful synthesis of a range of phosphonium- and ammonium-based ionic liquids was described. These were formed through simple neutralisation and protonation methods, which in some cases were both solvent and heat free reactions. Many of the created ILs which contained the $[(EH)_3NH]^+$ cation resulting in a solid or partially solid product and so were not suitable to the desired rare earth element separation tests at room temperature using neat ILs. Solubility tests showed $[P(butyl)_4]$[Cyanex272] and $[P(butyl)_4][(hexyl)_2POO]$ to be soluble in water, but a total of five ionic liquids were deemed sufficiently insoluble in water for further testing as hydrophobic ionic liquids for rare earth separation methods described in the following chapter.

3.5 References

[1] Ying, L. Synthesis, characterisation and applications of novel ionic liquids. MPhil Thesis, University of Waikato, Hamilton, New Zealand, 2006.

[2] Leach, M. T. O. Organophosphorus chemistry of camphene. PhD Thesis, University of Waikato, 1999.

[3] Alfassi, Z.; Huie, R. E.; Milman, B.; Neta, P., Electrospray ionization mass spectrometry of ionic liquids and determination of their solubility in water. *Analytical and Bioanalytical Chemistry* **2003,** *377*, 159-164.

[4] Dorbritz, S.; Ruth, W.; Kragl, U., Investigation on aggregate formation of ionic liquids. *Advanced Synthesis & Catalysis* **2005,** *347* (9), 1273-1279.

[5] Jackson, G. P.; Duckworth, D. C., Electrospray mass spectrometry of undiluted ionic liquids. *Chemical Communications* **2004,** (5), 522-523.

[6] Zhao, D., Analysis of ionic liquids and dissolved species by electrospray ionization MS. *Australian Journal of Chemistry* **2004,** *57* (5), 509-509.

[7] Zhou, T.; Chen, L.; Ye, Y.; Chen, L.; Qi, Z.; Freund, H. R.; Sundmacher, K., An overview of mutual solubility of ionic liquids and water predicted by COSMO-RS. *Industrial & Engineering Chemistry Research* **2012,** *51* (17), 6256-6264.

[8] Freire, M. G.; Neves, C. M.; Carvalho, P. J.; Gardas, R. L.; Fernandes, A. M.; Marrucho, I. M.; Santos, L. M.; Coutinho, J. A., Mutual solubilities of water and hydrophobic ionic liquids. *The Journal of Physical Chemistry B* **2007,** *111* (45), 13082-13089.

[9] Freire, M. G.; Carvalho, P. J.; Gardas, R. L.; Marrucho, I. M.; Santos, L. M.; Coutinho, J. A., Mutual solubilities of water and the $[C_nmim][Tf_2N]$ hydrophobic ionic liquids. *The Journal of Physical Chemistry B* **2008,** *112* (6), 1604-1610.

Chapter 4
Separation of the Rare Earth Elements using SILs

4.1 Introduction

The use of ILs as extractants in separation methods has been discussed in Chapter 1. ILs have shown potential for many industrially important separations, including cobalt and nickel[1, 2] and the rare earth elements. [3, 4]

The mechanism for these separations are often reported to be either cation or anion exchange mechanisms, with cation exchange appearing to be the most commonly reported. [5] Aside from the ion exchange mechanism, ion pairing extraction mechanisms are also reported. [6] The cation exchange mechanism can be expressed by the following equation:

$$M^{n+}{}_{(aq)} + mC^{+}{}_{(IL)} + mA^{-}{}_{(IL)} \rightleftharpoons M(A)_{n\,(IL)}^{(m-n)-} + mC^{+}{}_{(aq)} \tag{4-1}$$

Where M^{3+} is the metal (of type MX_3) in the aqueous phase, and C and A represent the cation and anion of the ionic liquid respectively. This mechanism results in the loss of the cation to the aqueous phase as extraction takes place, resulting in the gradual dissolution of the ionic liquid over multiple runs. Ion pairing mechanisms are commonly observed in neutral extractants but has also been observed in ionic liquid extraction systems. This mechanism is shown in Equation 1-2.

$$M^{n+}{}_{(aq)} + nX^{-}{}_{(aq)} + mA^{-}{}_{(IL)} \rightleftharpoons M(A)_{n(IL)}^{(m-n)-} + nX^{-}{}_{(IL)} \tag{4-2}$$

Ion pairing mechanisms are often considered to be more desirable as they do not result in the dissolution of the ionic liquid phase over time as the ion exchange mechanisms do. However, those who report ion pairing mechanisms often find lower extraction efficiencies compared to those obtained via ion exchange mechanisms. It has been suggested that in some cases that there is not always a single mechanism at work. For example, in their study of tributyl(2-ethoxy-2-oxoethyl)ammonium-based ILs for the separation of copper(II), Messadi et al. found that a cation exchange and ion pairing mode were concurrently driving extraction. [6]

4.1.1 Cobalt Extractions

The extraction and separation of cobalt and nickel is of high industrial importance around the world. Nickel is important as it used to form alloys with chromium to produce stainless steel, while cobalt is of high technological importance as it is a key component to rechargeable batteries found in many electronic goods including mobile phones and electric vehicles. [7] These two elements are mined and separated from some of the same ores, and therefore methods of separation are of interest. [7]

Aside from the industrial importance of cobalt, there are a few other reasons for the interest in cobalt extraction in this work. Many methods of cobalt extraction use organophosphorus extractants, such as the alkyl phosphoric, alkyl phosphonic and alkyl phosphinic acids commonly used for the extraction of the REEs. [8] For example, Cyanex272, which has been widely considered for REE extractions, was designed for cobalt/nickel separations achieving high separation factors which range in the thousands.

Upon extraction, cobalt also undergoes a colour change as it changes from octahedral coordination (pink) to tetrahedral coordination (blue). [9] Therefore, cobalt extraction tests provide quick visual confirmation that a particular extractant works for cobalt extraction, and therefore provide some indication as to whether a particular extractant is likely to work for the separation of rare earth elements which are too palely coloured to give visual evidence of extraction.

4.1.2 Separation Calculations

To describe and compare the extraction and separation abilities of different ionic liquids, a few different calculations can be done. Many papers report the distribution ratios and/or extraction efficiencies of separation methods involving the use of ionic liquids.

The distribution constant, or partition coefficient (Eq. 4-3) provides information about the extraction of a solute from the aqueous phase to the ionic liquid phase, taking into account the concentration of the solute in the IL phase and the aqueous phase after extraction has occurred. When the solute of interest only exists in the method in one form, this equation is the same as the distribution ratio (D). The larger this value, the better the extraction of the solute into the second phase.

$$D = \frac{[M]_{IL}}{[M]_{aq}} \tag{4-3}$$

In Equation 1-3, $[M]_{IL}$ is the concentration of the solute in the IL phase, and $[M]_{aq}$ is the concentration of the solute in the aqueous phase after extraction. The extraction efficiency can be calculated as a percentage (Eq. 4-4) to show the amount of solute extracted into the ionic liquid phase.

$$\%E = \frac{[M]_{IL}}{[M]_{aq}} \times 100 \tag{4-4}$$

When there are two solutes of interest in the extraction, the separation factor (β) can also be calculated from the distribution ratios of the individual solutes (Eq. 4-5). A large separation factor will indicate that the method used is suitable for the separation of two solutes. A large separation factor is often desired, however for some metals, such as cobalt and nickel, and many of the REEs, this can be difficult to achieve due to the similar properties of neighbouring elements.

$$\beta_{M_2}^{M_1} = \frac{D_{M_1}}{D_{M_2}} \tag{4-5}$$

Following the extraction, the separated elements are stripped from the column. The stripping method can be tested by calculating the stripping efficiency (Eq. 4-6) where $[M]_{aq}$ is the concentration of the solute in the aqueous solution used for stripping, and $[M]_{IL}$ is the concentration of the solute in the ionic liquid phase after extraction.

$$S\% = \frac{[M]_{aq}}{[M]_{IL}} \times 100 \tag{4-6}$$

For the separation of rare earth elements using ionic liquid extractant, a range of separation factors and extraction efficiencies have been reported. For example, using a liquid-liquid extraction method with the ammonium-based tricaprylmethylammonium dihexyl diglycolate, [A366][DHDGA], in a chloroform system, Khodakarami and Alagha reported high separation factors between the light and heavy rare earth elements, achieving separation factors as high as 1266.2 for the separation of lanthanum and erbium. [10] Separation factors between neighbouring elements in the periodic table were significantly lower, with a separation factor of 3.9 achieved for Pr/Nd. Therefore, it was suggested that this tested ionic liquid could be useful for separating the heavy rare earth elements (HREEs) and the light rare earth elements (LREEs). In another study, carboxylic acid-functionalised imidazolium ILs were found to selectively extract scandium from other rare earth elements, achieving extraction efficiencies as high as 99.5%, and large separation factors in the range of 10^3. [11]

There are a range of reports of REE separations using various ionic liquids and extraction methods, some of which showing that high extraction efficiencies and high separation factors can be achieved by ionic liquid extractants. Some of these methods can be read in reviews on the topic by Baba et al[12], Okamura et al. [13] and Barrueto et al.[14]

In this chapter, the applicability of the selected ionic liquids as extractants for the separation of the REEs will be tested. Extractions of cobalt are also tested as the separation of cobalt and nickel is another industrially important separation. Many of these separations use organophosphorus extractants, similar to those used in REE separations. Furthermore, cobalt is brightly coloured, and undergoes a colour change from pink to blue when extracted as it changes from octahedral to tetrahedral coordination. Therefore, cobalt provides a good visual indication of the applicability of the chosen IL extractants to REE separation.

4.2 Experimental

4.2.1 Materials

Concentrated nitric acid was obtained from Merck, and hydrochloric acid from Thermofisher. Cobalt(II) acetate tetrahydrate, lanthanum(III) nitrate hexahydrate and 80 mesh glass beads were from BDH Chemicals. Nickel(II) chloride hexahydrate came from M&B. Dyprosium(III) nitrate hydrate, ytterbium(III) nitrate pentahydrate, praseodymium(III) nitrate hexahydrate, gadolinium(III) nitrate hexahydrate, neodymium(III) nitrate hexahydrate, samarium(III) nitrate hexahydrate, and cerium(III) nitrate hexahydrate were sourced from Sigma Aldrich.

A solution of cobalt and nickel was made by dissolving cobalt(II) acetate tetrahydrate (0.09 g) and nickel(II) chloride hexahydrate (0.08 g) in type 1 water (250 mL). A lanthanum solution for liquid-liquid extraction tests was made by adding lanthanum(III) nitrate hexahydrate (0.14 g) to type 1 water (20 mL). For column separation tests, a lanthanum solution was made by dissolving lanthanum(III) nitrate hexahydrate (0.015 g) in type 1 water (100 mL). For the same purpose, a ytterbium solution was made by dissolving ytterbium(II) nitrate pentahydrate (0.016 g) in type 1 water (100 mL). A mixed lanthanide solution was made by dissolving the nitrates of lanthanum, cerium, praseodymium, neodymium, gadolinium, samarium, dysprosium, and ytterbium (0.043-0.045 g) in type 1 water (100 mL).

4.2.2 General Methods and Instrumentation

SEM:

Glass beads coated with [$(EH)_2NH_2$][Cyanex272] at 0, 0.5, 1, and 2 wt% were prepared for SEM by coating the samples in platinum using a Quorum 150v ESplus. SEM images were produced on a Hitachi Regulus SU8230 FE-SEM. SEM observations were carried out at 3.0 kV.

4.2.3 Liquid-liquid extraction

Cobalt extraction:

[$(EH)_2NH_2$][Cyanex272] (1 mL) was added to a cobalt solution (1 mL, 0.012 g L^{-1}) and stirred vigorously using a magnetic stirbar. Observations on the colour change were made after 10 s, 30 s, 60 s, 2 min, and 5 min.

Lanthanum extraction:

Lanthanum solution (2 mL, 2.06 g L^{-1}) was added to 1 mL IL and stirred with a stirbar for 2 minutes. The aqueous layer was removed from the IL layer and centrifuged for 5 minutes to ensure separation of remaining IL droplets from the aqueous layer. The aqueous layer was prepared for ICP-MS analysis as described above in **Section 4.2.2**. The same method was repeated with stirring for 30 minutes. These lanthanum liquid-liquid extractions were carried out using each of the ILs.

4.2.4 Column Preparation

Glass beads were prepared by adding the beads (10 g) to the IL (0.1 g) dissolved in pentane (20 mL). The solvent was removed by rotary evaporation, which also helped to evenly coat the beads. For small scale column separation experiments, glass wool was added to a Pasteur pipette, before loading the coated beads (3.1 – 3.2 g) down the pipette.

The column was preconditioned with Type 1 water (5 mL), followed by HCl (2 mL, 1 M), and another 5 mL water.

4.2.5 Scanning Electron Microscopy (SEM)

Glass beads coated with $[(EH)_2NH_2]$[Cyanex272] at 0, 0.5, 1, and 2 wt% were prepared for SEM by coating the samples in platinum using a Quorum 150v ESplus. SEM images were produced on a Hitachi Regulus SU8230 FE-SEM. SEM observations were carried out at 3.0 kV. Prior to coating glass beads with the IL, the IL was dried thoroughly to remove any remaining volatiles.

4.2.6 Column Separations

Cobalt/Nickel Separation:
A cobalt/nickel solution (Co^{2+} 9.3 g L^{-1}, Ni^{2+} 7.7 g L^{-1}) was made using cobalt(II) acetate hexahydrate and nickel(II) chloride hexahydrate. For the separation experiments, the cobalt/nickel solution (4 mL) was passed through the column and the eluate collected. The column was stripped using HCl (2 mL, 1M) and washed with Type 1 water (5 mL). This was repeated using the same column for 10 runs. The 1st, 2nd, 4th, 6th, 8th, and 10th collected eluates were made up as ICP-MS samples and analysed.

Lanthanide Extractions:
Following the same method as described above for cobalt/nickel separations, column separations of individual lanthanide elements, La and Yb, were carried out, followed by separation of combined La and Yb elements. Further separation tests were also carried out using an aqueous solution containing a mixture of eight lanthanide elements. These tests were all done as duplicates. Following extraction, the column was stripping using HCl (2 mL, 1M). The eluate of each stripping experiment was collected and prepared as samples for ICP-MS analysis.

4.3 Results and Discussion

4.3.1 Cobalt liquid-liquid extractions

The extraction of cobalt using the liquid-liquid extraction method was observed visually through the exchange of colour from the pale-pink aqueous cobalt solution to bright blue IL containing the extracted cobalt. The colour changes over the different time intervals can be observed in Figure 4.1. These show a fast extraction, with the most significant colour change occurring in under two minutes. The observed speed of this extraction indicates the suitability of the proposed column extraction method as extraction is likely able to occur within the time it takes the solution to pass through the column. It was predicted that the extraction of the lanthanides would occur faster than cobalt as is observed that ligand exchange in lanthanide hexaaqua complexes is typically faster than ligand exchange in similar cobalt complexes. [15]

Figure 4.1: Cobalt liquid-liquid extractions after 0 s, 10 s, 30 s, 2 min, and 10 min of stirring.

4.3.2 SEM images of IL-coated glass beads

In order to create supported ionic liquids, a support was selected. Glass beads were used as they are known to be robust, uniform in size and inert with a low surface area. [16] Images were collected of the glass beads coated with varying amounts of IL $[(EH)_2NH_2][Cyanex272]$. These images are shown in Figure 4.2. These images showed that the coating of the glass beads with the IL appeared to produce a reasonably even layer of IL on the glass beads. The coating was more pronounced on the 1% and 2% coated beads as not only was the change to the appearance of the surface area of the beads observed, but the IL film was easily visible in the way beads stuck together more with these higher coatings.

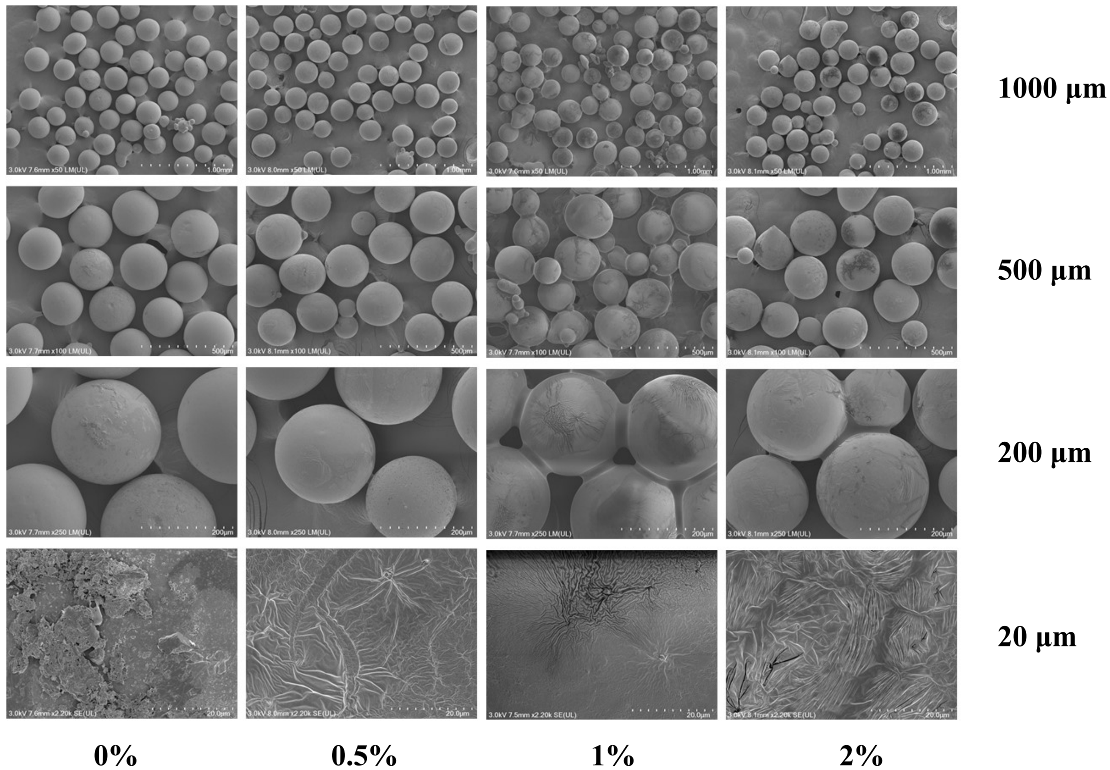

Figure 4.2: SEM images of glass beads coated with 0, 0.5, 1 and 2 wt% [$(EH)_2NH_2$][Cyanex272] IL. The magnification values given on right hand side refer to the size of the scale bar.

4.3.3 Cobalt-Nickel Column Separation

Initial column separation tests were completed as visual tests using cobalt and nickel. These metals were chosen as they are strongly coloured and would therefore give an immediate indication that the method was working for separation of elements from aqueous solution. Organophosphorus extractants, similar to those used in the extraction of the REEs, are applied to cobalt-nickel separations. Therefore, initial tests with cobalt provides a good indication of the potential applicability of the ILs for REE extraction.

With beads in the column coated with [$(EH)_2NH_2$][Cyanex272], a strong colour change for the cobalt test was observed, with the pale pink solution turning the beads blue as it passed through the column. This indicated the extraction of the cobalt from solution onto the beads, with the colour change caused by the change in cobalt from octahedral coordination to tetrahedral coordination.

A transfer of colour was also observed for separation tests with iron and nickel, turning the column orange and green respectively. The change of colour for the nickel tests were less pronounced, with the column becoming pale green. While the Ni complex is not likely to be as strongly coloured as the cobalt complex, the aqueous solution also retained some of its green colour, whereas the cobalt column eluate appeared to have lost all of its pale pink colouring. This may suggest that the IL can extract more cobalt than nickel. The quantitative extraction tests for cobalt/nickel separation confirmed this was the case, showing that IL $[(EH)_2NH_2][Cyanex272]$ was capable of extracting both cobalt and nickel, with a preference for cobalt extraction. This selectivity towards cobalt is not surprising given the inclusion of Cyanex272 as the anion in this IL which has been designed for the separation of cobalt from nickel, with reported separation factor of 7000 between pH of 5.3-5.5.[17]

Figure 4.3 shows the extraction efficiencies for both cobalt and nickel over multiple runs. Cobalt was found to have an average extraction efficiency of 67.7 % (range: 63.4 – 69.4%), and nickel had an average extraction efficiency of 24.4% (range: 21.6 - 26.9%). The average separation factor across the 10 runs was found to be 2.79. A summary of the results from individual runs is given in Appendix B.

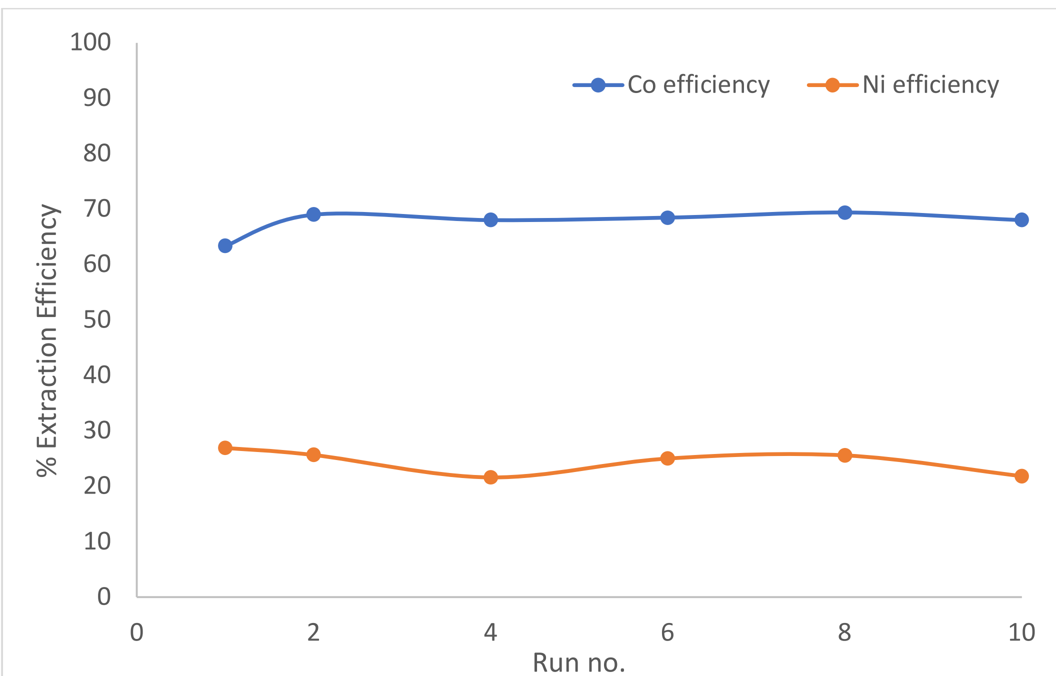

Figure 4.3: Cobalt/nickel column separation experiments over 10 runs

The extraction efficiencies, and in particular the separation factor, are comparably lower to many of the values reported in literature for the separation of cobalt and nickel using

ILs. For example, using an ionic liquid synthesised with n-octylamine and Cyanex 272 as ion precursors, Jing et al. were able achieve selective cobalt extraction with a separation factor of 976.9. In this method, a two-stage cross-flow extraction was used, with the aqueous solution undergoing two extraction steps in the diluted ionic liquid. [18]

In another study by Zante et al., the undiluted ionic liquid, trihexyl(tetradecyl)phosphonium chloride ([P_{66614}][Cl]) was used to create a supported ionic liquid membrane (SILM) and tested for cobalt/nickel separation. [19] Following a 1-hour extraction, cobalt extraction efficiencies reached 86%, and Co/Ni separation factors of 218 were achieved. Using the sample ionic liquid, separation factors as high as 50000 were achieved with undiluted phosphonium based ionic liquid, [P_{66614}][Cl], by Wellens et al. [2]

Therefore, compared to results discussed in the literature, the Co/Ni separation factor achieved by [$(EH)_2NH_2$][Cyanex272] in this work is low. However, the conditions for the above extractions are quite different to the conditions used for extraction with [$(EH)_2NH_2$][Cyanex272]. For example, Jing et al. used a two-stage cross-flow extraction method involving two subsequent 40 minute extraction steps. [18] Zante et al. created a supported ionic liquid phase using a polyvinylidene fluoride (PVDF) film and undiluted ionic liquid, however, they exposed the aqueous IL phase to their supported ionic liquid phase (SILP) for 60 minutes. In the final example given, Wellens et al. also achieved their results using a solvent extraction method, with intense stirring of the two phases for 10 minutes at 60°C. In all these example, larger contact times and higher temperatures likely contributed to the higher reported extraction efficiencies and separation factors. If tested using similar conditions, the separation of cobalt and nickel with [$(EH)_2NH_2$][Cyanex272] may see significant improvement of results.

The results from the repeated extraction experiments shown in Figure 4.3 show the stability of the column over multiple runs. After 10 runs, no significant decrease in extraction efficiencies was observed, indicating there is little loss of the ionic liquid over the course of multiple extraction and stripping steps. This recyclability of the column is highly advantageous because, once prepared, the column can carry out multiple extractions in a few easy and straightforward steps. While the extraction mechanism of the ionic liquids is not studied in this work, the stability of the column over multiple runs suggests that an ion pairing mechanism may be driving the extraction. However, stable extractions like these may also be observed where a combination of ion exchange and ion pairing mechanisms are acting. [6] However, with the use of a hydrophobic IL, it would be expected that minimal loss of the IL to the aqueous phase would occur.

4.3.4 Lanthanum Liquid-Liquid Extractions

The extraction efficiencies for the lanthanum liquid-liquid extractions are shown in Table 4.1. After an extraction time of 2 minutes, $[(EH)_2NH_2]$[Cyanex272] had extracted the most lanthanum from solution (96%), while $[(EH)_2NH_2]$[camPhPOO] had extracted the least, with results suggesting it had extracted -1.4% of the lanthanum from solution. This result suggests there was more lanthanum in the aqueous layer after extraction than there was to begin with, indicating the sample may not have been prepared or diluted correctly, or that the sample may have been contaminated with lanthanum from elsewhere. This result may be anomalous as the 30-minute experiment result shows good extraction and appears normal. A repeat of the 2-minute experiment may be useful to confirm this.

The remaining ionic liquids showed some promise for lanthanum extraction, all ranging from 26-54% extraction efficiency for the 2-minute extraction test. After the 30 minute extraction of lanthanum, all of the ionic liquids reached extraction efficiencies greater than 99%, except for $[(EH)_3NH]$[Cyanex272] which only extracted 23.8% La. While the extraction of La from solution was not as quick as predicted, these experiments show that the tested ionic liquids may be suitable for REE extraction.

Table 4.1: Extraction efficiencies for lanthanum liquid-liquid extraction after 2 and 30 minutes

Ionic Liquid	Extraction Efficiency (%)	
	2 minutes	30 minutes
$[(EH)_2NH_2]$[Cyanex272]	96.2	99.3
$[(EH)_3NH]$[Cyanex272]	26.1	23.8
$[(EH)_2NH_2][(octyl)_2POO]$	54.6	99.7
$[(EH)_2NH_2]$[camHPOO]	-1.4	99.9
$[(EH)_2NH_2]$[camPhPOO]	52.1	99.4

Maria et al. tested a range of ILs for the extraction and separation of lanthanides from solution using a simple liquid-liquid extraction method. With their ILs, they discovered that a contact time of 5 minutes was sufficient for extraction to occur. However, pH was a significant factor in the extractions, with higher pH levels resulting in higher extractions for all lanthanides and the lower pH levels resulting in higher selectivity among the lanthanide elements. It was also concluded that a larger ionic strength caused higher extractions and lower selectivity. [20] Therefore, the extraction results reported in this work may be improved with slight alterations to the method, including changes to the pH.

4.3.5 Lanthanum and Ytterbium Separations using SILs

The initial lanthanum and ytterbium separation tests using the SIL column method involved extraction experiments of separate lanthanum and ytterbium solutions, as well as a solution containing a mixture of both lanthanum and ytterbium. This was done as it allows for the comparison of results and speculation on the interference or any competition in the extraction experiments. La and Yb were chosen to represent the light and heavy REEs respectively. Therefore, they would be expected to give relatively good separation compared to two closer, more similar lanthanide elements. The results of these initial experiments seemed promising, with some of the ILs producing extraction efficiencies as high as 99.9%. The extraction efficiencies and distribution ratios of the extraction of the lanthanum solution and ytterbium solution are shown in Table 4.2. All REE extraction tests were done as duplicates, so the results given are the average of these two results.

Table 4.2: Results from extraction experiments of individual lanthanum and ytterbium elements

IL	**La extraction experiments**		**Yb Extraction experiments**	
	Distribution Ratio (D)	Extraction Efficiency (%)	Distribution Ratio (D)	Extraction Efficiency (%)
$[(EH)_2NH_2][Cyanex272]$	17.2	94.3%	840	99.9%
$[(EH)_3NH][Cyanex272]$	4.94	82.8%	3020	99.9%
$[(EH)_2NH_2][oct_2POO]$	13.7	91.9%	1904	99.8%
$[(EH)_2NH_2][CamHPOO]$	1.11	52.4%	7.19	85.5%
$[(EH)_2NH_2][CamPhPOO]$	1.73	60.6%	13900	99.9%

These results show higher extraction efficiencies of Yb compared to La across all ILs tested, with most ILs achieving extraction efficiencies above 99%. This difference can be expected due to the difference in size of La^{3+} and Yb^{3+}. The lanthanide contraction was discussed in Chapter 1 to describe the general trend of decreasing size of the ionic and metallic radii across the lanthanide series. Therefore, Yb^{3+} is smaller than La^{3+}, and will form more stable complexes with ligands, thus will be more readily extracted by the IL. [21] For the lanthanum extraction experiments, it was IL $[(EH)_2NH_2]$[Cyanex272] that achieved the highest extraction efficiencies, at 94.3%. This aligns with the results achieved for the lanthanum liquid-liquid extraction results which showed an extraction efficiency of 96.2% after a 2-minute extraction. $[(EH)_2NH_2]$[CamHPOO] showed the lowest extraction efficiencies for both the La and Yb extractions, with extraction efficiencies of 52.4% and 85.5% respectively.

Following these experiments, the La/Yb separation experiments were carried out. The extraction efficiencies and separation factors are given in Table 4.3. For the extraction of both La and Yb, $[(EH)_2NH_2]$[CamHPOO] achieved the lowest extraction efficiencies at 46.3% and 58.2% respectively. This aligns with the results from the single element extraction experiments where $[(EH)_2NH_2]$[CamHPOO] was also the poorest IL extractant for both elements.

Table 4.3: La/Yb column separation results showing extraction efficiencies and separation factors

IL	**Extraction Efficiencies**		**Separation Factor**
	La	Yb	
$[(EH)_2NH_2]$[Cyanex272]	95.5%	99.8%	55.3
$[(EH)_3NH]$[Cyanex272]	92.5%	99.8%	48.3
$[(EH)_2NH_2][oct_2POO]$	98.3%	99.8%	4.83
$[(EH)_2NH_2]$[CamHPOO]	46.3%	58.2%	1.63
$[(EH)_2NH_2]$[CamPhPOO]	58.1%	84.0%	5.15

These results also show the two Cyanex272-containing ILs and $[(EH)_2NH_2][oct_2POO]$ to be the best ILs for rare earth extraction from an aqueous solution. ILs containing the Cyanex272 anion also show high selectivity towards Yb, possibly indicating a preference towards the extraction of the HREEs.

4.3.6 Lanthanum and Ytterbium Stripping Experiments

Alongside the extraction tests, the stripping of the column was also tested using 1 M HCl. This was carried out by running 2 mL of 1 M HCl through the column following the extraction experiments and collecting the stripped solution. The ICP-MS results of the stripping experiments were used to calculate the stripping efficiency of HCl on the column. The stripping efficiencies of La and Yb for the single element separation experiments are shown in Table 4.4.

Table 4.4: Stripping efficiencies of La and Yb for single element separation experiments

ILs	**Stripping Efficiency (%)**	
	La	Yb
$[(EH)_2NH_2][Cyanex272]$	41.8%	34.5%
$[(EH)_3NH][Cyanex272]$	24.6%	17.2%
$[(EH)_2NH_2][oct_2POO]$	94.0%	1.31%
$[(EH)_2NH_2][CamPOO]$	74.6%	64.5%
$[(EH)_2NH_2][CamPhPOO]$	59.7%	18.1%

These results show moderate stripping efficiencies in most cases, with $[(EH)_2NH_2][oct_2POO]$ showing the lowest stripping efficiencies for Yb at only 1.31%. The highest stripping for Yb was achieved by $[(EH)_2NH_2][CamHPOO]$ at 64.5%. On the other hand, the stripping of La from the La column proved to be better, with the lowest stripping efficiency calculated to be 24.6% for the $[(EH)_3NH][Cyanex272]$ column. Interestingly, the highest and lowest stripping efficiency across these experiments were both achieved by $[(EH)_2NH_2][oct_2POO]$, with the La column resulting in a stripping efficiency of 94.0%. and the Yb column with a stripping efficiency of 1.31%. The low stripping efficiency may be due to the stability of the complex formed between this IL and Yb.

For the column tested for the separation of both La and Yb combined, thestripping efficiencies are given in Table 4.5. These results show a similar trend to the single element stripping experiments, with better stripping occurring for La in most cases. However, most of the results, particularly for the La stripping, show a lower stripping efficiency than the previous experiments.

Table 4.5: Stripping efficiencies for SILs in La/Yb separation tests

IL	Stripping Efficiency	
	La	Yb

$[(EH)_2NH_2][Cyanex272]$	35.0%	20.5%
$[(EH)_3NH][Cyanex272]$	39.0%	14.3%
$[(EH)_2NH_2][oct_2POO]$	48.3%	11.1%
$[(EH)_2NH_2][CamPOO]$	52.5%	54.4%
$[(EH)_2NH_2][CamPhPOO]$	59.1%	44.3%

4.3.7 Separation of Rare Earth Elements using SILs

Folllowing the separation tests involving two of the rare earth elements, the ILs were tested for the separation of multiple REEs in order to determine selectivities of the ILs, as well as the performance of the ILs for separations when a wider range of REEs were involved. A total of 8 REEs were selected for these separation tests, ranging from lanthanum to ytterbium to ensure tests covered a range of the light and heavy rare earths, with the solution prepared allowing for a 6 % loading of the IL when the column is filled with 3.15 g of glass beads coated with a weight percentage of 1 % IL. These tests were also done in duplicate, with any reported results being the average of the two. The extraction efficiencies of the ILs across the lanthanide series is shown in Figure 4.4Figure 4.4. Compared to previous separation tests, these extraction efficiencies are quite low, with $[(EH)_3NH][Cyanex272]$ producing the lowest extraction efficiencies for elements lanthanum, cerium, praseodymium and neodymium. The performance of this IL in comparison to others tested improves across the lanthanide series, with results showing one of the highest extraction efficiencies for the heavier elements, gadolinium, dysprosium, and ytterbium.

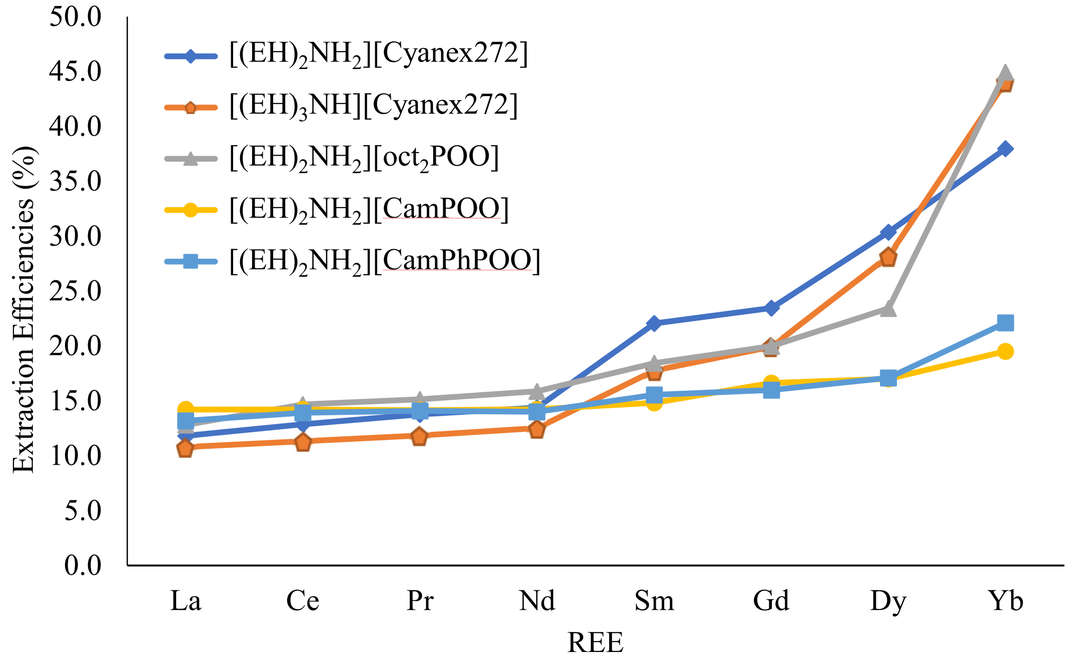

Figure 4.4: Extraction efficiencies for all tested ILs across the lanthanide series

The lower extraction efficiencies observed in these tests, compared to the previously discussed single element, or La/Yb separation tests, may be due to some degree of competitive extraction amongst the chosen REEs, as well as an overloading of the column. Calculating the number of moles of REEs extracted by the SIL shows than the total extracted REEs for the lanthanide extraction tests was greater than the total extracted REEs for the La/Yb tests. For example, IL $[(EH)_2NH_2][oct_2POO]$ extracted 2.38×10^{-7} mol of Ln^{3+} elements in the lanthanide extraction tests, and a total of 6.45×10^{-8} mol of La and Yb in the La/Yb extraction tests. The loading capacity of the ionic liquid appears to be quite low compared to other examples found in the literature. For example, Deng et al.[22] found the saturation loading capacity for the IL benzyltributylammonium dodecanedioic acetate ($[N_{444Bn}]$[DDA]) to be 0.433 mol/mol (the mole ratio of Y(III) to ILs). The results found in this work found the highest mole ratio for total lanthanide content to IL for $[(EH)_3NH]$[Cyanex272] to be 0.00483 mol/mol. However, these results cannot be considered entirely equal, as Deng et al. used a liquid-liquid extraction method with a longer extraction time of 30 minutes. With some variation in the mass of 1 % IL loaded glass beads added to the column (ranging from 3.10 – 3.20 g), it was assumed that an average 3.15 g beads were used to prepare the column for the sake of loading calculations. This therefore assumes 0.0315 g IL was present in the column, however this may vary due to uneven coating of glass beads, or loss of IL in preconditioning steps.

With all ILs, a general trend emerges whereby each IL appears to show selectivity towards the heavier REEs over the LREEs to some extent. Once again, this trend can be expected, as the size of the metal cation decreases across the series, therefore the smaller, heavier REEs form more stable complexes. This trend can also be seen in the separation factors shown for all tested ionic liquids in Tables 4.6-4.10. Based on these results, $[(EH)_2NH_2][camPhPOO]$ and $[(EH)_2NH_2][camPhPOO]$ show the lowest separation factors, and therefore the lowest selectivity towards any single element or group of elements. The remaining ILs all shown higher separation factors particularly between ytterbium and the lighter REEs. The highest separation factors were achieved by $[(EH)_3NH_2][Cyanex272]$, with a La/Yb separation factor of 6.57. $[(EH)_2NH_2][oct_2POO]$ and $[(EH)_2NH_2][Cyanex272]$ also showed good separation factors between Yb and the lighter REEs, with La/Yb separation factors of 5.71 and 4.57 respectively.

Table 4.6: Separation factors for the range of REEs tested using IL $[(EH)_2NH_2][oct_2POO]$

	La	Ce	Pr	Nd	Sm	Gd	Dy	Yb
La		1.17	1.21	1.28	1.53	1.69	2.08	5.71
Ce			1.04	1.10	1.31	1.45	1.78	4.90
Pr				1.06	1.27	1.40	1.72	4.72
Nd					1.20	1.32	1.62	4.46
Sm						1.11	1.36	3.73
Gd							1.23	3.37
Dy								2.75
Yb								

Table 4.7:Separation factors for the range of REEs tested using IL $[(EH)_2NH_2][camHPOO]$

	La	Ce	Pr	Nd	Sm	Gd	Dy	Yb
La		1.00	1.00	1.00	1.05	1.20	1.24	1.46
Ce			1.00	1.00	1.05	1.20	1.24	1.46
Pr				1.01	1.06	1.21	1.24	1.47
Nd					1.05	1.20	1.23	1.46
Sm						1.15	1.18	1.39
Gd							1.03	1.22
Dy								1.18
Yb								

Table 4.8: Separation factors for the range of REEs tested using IL $[(EH)_2NH_2][camPhPOO]$

	La	Ce	Pr	Nd	Sm	Gd	Dy	Yb
La		1.06	1.08	1.07	1.21	1.25	1.36	1.87
Ce			1.01	1.01	1.14	1.18	1.28	1.76
Pr				0.99	1.12	1.16	1.26	1.73
Nd					1.13	1.17	1.27	1.75
Sm						1.03	1.12	1.54
Gd							1.08	1.49
Dy								1.38
Yb								

Table 4.9: Separation factors for the range of REEs tested using IL $[(EH)_2NH_2][Cyanex272]$

	La	Ce	Pr	Nd	Sm	Gd	Dy	Yb
La		1.10	1.19	1.25	2.11	2.29	3.26	4.57
Ce			1.08	1.14	1.91	2.07	2.95	4.14
Pr				1.05	1.77	1.92	2.73	3.83
Nd					1.69	1.83	2.60	3.65
Sm						1.08	1.54	2.16
Gd							1.42	2.00
Dy								1.40
Yb								

Table 4.10: Separation factors for the range of REEs tested using IL $[(EH)_3NH][Cyanex272]$

	La	Ce	Pr	Nd	Sm	Gd	Dy	Yb
La		1.06	1.11	1.18	1.79	2.06	3.27	6.57
Ce			1.05	1.12	1.69	1.95	3.09	6.22
Pr				1.07	1.61	1.86	2.94	5.92
Nd					1.51	1.74	2.76	5.56
Sm						1.15	1.83	3.67
Gd							1.58	3.19
Dy								2.01
Yb								

In the literature, much of the interest in separation of the REEs considers separation of neighbouring elements, as well as separation of the LREEs from the HREEs. For example, in their extraction experiments using varying ratios of Cyanex572 and TBP, Dashti et al.[23]

achieved separation factors as high as 30.1 for a Pr/Er element pair. This result is significantly better than any of the results produced in this work for similar element pairs. For example, the best separation factors achieved for Pr/Dy and Pr/Yb in this work are 2.94 and 5.92 respectively, both of which were achieved by [$(EH)_3$NH][Cyanex272]. In another example, Devi et al.[24] considered the separation of yttrium(III) from neighbouring elements lanthanum(III) and cerium(III) using ionic liquids in a liquid-liquid extraction method. Using the IL [A336][Cyanex272] they reported separation factors as high as 134 and 148.5 for Y/La and Y/Ce separations respectively. These results are impressive considering the difficulty often faced in the separation of the REEs.

While reports on the use of ILs for the separation of the REEs are common, and there are many reports using SILs, the use of SIL for REE separation appears to be a rather small area of study. Of the publications using SILs for REE separation, the results reported are often comparable to those reported in this work. For example, using a polymer inclusion membrane as a support for Cyphos IL 104, Wang et al. was able to separate neighbouring elements, Yb(III) and Lu(III), with a separation factor of 1.37 under optimised conditions. [25]. While not between neighbouring elements, higher separation factors were achieved in this work for many of the separations without optimisations made to the method.

4.3.8 Stripping of REEs from SILs

The SIL columns used for REE separation were stripped following extraction experiments using 1 M HCl. This showed some success producing moderate to good stripping efficiencies for most elements. The stripping efficiencies for each of the SIL columns for each element are shown in Table 4.11. These are shown as the average stripping efficiencies from duplicate tests.

Table 4.11: Stripping efficiencies of lanthanide elements from SIL column

IL	Stripping Efficiency (%)							
	La	Ce	Pr	Nd	Sm	Gd	Dy	Yb
$[(EH)_2NH_2][Cyanex272]$	54.8%	61.8%	66.0%	79.1%	28.3%	101%	145%	187%
$[(EH)_3NH][Cyanex272]$	57.9%	60.7%	63.6%	69.0%	97.3%	80.1%	158.0%	341%
$[(EH)_2NH_2][oct_2POO]$	65.9%	73.7%	75.1%	62.5%	92.6%	70.4%	124%	355%
$[(EH)_2NH_2][CamHPOO]$	69.7%	69.3%	68.4%	69.1%	71.1%	114%	80.4%	87.1%
$[(EH)_2NH_2][CamPhPOO]$	58.6%	62.0%	62.9%	67.7%	68.6%	109%	74.3%	93.0%

These results show very high stripping efficiencies for many of the heavier rare earth elements, with the highest results showing an efficiency of 355 % for the stripping of Yb from the $[(EH)_2NH_2][oct_2POO]$ column. These high stripping efficiencies are possibly due to interferences which can be observed in ICP-MS. For many REEs, there are minimal interferences present in ICP-MS, however for Gd and Yb in particular, the presence of other REEs can cause interference in these measurements.[26] Some of these interferences are given in Table 4.12.

Table 4.12: Common polyatomic interferences for a selection of REEs[1]

Element	Polyatomic Interferences
^{163}Dy	$^{147}Sm^{16}O^{+}$
^{155}Gd	$^{139}La^{16}O^{+}$
^{157}Gd	$^{141}Gd^{16}O^{+}$
^{172}Yb	$^{156}Gd^{16}O^{+}$
^{173}Yb	$^{157}Gd^{16}O^{+}$

The interferences given above show those which include other REEs. These interferences may be a contributing factor to the high results achieved for the stripping of the REEs. Interferences for the lighter REEs can be observed, however these occur in the presence of elements outside the REEs. The high results may also be due to error with dilution and/or the subsequent calculation of the stripping efficiency, which may cause all the results to be proportionally incorrect. However, considering the three elements affected by high results are those which experience interferences from other REEs (all of which were present in the sample), it can be assumed that these results are at least in part affected by interferences.

The stripping of the lighter REEs has shown some promising results with stripping. In most cases, there seems to be some stripping preference for the heavier Sm, achieving stripping efficiencies as high as 97.3 %. Across all the SILs for elements from La to Sm, most of the stripping efficiencies lie between 50 – 70 %, with these generally increasing from La to Sm.

4.3.9 Reliability of Results

For each of the lanthanide separation tests using the SILs, each IL was tested in duplicate in order to determine the repeatability of the results. For the results reported in this chapter, it is the average of the duplicate result which is reported for all results except for the stripping experiment for the single element Yb column with $[(EH)_2NH_2]$[Cyanex272] which only 1 result was obtained due to issues faced with the ICP-MS analysis.

Using the duplicate results, the percentage difference between duplicates of the same test is calculated using the following equation:

$$\%Difference = \frac{|A - B|}{\frac{(A + B)}{2}} \times 100$$

where A and B refer to the extraction efficiency or stripping efficiency of a certain element calculated for the duplicate runs. Across all duplicate results, the average percentage difference between results was calculated to be 10.2%. For most of the results, the calculated percentage difference is below 10%, however there are two runs which appear to bring the average difference up. The $[(EH)_2NH_2][oct_2POO]$ and $[(EH)_3NH]$[Cyanex272] SIL column lanthanide separation tests had high percentage differences for most elements, with an average percentage difference of 20.3% and 22.1% respectively for the extraction experiments. These also had high percentage differences for the stripping experiments with average percentage differences of 16.2% and 25.9%. For the remaining columns, the average percentage differences for the extraction tests are all under 10%. The high differences observed in both the extraction and stripping results for $[(EH)_2NH_2][oct_2POO]$ and $[(EH)_2NH]$[Cyanex272] may be due to differences in the packing of the column and therefore differences to the way solutions passed through the column. For both of these SILs, it was observed that one of the two columns tested had a much slower elution compared to most columns. This time difference is likely due to differences in the packing of the column, with some beads potentially being more tightly packed than others. This difference in contact time would increase extraction time for a particular run, therefore resulting in a better extraction than a duplicate run which had a faster contact period.

Based on these results (shown in Appendix B), while there are some differences observed between duplicate results, for a majority of results, the differences between duplicate extraction and stripping efficiencies are within ranges suitable to ascertain whether the ILs created in this work could be suitable for REE separation. Further work could be done to improve the separation method, and to produce more reliable results.

4.4 Conclusion

The separation experiments described in this chapter tested five different ammonium phosphinate ionic liquids for their ability to extract and separate cobalt and nickel, lanthanum and ytterbium, and a mixture of eight different lanthanide elements. For the lanthanide extraction experiments using SILs, $[(EH)_3NH][Cyanex272]$ produced the highest separation factors between the light and heavy rare earth elements, including a separation factor of 6.57 for La/Yb separations. $[(EH)_2NH][oct_2POO]$ also performed well, with the highest separation factor between heavy REEs Dy and Yb. La/Yb separations resulted in high extraction efficiencies for most of the tested ionic liquids, showing the potential these ILs have in separations of this kind.

4.5 References

[1] Onghena, B.; Valgaeren, S.; Vander Hoogerstraete, T.; Binnemans, K., Cobalt(II)/nickel(II) separation from sulfate media by solvent extraction with an undiluted quaternary phosphonium ionic liquid. *RSC Advances* **2017,** *7* (57), 35992-35999.

[2] Wellens, S.; Thijs, B.; Binnemans, K., An environmentally friendlier approach to hydrometallurgy: Highly selective separation of cobalt from nickel by solvent extraction with undiluted phosphonium ionic liquids. *Green Chemistry* **2012,** *14* (6), 1657-1665.

[3] Kaim, V.; Rintala, J.; He, C., Selective recovery of rare earth elements from e-waste via ionic liquid extraction: A review. *Separation and Purification Technology* **2023,** *306*, 122699.

[4] Zhu, L.; Guo, L.; Zhang, Z.; Chen, J.; Zhang, S., The preparation of supported ionic liquids (SILs) and their application in rare metals separation. *Science China Chemistry* **2012,** *55* (8), 1479-1487.

[5] Billard, I.; Ouadi, A.; Gaillard, C., Liquid–liquid extraction of actinides, lanthanides, and fission products by use of ionic liquids: From discovery to understanding. *Analytical and Bioanalytical Chemistry* **2011,** *400* (6), 1555-1566.

[6] Messadi, A.; Mohamadou, A.; Boudesocque, S.; Dupont, L.; Guillon, E., Task-specific ionic liquid with coordinating anion for heavy metal ion extraction: Cation exchange versus ion-pair extraction. *Separation and Purification Technology* **2013,** *107*, 172-178.

[7] Crundwell, F.; Moats, M.; Ramachandran, V.; Robinson, T.; Davenport, W. G., *Extractive metallurgy of nickel, cobalt and platinum group metals*. Elsevier: Oxford, United Kingdom, 2011.

[8] Flett, D. S., Solvent extraction in hydrometallurgy: The role of organophosphorus extractants. *Journal of Organometallic Chemistry* **2005,** *690* (10), 2426-2438.

[9] Cotton, F. A., Wilkinson, G., Murillo, C.A., Bockmann, M., *Advanced inorganic chemistry*. 6th ed.; Wiley: New York, 1999.

[10] Khodakarami, M.; Alagha, L., Separation and recovery of rare earth elements using novel ammonium-based task-specific ionic liquids with bidentate and tridentate O-donor functional groups. *Separation and Purification Technology* **2020,** *232*, 115952.

[11] Chen, Y.; Wang, H.; Pei, Y.; Wang, J., Selective separation of scandium(III) from rare earth metals by carboxyl-functionalized ionic liquids. *Separation and Purification Technology* **2017,** *178*, 261-268.

[12] Baba, Y.; Kubota, F.; Kamiya, N.; Goto, M., Recent advances in extraction and separation of rare-earth metals using ionic liquids. *Journal of Chemical Engineering of Japan* **2011,** *44* (10), 679-685.

[13] Okamura, H.; Hirayama, N., Recent progress in ionic liquid extraction for the separation of rare earth elements. *Analytical Sciences* **2021,** *37* (1), 119-130.

[14] Barrueto, Y.; Hernández, P.; Jiménez, Y. P.; Morales, J., Properties and application of ionic liquids in leaching base/precious metals from e-waste. A review. *Hydrometallurgy* **2022,** *212*, 105895.

[15] Atkins, P. W.; Shriver, D. F., *Shriver & Atkins' inorganic chemistry*. 4th ed.; Oxford University Press: Oxford, 2006.

[16] Giddings, J. C.; Keller, R. A., *Advances in chromatography : Volume 9*. First edition. ed.; CRC Press: 2021.

[17] Ayanda, O. S.; Adekola, F. A.; Baba, A. A.; Ximba, B. J.; Fatoki, O. S., Application of Cyanex® extractant in cobalt/nickel separation process by solvent extraction. *International Journal of Physical Sciences* **2013,** *8*, 89-97.

[18] Jing, X.; Wu, Z.; Zhao, D.; Li, S.; Kong, F.; Chu, Y., Environmentally friendly extraction and recovery of cobalt from simulated solution of spent ternary lithium batteries using the novel ionic liquids of $[C_8H_{17}NH_2]$[Cyanex272]. *ACS Sustainable Chemistry & Engineering* **2021,** *9* (6), 2475-2485.
[19] Zante, G.; Boltoeva, M.; Masmoudi, A.; Barillon, R.; Trébouet, D., Selective separation of cobalt and nickel using a stable supported ionic liquid membrane. *Separation and Purification Technology* **2020,** *252*, 117477.
[20] Maria, L.; Cruz, A.; Carretas, J. M.; Monteiro, B.; Galinha, C.; Gomes, S. S.; Araújo, M. F.; Paiva, I.; Marçalo, J.; Leal, J. P., Improving the selective extraction of lanthanides by using functionalised ionic liquids. *Separation and Purification Technology* **2020,** *237*, 116354.
[21] Housecroft, C. E.; Sharpe, A. G., *Inorganic chemistry*. Pearson: Harlow, 2012; Vol. 4th ed.
[22] Deng, Y.; Ding, Y.; Huang, Z.; Yu, Y.; He, J.; Zhang, Y., Boosting the extraction of rare earth elements from chloride medium by novel carboxylic acid based ionic liquids. *Journal of Molecular Liquids* **2021,** *329*, 115549.
[23] Dashti, S.; Sadri, F.; Shakibania, S.; Rashchi, F.; Ghahreman, A., Separation and solvent extraction of rare earth elements (Pr, Nd, Sm, Eu, Tb, and Er) using TBP and Cyanex 572 from a chloride medium. *Minerals Engineering* **2021,** *161*, 106694.
[24] Devi, N.; Sukla, L. B., Studies on liquid-liquid extraction of yttrium and separation from other rare earth elements using bifunctional ionic liquids. *Mineral Processing and Extractive Metallurgy Review* **2019,** *40* (1), 46-55.
[25] Wang, Y.; Chen, L.; Yan, Y.; Chen, J.; Dai, J.; Dai, X., Separation of adjacent heavy rare earth lutetium(III) and ytterbium(III) by task-specific ionic liquid Cyphos IL 104 embedded polymer inclusion membrane. *Journal of Membrane Science* **2020,** *610*, 118263.
[26] May, T. W.; Wiedmeyer, R. H., A table of polyatomic interferences in ICP-MS. *Atomic Spectroscopy* **1998,** *19*, 150-155.

Chapter 5

Conclusions and Suggestions for Future Work

In this work, a series of phosphorus-based ionic liquids were successfully prepared using a simple protonation reaction between secondary and tertiary amines and various phosphinic acids. Five of these ionic liquids were selected to be tested for the separation of the REEs from aqueous solution through liquid-liquid extraction methods, or a column extraction method using ionic liquids supported on glass beads. Results showed the potential of these ionic liquids for REE separation, with [$(EH)_3NH$][Cyanex272] showing moderate extraction efficiencies, and producing the highest separation factors between the light and heavy rare earth elements.

However, the extraction method was not perfect, with low extraction efficiencies compared to some literature studies. Future work may look to improve the extraction method and fine tune the extraction. This might be achieved through slight adjustments to the pH of the aqueous solution as it is well known that REE separations can greatly rely on small changes to the pH. Tests with a lower concentration of REE solution should also be tested. Liquid-liquid extraction tests and separations of single elements La and Yb showed high extraction efficiencies greater than 90 %. Therefore, the lower extraction efficiencies achieved for the separation tests for multiple REE separations may be due to the column being overloaded. Lower REE concentration may achieve better extractions.

There was also some synthesis work described in this thesis, some of which was unsuccessful, or abandoned due to time constraints. Further work could be done to improve the yield, to purify, and fully characterise the product camP(O)(OH)($CH_2N^iBu_2$).

Appendix A: Calculation Examples

Solubility test calculation example (for IL [(EH)$_2$NH$_2$][Cyanex272]):

The ICP-MS result showed P concentration in aqueous solution was 12.6 ppm, or 0.0126 g/L. The percentage of P present in the IL was calculated based on molecular weight:

$$\%P\ in\ [(EH_2)NH_2][Cyanex272] = \frac{P\ g\ mol^{-1}}{IL\ g\ mol^{-1}} \times 100 = \frac{31\ g\ mol^{-1}}{532\ g\ mol^{-1}} \times 100 = 5.83\ \%$$

$$Solubility = \frac{[P]gL^{-1}}{\%P\ in\ IL} = \frac{0.0126\ g\ L^{-1}}{5.83\ \%} = 0.216\ g\ L^{-1}$$

Example Calculations used for extraction and stripping of SILs:

La solution (aq$_i$) =	516.071 ppb (aq solution before extraction)
Extracted solution (aq$_f$) =	59.047 ppb (aq solution after extraction with IL)
Dilution factor =	4
V of solution passed through column =	5 mL

$$Actual\ concentration\ in\ aq_i = 516.071 \times 4 = 2064.284\ ppb$$
$$Actual\ concentration\ in\ aq_f = 59.047 \times 4 = 236.188\ ppb$$

This gives the initial concentration and the concentration of the aqueous solution after is has passed through the column. To calculate what was left on the column, the following equation was used:

$$[M]_{IL} = [M]_i - [M]_f = 2064 - 236 = 1828\ ppb$$

This can then be used to calculate the extraction efficiency and distribution ratio:

$$\%E = \frac{[M]_{IL}}{[M]_i} \times 100 = \frac{1828}{2064} \times 100 = 88.6\%$$

$$D = \frac{M_{IL}}{M_f} = \frac{1828}{236} = 7.74$$

For the stripping experiment, the ICP-MS result showed a concentration of 1003.46 ppb (actual conc = 4013.8 ppb).

Due to the use of different volumes used in the extraction and stripping experiments, this needed to be accounted for in these calculations. This was done by converting relevant concentrations to g L^{-1} and including the volumes in the stripping experiments:

Stripped solution = 4013.8 / 1000000 = 0.00401 g L^{-1}
Initial La solution = 0.00206 g L^{-1}
Final La solution = 0.000236 g L^{-1}
La column conc = 0.00206 – 0.000236 = 0.00182 g L^{-1}

$$Stripping\ efficiency = \frac{V_S[M]_{aq}}{[V]_E[M]_{IL}} \times 100 = \frac{0.005\ mL \times 0.00182\ g\ L^{-1}}{0.002\ mL \times 0.00401 g\ L^{-1}} \times 100$$
$$= 87.8\%$$

Appendix B: Cobalt/Nickel Extraction Results

Table A.1: Extraction efficiency results for cobalt/nickel separation experiments over 10 runs using $[(EH)_2NH][Cyanex272]$ SIL.

Run	**Extraction Efficiency (%)**		**Separation Factor**
	Cobalt	**Nickel**	
1	63.4%	26.9%	2.35
2	69.0%	25.7%	2.69
4	68.0%	21.6%	3.15
6	68.4%	25.0%	2.74
8	69.4%	25.6%	2.71
10	68.0%	21.8%	3.11

Appendix C: Percentage Difference Results

Table A.2: Percentage differences between duplicate results for lanthanide extraction experiments.

IL	% Difference for individual elements								Average % Difference
	La	**Ce**	**Pr**	**Nd**	**Sm**	**Gd**	**Dy**	**Yb**	
$[(EH)_2NH_2][Cyanex272]$	6.57%	1.75%	5.68%	2.24%	2.37%	5.91%	4.25%	3.43%	4.02%
$[(EH)_3NH][Cyanex272]$	26.7%	21.9%	22.9%	22.2%	22.0%	20.0%	24.6%	16.4%	22.1%
$[(EH)_2NH_2][oct_2POO]$	36.8%	24.9%	24.9%	20.7%	10.2%	0.036%	15.8%	28.9%	20.3%
$[(EH)_2NH_2][CamHPOO]$	3.76%	0.22%	2.02%	0.69%	2.86%	2.66%	2.72%	4.15%	2.39%
$[(EH)_2NH_2][CamPhPOO]$	9.43%	6.06%	12.93%	9.33%	6.75%	0.39%	4.28%	13.3%	7.81%

Table A.3: Percentage differences between duplicate results for lanthanide stripping experiments.

IL	% Difference for individual elements								Average % Difference
	La	Ce	Pr	Nd	Sm	Gd	Dy	Yb	
$[(EH)_2NH_2][Cyanex272]$	5.12%	3.14%	0.46%	3.68%	8.70%	16.0%	13.0%	12.9%	7.87%
$[(EH)_3NH][Cyanex272]$	25.6%	21.9%	22.4%	21.1%	22.8%	19.0%	27.4%	45.6%	25.8%
$[(EH)_2NH_2][oct_2POO]$	32.7%	20.6%	20.3%	16.4%	6.44%	0.48%	16.3%	16.1%	16.2%
$[(EH)_2NH_2][CamHPOO]$	13.0%	9.28%	7.49%	7.93%	11.3%	11.9%	12.1%	14.0%	10.9%
$[(EH)_2NH_2][CamPhPOO]$	14.6%	10.3%	17.1%	13.0%	11.5%	1.03%	1.66%	5.85%	9.4%